This document should be considered a "work in progress." It has not gone through an external peer review process. It should not be cited in any reports until it has been completed and undergone a thorough peer review process.

Effects of Fluctuating Flows from Glen Canyon Dam on the Early Life History Stages of Rainbow Trout in the Lee's Ferry Reach of the Colorado River

FY2003 Draft Report

By:

Josh Korman[1]
Matt Kaplinski[2]
Joseph E. Hazel, III[2]
Ted Melis[3]
Jeff Sneep[1]
Chris Magirl[4]

Prepared for:

Grand Canyon Monitoring and Research Center
Flagstaff, Arizona

January 16, 2004

[1]Ecometric Research Inc.
3560 W 22nd Ave., Vancouver, BC, V6S 1J3

[2]Namtek Inc., Northern Arizona University
Box 4099, Flagstaff, AZ 86011-4099

[3]Grand Canyon Monitoring and Research Center
2255 N. Gemini Dr., Flagstaff, AZ, 86001

[4]USGS, 1675 W Anklam Road
Tucson, AZ, 85745

(Text Only, Companion Document contains Tables and Figures)

Executive Summary

An experimental alteration of the hydrograph from Glen Canyon Dam, targeted at reducing the recruitment rate of rainbow trout through increased daily fluctuations in flow, was implemented from Jan.-Mar., 2003. This report describes the impact of the experimental flow regime on the early life stages of rainbow trout in the Lee's Ferry reach. The study consisted of 3 components. First, we measured the timing of redd excavation and the distribution of redds across elevations (i.e., redd hypsometry) to estimate the potential egg and alevin mortality caused by the experimental flow regime. Second, we quantified the relationships between spawning habitat preference and depth, velocity, and substrate to evaluate the feasibility of controlling spawning elevations through changes in discharge. Finally, we estimated seasonal trends in rainbow trout fry recruitment and survival using length-frequency data and high-resolution ageing information integrated in a stock synthesis model. Estimates of recruitment and survival can be compared across years under different flow regimes form Glen Canyon Dam to evaluate the extent to which operations effect the production of young fish. Monitoring changes in fry density and distribution over the summer can potentially be used to evaluate the effects of operations on seasonal or shorter time-scales. Information from the redd survey, habitat use, and fry components of the study were used to provide a series of recommendations for future experimental flows targeted at reducing the production of young rainbow trout in the Lee's Ferry reach.

The overall effect of the Jan.-Mar. 2003 experimental flow on the mortality of eggs was derived by combining data on redd hypsometry, gravel temperatures, and the timing of redd excavation. Of the redds excavated before Apr. 1, 25% were located above 12 kcfs and would been stranded above the water surface after this date. The duration of exposure at 12 kcfs prior to Apr. 1 was 11.5 hrs and exceeded the 10 hr. duration where total alevin mortality occurred based on field experiments in the Lee's Ferry reach conducted by Montgomery and Tinning (1993). Thus, eggs and alevins at 12 kcfs and higher were very likely already dead before the change in flow on Apr. 1. The duration of exposure at 8 kcfs was 9 hrs. Considering the daily application of this exposure frequency and elevated temperatures at 10

kcfs in Mar., it is likely that very little of the egg deposition above 8 kcfs survived until Apr. 1, corresponding to a 36-42% loss prior to the flow change. The loss of egg deposition due to enhanced fluctuating flows up to Apr. 1 therefore ranged from 25% - 40%. It is likely that the egg deposition after Apr. 1 above 8 kcfs (36%) was lost due to lethal temperatures associated with Sunday low-flow periods. In summary, the total egg deposition loss due to Glen Canyon Dam operations in 2003 ranged from 30 - 40% with about half of this mortality being a direct consequence of the enhanced fluctuating flows.

The spawning habitat preference models we developed for rainbow trout in the Lee's Ferry reach were useful for evaluating the extent to which increased discharge during the Jan. - Mar. experimental flow period altered the elevations where spawning occurred. Depths of 0.5 – 1.5 m, velocities of 0.3 – 1 m/sec, and D85 values of 15-45 mm were preferred. Weighted useable area computations showed that higher discharges increased total spawning habitat availability at sites that had spawning habitat located at higher stages such as Four Mile and Powerline Bars, and reduced spawning habitat availability at deep-water redd sites such as Ferry Swale. The model also showed that the stages of preferred suitable spawning habitat at Four Mile and Powerline Bars were increased under higher discharges. Such changes in spawning habitat availability would increase the proportion of redds that would be dessicated and increase the duration of exposure. The redd hypsometry study showed that there was a significant proportion of redds excavated in deep-water that would not be dewatered at flows as low as 5 kcfs. The large decline in spawning habitat availability at Ferry Swale under high discharge suggests that spawning at deep-water sites could be suppressed through maintenance of high flows through the entire spawning period, however this conclusion needs to be validated by additional flow experiments. There was a large proportion of total redds formed at stages below 5 kcfs (40-50%) in the Lee's Ferry reach, and we are uncertain about the efficacy of using high flows to reduce this proportion.

As expected, Young-of-Year (YoY) forklength increased over the summer and fall while densities generally declined. Talus shorelines had much higher densities compared to lower angle habitats (cobble bars and vegetated/sandy shorelines) and tended to attract or support slightly larger fish. The otoliths of 266 YoY rainbow trout captured between Apr. –

Oct. sample periods were extracted and successful age determinations were made for 237 of these fish. Hatch checks were clearly evident on all otoliths. Emergence checks tended to be subtler and could not always be identified, thus age was determined relative to the hatch date. There was little error in the estimation of days from hatch based on a blind-test using hatchery fish of known age. There was a very strong relationship between forklength and daily age from hatch. The best-fit von Bertalanffy relationship explained over 87% of the variation in forklength (n = 237). No seasonal trend in mean size-at-age was apparent. In 2003 the majority of hatching occurred between mid-Mar. and late-May with a peak in late-Apr. A weekly striping pattern was evident in at least 51% of the otoliths that were examined. The atypical increment formed every 7 days that caused the striping pattern tended to be 25% wider (3.12 microns) compared to the other increments (2.51 microns) when averaged across all striping cycles and fish, and the difference was statistically significant. It is very likely that the larger width of atypical increments that occurred with a periodicity of exactly 7 days were caused by Sunday-steady low flows. Thus, steady flows likely increase the growth rates of young trout and in turn may improve their survival.

The stock synthesis model was able to provide a good fits to the observed monthly length-frequency distributions. The most likely estimate of the weekly survival rate ranged from 0.88 to 0.90 across alternate recruitment models when the survival rate was assumed to be constant over the simulation period. The survival estimates were very precisely defined and precision was not dependent on the form of the recruitment model. 95% confidence limits were 0.88 +/- 0.015 for time-independent and best-fit Beta distribution recruitment models. All constant-survival models tended to over predict the number of fish present in the 45-75 mm forklength range on the Sept. sample period. This suggests that the survival rate between the late-Jul. and early-Sep. trips was somewhat lower than the average rate for the rest of the summer, or that there was a displacement of fish from low angle habitats between these two periods. These effects could have been caused by the large change in the minimum flow from 10 to 5 kcfs that occurred after the labor-day weekend.

Results from the redd surveys were used to define more effective flow regimes to reduce survival rates of rainbow trout eggs and alevins in the Lee's Ferry reach. Increased

fluctuations in flow targeted at increasing egg mortality should be conducted over a four-month period between Feb. and May to coincide with the majority of spawning activity. We estimated that 50 - 60% of the total amount of spawning occurred after Mar. 31. Terminating high flows after this date probably increased the number of redds excavated at lower stages where temperature and exposure impacts would be less severe. If increased fluctuating flows are to be implemented as part of a longer-term strategy, we do not recommend delaying the timing of the morning increase in discharge as was done in 2003. Significant temperature-induced mortality can be achieved through implementation of low steady flows every Sunday. This strategy will result in lethal or sub-optimal temperatures occurring once per week above the Sunday minimum flow elevation by about mid-Mar.

Three flow recommendations for Glen Canyon Dam were made based on results from the 2003 YoY survey and analysis: 1) Fluctuating flows targeting YoY rainbow trout should be implemented from Apr. through July to coincide with the timing of hatch; 2) Summer steady flows very likely improve the growth of YoY rainbow trout and should be minimized if the objective is to reduce rainbow trout densities; and 3) Sudden reductions in the minimum daily flow have the potential to strand or displace many YoY rainbow trout in the Lee's Ferry reach.

Acknowledgments

This project was supported through a cooperative agreement between the USGS and Ecometric Research Inc. as part of the science evaluation for the 2003 Glen Canyon Dam experimental flow program. Dr. Steven Campana of the Canadian Department of Fisheries and Oceans performed the analysis of otolith microstructure and provided suggestions on the analysis and interpretation of otolith data. Steve Hall, Dave Foster, Scott Decker, Gene Tisdale, Elizabeth Fuller, Alexis Hall, Matt Morales, Mark Pillar, and Chris Franke participated in the field surveys. Scott Decker and Steve Hall provided useful comments on the survey design. Carol Fritzinger, Mike Yard, Dave Foster, Brian Derker, Lars Niemi, Steve Jones, and Rocky Levette provided logistical support. Nancy Hornewer of the USGS provided discharge data.

Table of Contents

1.0 Introduction

Predation and competition by non-native salmonids has been identified as a potentially important factor contributing to the continued decline of humpback chub and other native fishes in Grand Canyon. To test this hypothesis, members of the Glen Canyon Dam Adaptive Management Workgroup elected to actively reduce the abundance of rainbow trout in Grand Canyon through a combination of mechanical removal and changes in discharge. A large-scale mechanical removal program was initiated in Jan. 2003 to reduce non-native fish densities in a 16-mile section of the Colorado River that is heavily used by the largest humpback chub aggregation in Grand Canyon. An experimental alteration of the hydrograph from Glen Canyon Dam, targeted at reducing the recruitment rate of rainbow trout through increased daily fluctuations in flow, was implemented in Jan.-Mar., 2003 and 2004.

The experimental hydrograph consisted of a increasing the maximum daily range in flows from a normal range of approximately 7–12 kcfs to 5-20 kcfs between Jan. and Mar. (Fig. 1.1). The flow regime exceeded both the maximum daily flow fluctuation and the ramping rates specified in the Glen Canyon Dam Record of Decision. High flows during the day were intended to increase the elevations where rainbow trout would spawn. Reduced flows at night were intended to increase the mortality rate on eggs and alevins on exposed portions of the gravel bars. The increased fluctuations in flows were also hypothesized to potentially reduce the survival of Young-of-Year (YoY) trout that had already emerged. A reduction in the maximum daily discharge on Apr. 1. to ca. 12 kcfs was intended to strand all surviving egg deposition above this elevation.

This report presents the results from the first year of a two-year study designed to assess the effects of the 2003/2004 experimental flow regime on early life stages of rainbow trout in both the Lee's Ferry reach and in Grand Canyon. We chose to work only in the Lee's Ferry reach in 2003 for a number of reasons. The fishery for rainbow trout in the Lee's Ferry reach is a valuable resource and understanding how operations from Glen Canyon Dam affect it is highly relevant to the overall GCD Adaptive Management Program. Reducing the

production of young fish in the Lee's Ferry reach would likely increase the size of catchable fish and is therefore a potential management tool for this resource. Many of the methods designed to meet the objectives of this project have never, or only rarely, been attempted in a river system as large as the Colorado River. We therefore elected to conduct the first year of the study in the Lee's Ferry reach due to its logistical advantages. Finally, juvenile or adult rainbow trout emigrating from the Lee's Ferry reach to Grand Canyon may be an important source of recruitment to the population in Grand Canyon. If this is the case, understanding the impacts of dam operations on the recruitment and survival young rainbow trout in the Lee's Ferry reach is highly relevant to understanding how operations effect the population in Grand Canyon. We will attempt to address this issue as part of the FY 2004 study that will be conducted in both the Lee's Ferry reach and in Grand Canyon.

The 2003 Lee's Ferry study consisted of three components. First, we measured the timing of redd excavation and the distribution of redds across elevations (i.e., redd hypsometry) to estimate the potential egg and alevin mortality caused by the experimental flow regime. Second, we quantified the relationships between spawning habitat preference and depth, velocity, and substrate to evaluate the feasibility of controlling spawning elevations through changes in discharge. Finally, we estimated seasonal trends in rainbow trout fry recruitment and survival using length-frequency data and high-resolution ageing information integrated in a stock synthesis model. Estimates of recruitment and survival can be compared across years under different flow regimes form Glen Canyon Dam to evaluate the extent to which operations effect the production of young fish. The fry component of this study also has the potential to help evaluate the effects of dam operations over shorter time-scales. Information from the redd survey, habitat use, and fry components are used to provide a series of recommendations for future experimental flows targeted at reducing rainbow trout recruitment rates in the Lee's Ferry reach.

2.0 Redd Hypsometry and Timing

Evaluation of the effects of the Jan.-Mar. 2003 enhanced fluctuating flows on the survival of rainbow trout eggs and alevins incubating in gravel substrates requires data on both seasonal timing and hypsometry of redd excavation. Timing of excavation determines the proportion of the total egg deposition potentially effected by the experimental flows. Within that proportion, redd hypsometry determines the extent of egg and alevin mortality caused by exposure- and temperature-induced impacts.

There is a considerable body of literature documenting the effects of fluctuating flows on the eggs and alevin stages of salmonids. Several studies have shown that salmonid eggs can tolerate long periods of dewatering. Reiser and White (1983) found that eggs dewatered for as long as four weeks (steelhead) and 1-5 weeks (chinook) showed essentially no effect on hatching success, or on the development and growth rate of alevins and juveniles, provided the sediment moisture content was maintained at 4% or higher. In a laboratory setting, Becker et al (1982) determined that the pre-hatch phases of chinook salmon development were tolerant to dewatering but that post hatch alevins were highly susceptible. Reiser and White (1983) cited the proximity of the redd to local ground water as one factor that might influence egg survival during dewatering. Chapman et al. (1986) found that flow fluctuations on the Columbia River did not prevent females from building redds and laying eggs above the minimum flow elevation. They found that 85% of the redds constructed above the minimum flow elevation that were subjected to regular dewatering contained live embryos. Exposure of redds may result in elevated temperatures that induce lethal or sub-lethal effects such as developmental abnormalities. A maximum lethal temperature for rainbow trout eggs of 16 C has been well determined from numerous hatchery studies (Piper et al. 1986) and increased mortality and developmental abnormalities have been shown to occur at temperatures as low as 13 C (Raleigh et al. 1984, Crisp 1981, McEwan and Jackson 1996).

Angradi et al. (1992) mapped the elevation of rainbow trout redds in Glen Canyon from Dec. 1990 to Apr. 1991 at four locations (4, 6, 8.9, and 14 Mile Bars). They found that

the peak of spawning occurred between late Mar. to early May with 29%, 59%, and 83% of the redds located above 11, 8, and 5 kcfs, respectively. Montgomery and Tinning (1993) conducted laboratory and experimental field trials to measure the survival of rainbow trout eggs and alevins in Glen Canyon under fluctuating flows. They found that the moisture content of exposed sediments (9%) was well above the 4% minimum threshold for egg hatching estimated by Reiser and White (1983). In laboratory studies, they found that periods of exposure of up to 12 hrs. had no influence on hatching success, but that total mortality occurred when exposure was 15 hrs. (see Table 2.1 for a summary of results). Alevin survival rates were much more sensitive to exposure, with almost no survival at exposures of 12 hrs. or more. Both field and laboratory studies showed that an exposure period of 6 hrs. reduced alevin survival rates by 50% and that morality rates from exposure periods as low as 3 hrs. could be as high as 60% if temperatures exceeded 11 C. In the field, an exposure of 10 hrs. resulted in 100%l mortality of alevins, while 15 hrs. of exposure was required to produce the complete mortality rate in the laboratory. The authors suggest that differences in sediment moisture content and temperature regimes were the likely factors causing differences between laboratory and field results.

In this study, we counted redds and surveyed their locations in the Lee's Ferry reach from Feb. to May, 2003. The survey information allowed us to quantify redd hypsometry, which in conjunction with discharge data, was used to determine the durations of exposure. We also collected data on intergravel temperatures at a range of stages to improve our assessment of the extent of mortality resulting from exposure. Monthly redd count data were used as input to a model that estimated the timing of redd excavation and the total number of redds excavated over the spawning season. This information was used in conjunction with redd loss estimates to determine the overall impact of the fluctuating flow experiment on egg-to-alevin survival in 2003.

2.1 Methods for Redd Hypsometry and Timing Study

Methods used for intensive redd surveys at four sites in the Lee's Ferry reach are described in Section 2.2.1. Methods for a system-wide redd survey of the Lee's Ferry reach are described in Section 2.1.2. Modelling and analytical methods used to interpret the redd count data are described in Section 2.1.3.

2.1.1 Methods for Redd Surveys at Intensive Sites

Intensive redd surveys in the Lee's Ferry reach were conducted monthly from Feb. – May, 2003 (Table 2.2) at Four Mile Bar (FM), Ferry Swale (FS), Powerline Bar (PL), and Pumphouse Bar (PH) (Fig. 2.1). Criteria used to define redds included the presence of a pit which was usually composed of a coarse deposit, a sorted finer deposit downstream of the pit (tail spill), appropriate grain sizes (5 – 50 mm), and a lack of algae or macrophytes on the sediment in the vicinity of the redds. During the early surveys, a small fraction of redds were excavated with a shovel to determine egg presence and ensure that our criteria were sound. Identification of redds was likely more accurate when they were exposed or in shallow water (< 1m). In deeper water, the presence of fish exhibiting spawning behaviours was used to help identify redds. Redd surveys were conducted by systematically traversing each site by foot and boat at the minimum daily discharge. At sites where redd densities were high, spray-painted rocks were used to mark redds so they were not double-counted. These rocks were removed at the end of each survey. All redds were counted at every site on each survey and we made no attempt to determine the month of origin for individual redds in the field.

Redd locations were surveyed with an electronic total station equipped with a digital data collector. A survey rod was placed over the central pit of each redd to obtain its position. For deeper redds, elevations were computed by subtracting the total depth of the redd from the surveyed elevation of the water surface. Total depth was measured using a Lowrance depth-sounder mounted on a 7 m aluminum hulled motorized boat. The boat was spatially referenced with the total station by targeting a prism cluster mounted on a mast directly above the transducer. Point data were referenced to the Arizona State Plane NAD83, Arizona

Central (FIPS 202) coordinate system, in meters, using benchmarks within a previously established control network. Survey accuracy in the field was maintained by horizontal and vertical checks of positional error between known reference points. Upon completion of each survey, field data were edited for spurious rod heights and miscodes. Ground point data had a positioning accuracy of better than 0.05 m and vertical accuracy that varied from 0.03 to 0.05 m. Bathymetric point data had a positioning accuracy of better than 0.25 m and a vertical accuracy of 0.1 m or less.

Stage-discharge relationships were empirically developed for each site and used to translate surveyed redd elevations into their discharge equivalents. Water elevations were surveyed at 5, 8, 12, 15, and 20 kcfs at each site. Water elevations surveys were almost always conducted at steady discharges, which allowed us to assume that discharge at the site was equivalent to the discharge from Glen Canyon Dam at the time of the survey. In the few cases when this assumption did not hold, we routed the relevant portions of the Glen Canyon Dam discharge record to the location of the study sites using a one-dimensional unsteady flow model (Wiele and Griffin 1997). Under unsteady flow, only data within 2 kcfs of the targeted discharges (5, 8, 12, 15, and 20 kcfs) were used in the estimation of the stage-discharge relationships. The stage-discharge data were plotted and a 2^{nd} order polynomial was fit to the data (Fig. 2.2). The morphology and large size of Four Mile Bar required the development of two independent stage-discharge relationships.

Continuously recording temperature loggers were buried in the gravel at an assumed egg pocket depth of 15 cm (Kondolf 2000) at a range of elevations at Four Mile and Powerline Bars during the first sampling period in Feb. The loggers were retrieved by staking-out their locations on the final survey in May. Temperature loggers recorded instantaneous temperature at a one-hr. interval.

2.1.2 Methods for Rapid Assessment Technique (RAT) Redd Surveys

Intensive sites were chosen because they were historically important spawning sites that likely made a significant contribution to the total number of redds excavated in the Lee's

Ferry reach. These sites were not necessarily representative in terms of the timing of redd excavation or hypsometry. We therefore used a "rapid assessment technique" (RAT) survey during the Mar., Apr., and May sampling sessions to derive a rough but system-wide estimate of redd numbers and hypsometry. Surveys were conducted by foot and by boat typically during steady flows. Surveys were initiated early in the morning working in a downstream direction from Glen Canyon Dam to maximize the length of time at steady-low discharge.

On each survey we visited all historical spawning locations (M. Yard, GCMRC, unpublished data presented in Foster 2002) and examined additional locations that had potential spawning habitat. The height of each redd above the water surface was estimated using an Abney level mounted to a survey rod. The depth of submerged redds was measured with either a survey rod or a depth sounder. If discharge from Glen Canyon Dam was not steady at the time of the survey, we used an unsteady flow model (Wiele and Griffin 1997) to predict discharge at each site at the time of the survey. The elevation of the water surface was estimated using the discharge at the time of the survey and the nearest stage-discharge relationship from the STARS model (Randle and Pemberton 1987). Redd elevations were then translated into their discharge-equivalent using the appropriate stage-discharge relationship and the heights of the redds above or below the water surface at the time of each survey.

2.1.3 Redd Count Model

The total numbers of redds and the timing of excavation over the spawning season can be estimated from repeated redd counts. The Area-Under-the-Curve (AUC) method is the traditional method for analyzing such data (Irvine and Nelson 1995). The number of redds counted per survey is plotted as a function of time (e.g., weeks from start of spawning run) and linear interpolation is used to generate a curve. The integral, or total area-under-the-curve, determines the number of redd-weeks, which is in turn divided by an estimate of redd survey life (SLR in units of weeks) to determine the total number of redds excavated (E) over the season,

(2.1) $$E = \frac{AUC}{SLR}$$

Redd survey life is the time required for a redd to loose the characteristics that make it discernable from other irregularities in the substrate. Survey life will be determined by a number of factors including substrate characteristics, slope, beach traffic, and inundation frequency. If survey life is longer or equal to the length of time between the start and end of spawning and there is no redd superimposition, the peak redd count will be equivalent to the total number of redds excavated over the season. However, if survey life is shorter than the duration of the spawning period, the total number of redds will be higher than the peak count. This latter situation is certainly the case for rainbow trout in the Lee's Ferry reach, where a substantial amount of spawning occurs over a period of 3-5 months.

The AUC method has a few significant limitations:

1. it is difficult to characterize uncertainty in the estimate of the total number of redds;
2. an arbitrary assignment of the beginning and ending spawning dates is required if the first and last surveys have non-zero counts; and
3. the method does not explicitly take into account arrival timing, and is therefore not useful for determining the proportion of redds excavated before a certain date.

All issues, especially 3), are highly relevant in the case of evaluating the impacts of the Jan.-Mar. 2003 experimental flows. More recently, maximum likelihood methods have been used to fit migration- or spawn-timing models to periodic count data in order to estimate escapement (Hilborn et al. 1999, Korman et al. 2002). These models overcome all three weaknesses of the AUC-method described above and are highly applicable to estimating the timing of rainbow trout spawning in Glen Canyon. In this analysis, we modified the modeling approach to include the effects of redd superimposition. Increased rates of redd superimposition will increase the total redd-to-observed redd ratio and therefore will have the same general effect as reducing redd survey life. While redd superimposition can be thought of as a component of redd survey life, the extent of superimposition will likely vary over the

duration of the run, with increased superimposition occurring later in the spawning season as spawning habitat saturates. Such a dynamic would tend to underestimate the magnitude of the late component of the spawning run.

We developed a model that estimated the magnitude and timing of redd excavation from periodic redd counts and assumptions about redd survey life and the rate of redd superimposition. The total number of redds observed on any week (RP_t) was modeled based on the equation,

(2.2) $$RP_t = A_t - F_t - S_t$$

where, A_t is the cumulative number of redds excavated up to and including week t, F_t is the cumulative number of redds that have been lost due to fading as they exceed their survey life, and S_t is the cumulative number of redds that are obscured from superimposition.

The timing and magnitude of redd excavation was modeled using a Beta distribution,

(2.3) $$A_t \propto E\int_0^t \theta_t^{(\alpha-1)}(1-\theta_t)^{(\beta-1)}dt$$

where E is the total number of redds excavated over the spawning season, and α and β are parameters of the beta distribution that define the timing of spawning. θ_t represents the proportional date of the run and ranges from 1/52 on the first week to 1 on the last week (T), that is $\theta_t = t/T$. Note that the form of the Beta distribution in eqn. 2.3 returns the cumulative frequency so the number of redds excavated on week t (A_t) is A_t - A_{t-1}. We modeled the number of redds that exceeded their survey life on week t as,

(2.4) $$F_t = A_{ct-SLR} - S_{ct-SLR}$$

where SLR is the survey life in weeks. In other words, the number of redds lost due to fading does not include those already lost due to superimposition.

Assuming a limited area of spawning habitat, the number of new redds that are superimposed on top of old redds on any week will be a function of the numbers of redds being excavated on that week and the number of redds present at a site relative to the total number of redds the site can support. We modeled the number of redds superimposed on any week (S_t-S_{t-1}) as,

$$S_t - S_{t-1} = A_t * SP \max \frac{RP_{t-1}^{SPsl}}{RP_{t-1}^{SPsl} + SPhalf^{SPsl}} \quad (2.5)$$

where, *SPmax* is the maximum proportion of new redds that can be superimposed on existing redds, *SPhalf* is the total number of redds present where the superimposition rate is reduced to ½ of its maximum value, and *SPsl* is the slope of the relationship.

The total number of redds excavated over the spawning season (*E*) and arrival model parameters (α, β) were fit to the observations of total redd counts across the four survey periods (RAT + Intensive sites) under different assumptions concerning survey life and the rate of superimposition. A spatial analysis of the redd count data at intensive sites (described below) was used to estimate the combined effect of redd survey life and superimposition on redd longevity. The predicted redd timing curve was used to estimate the total number of redds excavated over the entire season and the proportion excavated prior to Apr. 1. The latter estimate determined the total population of redds potentially affected by the Jan. – Mar. 2003 enhanced fluctuating flows. Observation error was assumed to be normally-distributed. Most-likely parameter estimates (MLEs) were computed by minimizing the sums of squares between the observed and predicted total redd counts over the four survey periods. As we did not conduct a RAT survey in Feb., we used the ratio of the intensive-to-RAT survey counts in Mar. (1.08) to expand the Intensive-site count in Feb. to a total (RAT + Intensive) count.

We did not attempt to measure survey life or the rate of redd superimposition rate directly in the field, however an estimate of their combined effect was derived from a spatial analysis of the redd survey data. From the AUC method, the total number of redds that are

excavated over a defined period is the ratio of the area-under-the-curve between two survey dates that span this period and the survey life (eqn. 2.1). We rearranged the AUC equation to estimate survey life based on the ratio of AUC to the actual number of redds excavated. Each intensive survey site was divided up into a grid of 1 m^2 cells using a Geographic Information System (GIS) and the presence or absence redds in each cell on each survey period was determined. The number of cells which contained a redd on survey *x* but not on survey *x-1* provided a minimum estimate of the actual number of new redds deposited between the two surveys (the denominator). The number of cells which contained a redd on survey *x-1* but not on survey *x* provided an estimate of the number of redds lost due to fading as they exceeded their survey life. Under the assumption of no redd superimposition, the number of cells with a redd present in two consecutive sampling periods provided an estimate of the number redds which were present on the first survey that did not fade by the second. The total number of cells that contained a red, whether new or counted on a previous survey, was equivalent to the number of redds present at-a-site. We computed the AUC between the first and last surveys and divided by the estimated number of "New" redds that were excavated on over this period to estimate survey life. These calculations were done for all four intensive survey sites.

2.2 Results from Redd Hypsometry and Timing Study

Redd counts at intensive sites increased steadily between the Feb. and Apr. sampling trips (Fig. 2.3a). Four Mile Bar comprised 65% of the total redds among the four intensively monitored sites. 30% of the redds were located below 5 kcfs and 46% were below 8 kcfs on the Mar. survey (Fig. 2.3b). 33% of the redds were located above 12 kcfs and would have been dewatered after the flow change on Apr. 1 (Fig. 1.1, Table 2.2). Redd hypsometry varied considerably between sites (Fig.'s 2.4 and 2.5). Four Mile and Powerline Bars had the highest percentage of redds above 12 kcfs. All redds at Ferry Swale were below 5 kcfs. There was considerable variation among sites in terms of the apparent timing of redd excavation. Spawning was earliest at the two most upstream sites (Powerline and Pumphouse Bars) with the majority completed by the Mar. survey. In contrast, the most downstream site (Four Mile

Bar) showed an increase in redds between the Apr. and May sampling periods. Ferry Swale, located between the upper two sites and Four Mile Bar, showed an intermediate timing.

The RAT survey documented 21 additional spawning locations in the Lee's Ferry reach that were dominantly deep-water redd sites (Table 2.3, Fig. 2.1). The peak count of redds (427) occurred during the Apr. sampling trip (Fig. 2.6) and was less than the peak count across the four intensive sites (510). There was a considerably higher proportion of redds below 5 and 8 kcfs based on the RAT surveys relative to the distribution at intensive sites. The peak redd count summed across RAT and Intensive surveys was 936 and occurred during the Apr. survey (Table 2.4). The total percentage of redds from the combined surveys above 5, 8, and 12 kcfs prior to the Apr. 1 flow change was 62, 42, and 25%, respectively. Redd hypsometry was fairly stable from Mar. through May.

Estimates of redd survey life based on a spatial analysis of redd count data were reasonably consistent among intensive survey sites. The number of 1 m^2 grid cells that contained redds was very similar to the total number of redds counted, indicating that there were only rare cases when more than one redd was present in a 1 m^2 cell (Table 2.5). Estimates of survey life based on the ratio of the Area-under-the-Curve of the number of cells with redds present to the number of cells with new redds (e.g., Fig. 2.7) ranged from 4.6-6.8 wks. with an average of 6.2 wks. (Table 2.6). Survey life was very consistent among all sites that had a reasonably high proportion of redds that were exposed for part of the day (PH, PL, FM). The lower survey life at Ferry Swale is not surprising. Redds were located in relatively mobile pea gravel that and were exposed to high velocities. Redds at Ferry Swale were also permanently submerged which would have increased the rate of algal recolonization following excavation (Angradi 1992). Given these characteristics, redds at Ferry Swale likely faded quite quickly if they were not actively maintained. Our spatial analysis cannot be used to determine if a cell classified as an "Old" redd (Table 2.5) was actually a new redd excavated on top of an existing redd. When we assumed that 100% of "Old" cells were superimposed by new redds to provide a maximum estimate of the number of new redds excavated between months, survey life dropped to an average of 4.7 weeks (Table 2.6). This is likely a lower bound on survey life, although it is possible that more than one instance of superimposition in

a cell could occur between sample periods. We used a survey life estimate of five weeks for calculations of the total redds excavated in 2003 and the proportion excavated before Apr. 1. The majority of spawning sites in the Lee's Ferry reach were permanently submerged (Table 2.3) and therefore likely had redd survey lives closer to the estimate for Ferry Swale.

The redd count model was able to fit the observed redd count data almost perfectly. (Fig. 2.8a). This is not surprising as the model contained as many parameters (4 assuming no redd superimposition) as there were data points. The model predicted that there was a substantial amount of spawning in Jun. and Jul (Fig. 2.8b). While we counted many redds in late May, we observed very few spawning fish during this survey. We suspect that if we had conducted a survey in late Jun. very few redds would have been observed. Unfortunately, because we did not conduct a Jun. survey there was no data to force the spawn-timing curve to end by late May and this resulted in the substantial amount of spawning estimated for Jun. and Jul. When we assumed that few redds would have been present by late June, which corresponds to an end in spawning activity by late May given a survey life of 5 wks. (yellow point in Fig.. 2.8a), the model provides a plausible fit to the Feb.-May data. The revised timing curve peaks at a similar date relative to the "Feb-May data only"-curve, but has a much steeper descending right-hand limb. The revised model predicted a run size of 3,200 redds with 52% excavated prior to Apr. 1. The "Feb.-May data only" fit predicted a run size of 4,200 redds with 42% excavated prior to Apr. 1. The peak of spawning derived from either of these curves was about two months later than the average peak estimated for the 1990's that occurred in late Jan. (Fig. 2.8b). This shift in spawn timing is consistent with anecdotal observations by the Arizona Game and Fish Department and fishing guides (D. Foster, Marble Canyon Fishing Guides, Marble Canyon, AZ, pers. comm..) that the peak of spawning has moved from early-winter to spring.

Alternate assumptions concerning redd survey life and superimposition provided equally plausible fits to the observed change in the total number of redds over survey periods (Fig. 2.9). For example, an assumed survey life of 5 weeks resulted in an estimate of 4,200 redds with 42% being excavated before Apr. 1. In contrast, increasing survey life to 10 weeks produced 2,100 redds with 53% excavated prior to Apr. 1. The effect of increasing the redd

superimposition rate produced a similar type of response to reducing survey life, which was to generate a larger and later run. With an assumed survey life of 5 weeks, increasing the maximum rate of superimposition from SPmax=0 to SPmax=0.8 (with *SPhalf*=1000 and *SPsl*=3) produced 5,600 redds with only 35% excavated before Apr. 1 (Fig. 2.10). Increasing the sensitivity of the superimposition rate to the number of redds present (SPhalf=500) increased the total number of redds to 10,000 and reduced the percentage of redds excavated before Apr. 1 to 31%.

A sensitivity analysis of the effects of survey life and the maximum rate of superimposition on parameters of interest was conducted (Fig. 2.11). Assuming no superimposition, the percentage of redds excavated before Apr. 1 was as low as 42% with a survey life of 5 weeks and as high as 66% with a survey life of 16 weeks. The pre. Apr. 1 percentage ranged from 35% at a maximum superimposition rate of 0.8 to 42% with no superimposition (assuming *SLR*=5 and *SPhalf*=1000). Our 5-6 week estimate of survey life (Table 2.6) implicitly accounts for the effects of redd superimposition, so the sensitivity analysis on survey life alone is of most relevance. A survey life of 4-8 weeks very likely brackets the total range possible, which corresponds to 40-50% of total redds being excavated before Apr. 1.

Intergravel temperatures at Four Mile and Powerline Bars were highly variable and depended principally on seasonal changes in air temperature and the timing of inundation. Maximum daily temperatures at elevations >=10 kcfs at Four Mile Bar in Feb. were higher than those at Powerline Bar and approached the maximum recommended temperature limit for rainbow trout eggs (Fig. 2.12). As the season progressed, differences between sites became more pronounced. Lethal (16 C) temperatures occurred at all elevations >=10 kcfs by Mar. at Four Mile Bar. At Powerline Bar lethal temperatures did not occur until Apr. and then only at elevations >=15 kcfs. Differences in temperature regimes among sites were likely controlled by the ca. 3 hr. delay in the morning rise in discharge at Four Mile Bar (11.6 miles downstream of dam) relative to Powerline Bar (1.3 miles downstream). Under normal operations (e.g., post Apr. 1), flows began to rise by ca. 6:00 am at Powerline Bar and by 9:00 am at Four Mile Bar. This lag provided sufficient time for increased ambient air temperatures

and solar radiation to increase intergravel temperatures at exposed elevations at Four Mile Bar prior to their inundation, but not at Powerline Bar (Fig. 2.13). During the Jan. – Mar. experimental flow period, the morning increase in discharge from Glen Canyon Dam was delayed until 9:00. This delay resulted in lethal temperatures at Four Mile Bar at elevations >=10 kcfs during a month when this would likely not have occurred under normal weekday operations. Intergravel temperatures on Sunday were noticeably different when normal operations resumed on Apr. 1 (Table 2.7). Sunday flows during Jan-Mar. 2003 followed the experimental flow range of 5-20 kcfs, but were steady at 8 kcfs after Mar. 31. The effects of this change were very apparent in the gravel temperatures at both Four Mile and Powerline Bars. Lethal or sub-optimal temperatures at elevations >=10 kcfs were reached at both sites every Sunday after the flow change.

2.3 Conclusions from Redd Hypsometry and Timing Study

The overall effect of the Jan.-Mar. 2003 experimental flow on the mortality of eggs and alevins can be derived by combining data on redd hypsometry, gravel temperatures, and the estimates on the timing of redd excavation. Of the redds excavated before Apr. 1, 25% were above 12 kcfs (Table 2.4) and would been stranded above the water surface when normal operations resumed. The duration of exposure at 12 kcfs prior to Apr. 1 was 11.5 hrs (Table 2.8) and exceeded the 10 hr. duration where total alevin mortality occurred based on field experiments conducted in the Lee's Ferry reach by Montgomery and Tinning (1993) (Table 2.2). Thus, eggs and alevins at 12 kcfs and higher were very likely already dead before the change in flow on Apr. 1. The duration of exposure at 8 kcfs was 9 hrs. Considering the daily application of this exposure frequency and the high intergravel temperatures observed at 10 kcfs in Mar. (Fig. 2.12), it is likely that very little of the egg deposition above 8 kcfs survived until Apr. 1, corresponding to a 36-42% loss (Table 2.4). The loss of egg deposition due to enhanced fluctuating flows up to Apr. 1 therefore ranged from about 25% - 40%. As 50 - 60% of the egg deposition occurred after Apr. 1, these mortality estimates reduce to 10-16% when the entire 2003 spawning run is considered. It should be noted that the post-Apr. 1 egg deposition above 8 kcfs (36%) was likely lost due to lethal temperature effects associated with

Sunday low-flow periods (Table 2.7). The total egg deposition loss due to Glen Canyon Dam operations in 2003 therefore ranged from 30 - 40% and about half of this mortality was a direct consequence of the enhanced fluctuating flows. Strictly speaking, the pre.-Apr 1 mortality at 8-12 kcfs and the mortality after Apr. 1 cannot be attributed to the Jan.-Mar. experimental flow as it would have occurred under normal operations anyways.

Lethal or sub-optimal egg incubation temperatures were reached at all elevations of 10 kcfs and higher at Four Mile Bar as early as Mar. (Fig. 2.12). At Powerline Bar, average maximum temperatures at 10 kcfs and high generally did not become a problem until May. The delay in the morning rise in discharge in Mar. 2003 therefore resulted in increased temperature-related mortality during a period when it would not likely have occurred, except perhaps during Sunday-low flows. However, lethal or sub-optimal temperatures occurring prior to inundation were more severe and regular during the later part of the spawning period (Apr.-May) because elevated air temperatures and solar radiation resulted in higher intergravel temperatures, counteracting the effect of the earlier rise in discharge. Maximum daily intergravel temperatures at elevations of 10 kcfs and higher above 15 C were recorded by Montgomery and Tinning (1993) at 9 Mile Bar. Flows over their study period (Mar. 16-Apr. 7, 1991) generally ranged from 3-20 kcfs on a daily basis, with no restriction on ramping rates. Consequently, the temperature loggers at their study site were usually inundated quite early in the morning and showed little daily variation in maximum temperatures during the weekday. On weekends however, flows generally did not exceed 10 kcfs and resulted in elevated temperatures at the 10kcfs stage and higher. We also observed a 'Sunday-only' temperature effect (Table 2.7) when normal operations resumed on Apr. 1.

The delay in the morning rise in discharge in 2003, while effective at producing lethal or sub-optimal incubation temperatures at downstream spawning locations, was expensive because power was purchased at a higher rate relative to the cost of producing it from Glen Canyon Dam (C. Palmer, Western Area Power Administration, Salt Lake City, UT, pers. comm.). Achieving lethal or sub-optimal gravel temperatures one day per week would likely produce the same overall mortality as achieving such temperatures everyday. It is quite likely that the maximum temperatures we observed in Jan-Mar due to the delay in the timing of the

discharge increase would have occurred on Sunday under normal operations of steady 8 kcfs (Table 2.7). Steady-low flows on Sunday would have the advantages of effecting upstream spawning sites and reducing lost power revenues. As there are a substantial percentage of redds between 5 and 8 kcfs (Table 2.4) a Sunday daytime low flow of 5 kcfs would result in a larger increase in egg and alevin mortality due to temperature impacts.

3.0 Spawning Habitat Preference

Increased flow fluctuations from Glen Canyon Dam implemented in Jan. – Mar. 2003 were in part designed to increase the elevations where rainbow trout would spawn. In theory, higher maximum discharges would lead to increased depth and velocities and shift preferred spawning habitat to higher elevations where daily periods of exposure would be more severe. A proportion of redds deposited at the highest elevations would be completely dewatered following a reduction in the maximum discharge after Mar. 31. Partial or permanent exposure of redds would lead to increased or complete mortality of incubating life stages and potentially reduce the population size of rainbow trout in Grand Canyon.

Physical characteristics of salmonid spawning habitat have been well documented. In Montgomery and Tinning's (1993) review of rainbow trout spawning habitat characteristics, average water velocities and depths ranged from 0.3-1.0 m/sec and 0.3-0.8 m, respectively. There are no estimates of velocity and depth preferences for rainbow trout spawning in the Lee's Ferry reach or Grand Canyon, however a number of studies have examined gravel characteristics in spawning habitat. Kondolf et al. (1989) reported a median grain size (D50) for redds located below Glen Canyon Dam (Four- and Eight-Mile Bars) of 10 mm. The average D50 from four spawning areas in Glen Canyon measured by Angradi et al. (1992) was 46 mm, with sites closest to the dam having coarser material relative to spawning sites located downstream. Site morphology has also been shown to play an important role in determining spawning habitat preference. Many salmonid species have been observed to preferentially spawn where stream water down-wells into the gravel bed. Spawning is often observed at pool tail-outs where the lower water surface elevation of the downstream riffle creates a hydraulic gradient that induces down-welling (Kondolf 2000).

Habitat preference is usually computed as the ratio of the relative utilization of a particular habitat characteristic (e.g. proportion of total redds at depths 0.2-0.4m) to the relative total availability of that condition (Bovee 1982). Preference values for particular conditions that are larger than one indicate preferential use of that condition while values less

than one indicate avoidance. Preference curves are often used in conjunction with discharge-driven predictions of depth and velocity to compute Weighted Useable Area (WUA). WUA is simply the product of the preference for a particular location and the area of that location. In a two-dimensional application, an area is divided into a series of grid cells, and the sum of the product of the area of these cells and their preferences determines the total WUA at-a-site. Predictions of changes in depth and velocity as a function of discharge are used to evaluate how habitat availability changes in response to flow.

In this section of the report we present results that document rainbow trout spawning habitat preference for depth, velocity, and grain size of the bed for in the Lee's Ferry reach. We conducted intensive surveys of substrate characteristics and of depths and velocities across a range of discharges. Interpolated spatial fields of habitat characteristics developed from these data were used in conjunction with site-specific spawning preference relationships to predict how spawning habitat availability would change as a function of discharge from Glen Canyon Dam.

3.1 Methods for Spawning Habitat Preference Study

3.1.1 Methods for Spawning Habitat Preference Data Collection

We measured depth, water velocity, and grain size at Four Mile Bar, Ferry Swale, and Powerline and Pumphouse Bars (fig. 2.1) across an evenly-spaced grid, and over all redds that were identified during the redd surveys. The locations of all habitat measurements were surveyed with an electronic total station equipped with a digital data collector (see Section 2.1.1 for additional details concerning survey methods and accuracy). Measurements of depth and velocity were taken at steady flows of 5, 8, 12, and 20 kcfs. Measurements in shallow areas were made by wading with a Swoffer current meter attached to a topset wading rod. Velocities were taken at $6/10^{th}$ of the total depth and 8 cm off the bottom. For areas that could not be waded, velocities were measured by lowering the impeller of the current meter to $2/10^{th}$ and $8/10^{th}$ of the total depth using a ¾" steel pipe mounted to a sliding attachment at the bow

of a 7m aluminum-hulled motorized boat. It was not always possible to lower the impeller to $8/10^{th}$ of the total depth when water velocities or depths were high. In these cases, the depth of the measurement was usually 1.5 m. The depth of each velocity measurement was always recorded. Total depth was measured with a Lowrance depth-sounder.

Grain size of the bed was characterized using a modified Wolman pebble count. On exposed areas of the bars, a 40-m transect was equally divided into eight 5-m sections. The b-axis for each stone located immediately below the tape at 0.5 m increments was used to classify the particle into one of 18 categories of a modified Wentworth scale (Table 3.1). The starting and ending points of the transect were surveyed and interpolation was used to compute the spatial coordinates at the center of each 5-m section. A 1-m^2 wooden square, equally divided into 81 0.1-m increments, was used to select stones in areas that were not sampled by the transect method. An underwater video camera was used to measure grain size for areas that were submerged at the time of the survey. The video camera was equipped with a topside daylight viewing screen and digital video recording device. Two parallel lasers, located 10 cm apart on top of the camera, provided a horizontal scale for images of the bottom. A short video segment (5-10 sec.) was recorded at each location when the laser points became visible on the substrate. A microphone was used to record a location identifier on the audio track of the videotape. Following the field survey, digital video was downloaded onto a computer in an AVI-format using commercially available digital video editing software. These files were then loaded into a custom-software application (BVIS) to capture a single still image from the video segment for each measurement location (BVIS can be downloaded at http://www.mountainsoft.net). The user identified the laser points on the still image so that the scale of the image could be determined. A transect that intersected the laser points was then automatically drawn across the entire width of the image and divided into 15 equal widths. The b-axis of each stone located at the intersection of the transect and width boundaries was measured by the user and automatically recorded by the software. By measuring stones along an axis where the scale is known, the width of the stones in pixels could be translated into an absolute unit of measurement (mm).

3.1.2 Methods for Analysis of Spawning Habitat Preference Data

Six statistical descriptors were used to characterize particle size on the bed. D15, D50, and D85 refer to the sizes for which 15%, 50%, and 85% of the sample is finer. The geometric mean (DG), the geometric sorting index (SG), and skewness (SK) were computed using the formulas summarized by Kondolf et al. (1989) where,

(3.1) $$DG = \sqrt{D15 * D85}$$

(3.2) $$SG = \sqrt{\frac{D85}{D15}}$$

(3.3) $$SK = \frac{\log(\frac{DG}{D50})}{\log(SG)}$$

Computation of grain size statistics at each habitat measurement location were based on a minimum of 10 measurements for terrestrial surveys and 15 measurements for video surveys of submerged substrate.

Water velocity at specific depths at each measurement location was estimated by assuming a logarithmic vertical velocity profile (Gordon et al. 1994). The slope of the log depth-velocity relationship for each location was computed based on velocity measurements taken at two depths. The average water column velocity at 60% of the total depth, and the velocity 10 cm off the bottom were then computed. The latter estimate provided an index of the velocity that a fish would encounter when excavating a redd. The slope (b) of log depth-velocity profile was also used to compute shear stress (τ, in units of $N*m^{-1}*s^{-2}$) from,

(3.4) $$\tau = \rho \times (b / 5.75)^2$$

where, ρ is the density of water (998 kg/cm^3 at 20 C). With this formulation, critical shear stress is directly proportional to substrate size. For example, a shear stress of 23 Nm^{-1}s^{-2} would be expected to move a substrate particle 23 cm in diameter. The vulnerability of bed movement could therefore be assessed by comparing shear stress with statistics quantifying particle size on the bed (Leopold 1994).

At each survey site, spatial grids of water depth and bottom velocity at specific discharges, and substrate characteristics (e.g., D50), were interpolated from point values using a Universal (linear drift) Kriging algorithm (M. Boeringa, Amsterdam Water Supply, Amsterdan, the Netherlands, unpublished data). A summary of the input data used for these interpolations is provided in Table 3.2. Grid size for the modeled areas at each site was determined based on computational constraints and was 2 m^2, 1 m^2, and 1.5 m^2 for Four Mile Bar, Ferry Swale, and Powerline Bar, respectively. Pumphouse Bar was excluded from the analysis because the there were not enough redds to define habitat preference with any degree of certainty (Fig. 2.3a).

A variety of spatial interpolation routines, including alternate Kriging algorithms (quadratic drift, linear and gaussian) and regularized and tensioned splines were assessed using a cross-validation procedure. Surfaces were interpolated using a random selection of 90% of the data for each of the algorithms being assessed. The remaining 10% of the sample points were then compared to the predicted values to estimate accuracy. Ten random draws were performed from topographic and velocity data at Four Mile Bar. Universal Kriging (linear drift) was the most accurate interpolation algorithm in all cases. The accuracy of interpolated topography and velocity measurements was +/- 5 cm and +/- 4 cm/sec, respectively. Portions of interpolated surfaces of depth and velocity located above the water elevation at the time of the survey, an artifact of the interpolation procedure, were removed by overlaying polygons that defined the waters edge. These polygons were digitized from surveyed points along the waters edge at each site at the four discharge levels. All interpolated surfaces above the waters edge for each discharge were removed.

We needed to determine which cells of the interpolated surfaces of depth, velocity, and substrate contained redds, as preference for any habitat condition depended on the proportion of habitat that contained redds relative to the amount of that habitat condition over the entire site. As depth and velocity interpolations depended on discharge, it was important to select a redd survey where the discharge at which the redds were formed was known. We overlaid the locations of redds from the Mar. survey on to the interpolated surfaces. The Mar. survey was selected because the redd-forming discharge could be better determined relative to later surveys. The vast majority of redds present during the Mar. survey would have been created at either 5 or 20 kcfs as increased ramping rates during the Jan. – Mar. 2003 experimental flow period limited the amount of time at intermediate discharges. Less than 25% of the redds at Four Mile Bar were located at or below 5 kcfs in Mar. (Fig. 2.5) so the other 75% of the redds must have been created at 20 kcfs. At 5 kcfs, submerged redds tended to be in water less than 10 cm deep and we observed no spawning activity at this flow during any of our surveys. Thus, redds located at or below 5 kcfs were very likely created at 20 kcfs as well. At Powerline Bar only a small fraction of redds were located at or below 5 kcfs so it is reasonable to assume that the dominant redd-forming discharge was also 20 kcfs. At Ferry Swale we only observed spawning activity at 5 kcfs during Feb. and Mar. surveys. Fish were unable to hold over most redds at 20 kcfs, very likely due to excessive velocities. Redds created at Ferry Swale prior to Apr. 1 were therefore likely formed at 5 kcfs. The total number of wetted cells at each site at the redd-forming discharge and the number of cells with redds was 10,763/213, 18,028/56, and 4,980/99 for Four Mile Bar, Ferry Swale, and Powerline Bar, respectively.

A linear discriminant function analysis (DFA) was used to determine which habitat variables best classified grid cells into "redd" or "non-redd" groups (Systat 1997). All "redd" cells, and an approximately equal number of "non-redd" cells, selected at random across the entire site area, were used as input to the DFA. Utilization, availability, and preference were computed for the three most important variables identified in the DFA. The number of "redd" and "non-redd" cells among 16 depth (0 – 3 m in 0.2 increments), 10 bottom velocity (0 – 1.8 m/sec in 0.2 increments), and 15 D85 categories (0 – 70 mm in 10 mm increments) were computed for each site at its "redd-forming" discharge. Spawning utilization ($U_{c,i}$) for each

variable type ‘c’ and increment ‘i’ was computed as the ratio of the number of cells with redds at that increment relative to the total number of cells with redds. Total availability ($A_{c,i}$) was computed as the ratio of the total number of cells at that increment relative to the total number of wetted cells in the site. Plots of utilization and availability as a function of the increment value showed continuous relationships with some scatter likely due to small sample sizes for some increments. Utilization and availability relationships were therefore smoothed by fitting a Beta distribution to the data,

(3.5) $$X_{c,i} = YMax \int_0^i \theta_i^{(\alpha-1)} (1-\theta_i)^{(\beta-1)} di$$

where $X_{c,i}$ refers to utilization or availability, α and β are parameters of the Beta distribution that define its shape, θ_i represents the proportional value of the habitat variable that ranges from 0 to 1, and *Ymax* is a scalar. Note that eqn. 3.5 returns the cumulative frequency, thus point densities for utilization and availability for increment ‘i’ were calculated as the difference between adjacent increments (e.g., $X_{c,i} - X_{c,i-1}$). The model was fit to the data by minimizing the sum of squared differences between predictions and observed ratios using a non-linear iterative search procedure.

Spawning habitat preference ($P_{c,i}$) was computed as the ratio of smoothed values of utilization and availability,

(3.6) $$P_{c,i} = \frac{U_{c,i}}{A_{c,i}}$$

Spawning preference values larger than one indicated preferential use of that condition while values less than one indicated avoidance. Linear interpolation was used to predict preference for any continuous depth (D), velocity (V), or D85 value associated with a particular grid cell. Habitat values for each grid cells at specific discharges were derived from the interpolated surfaces of depth, velocity, and D85. The overall spawning preference for each grid cell at a specific discharge was computed as the product of the three variable-specific preferences,

(3.7) $$P = P_D * P_V * P_{D85}$$

Weighted useable area at specific discharges was computed as the product of the sum of the overall preference values of all grid cells and the cell area. Note that the overall preference model assumes that each habitat component acts independently on the overall preference and that there are no interactions among variables. However, the model does not assume that all habitat variables are equally important as variables that show little preference would have values close to one.

3.2 Results from Spawning Habitat Preference Study

Grain size statistics for the stream bed varied across the three sampling sites (Table 3.3). The median grain size (D50) and presence of larger particles (D85) was lower at Ferry Swale compared to the other sites. Powerline Bar had a higher fraction of smaller particles (D15). Grain sizes at Four Mile Bar and Ferry Swale were generally well sorted (low values of SG), but this was not the case at Powerline Bar. All sites showed a negative skew to the particle size distributions indicative of a longer tail extending into finer sediment sizes. Negative skew is a common characteristic of stream gravels used by spawning salmonids (Kondolf et al. 1989). D16, D50, and D86 values reported by Kondolf et al. (1989) for Four Mile and Twelve Mile Bars were 1, 10, and 30 mm, respectively and were considerably finer than the statistics at Four Mile Bar in 2003. This difference could reflect a coarsening of the bed over time or differences in sampling methodology. Kondolf et al.'s statistics were based on substrates collected from the surface to 10-15 cm depth, while the statistics presented in the upper portion of Table 3.3 were based on surface samples only. A limited sample of sediment collected in 2003 using Kondolf et al's methodology (Table 3.3 lower portion) showed that grain size of sediments from 0-15 cm depth were generally lower than the grain size from sediments collected on the surface. Differences in our statistics from previous estimates are therefore partially the result of differences in methods. Surficial grain size statistics defining particle size (D15, D50, D85, DG) were reasonably well correlated with

each other (Table 3.4). Statistics reflecting the shape of the grain size distribution (SG and SK) were not correlated with the other metrics or each other. Correlations among particle size statistics were highest at Four Mile Bar and Ferry Swale where variance in particle size (SG) was low relative to Powerline Bar.

Discriminant functions predicted the presence of redds in grid cells based on habitat characteristics with an accuracy of 76-84% (Table 3.5). The functions explained 59%, 62%, 46%, and 45% of the variance between "redd" and "non-redd" cells for Powerline Bar, Ferry Swale, Four Mile Bar, and all sites combined, respectively. Accuracy was highest at Powerline Bar (84%) and Ferry Swale (79%) and lowest at Four Mile Bar (76%) and for all sites combined (73%). More than half the sample size of the "all sites combined" analysis was made up of cells from Four Mile Bar. As a result, the pattern at Four Mile Bar dominated the pattern for "all sites combined". The models tended to predict more false-positives (cells without a redd incorrectly predicted as having one) than false-negatives (cells with a redd incorrectly predicted as not having one). This pattern could reflect error in model formulation or structure, such as not accounting for interactions among variables or failure to include variables that are important components of spawning habitat preference. An alternate explanation for the large number of false-positives is that some of the quality spawning habitat is under-utilized because there are fewer spawners than there is habitat. Depth, bottom velocity, and D85 were the most important variables for discriminating among "redd" and "non-redd" cells at Powerline Bar and Ferry Swale. Depth and D85 were the most important variables at Four Mile Bar and when all sites were combined. Water depth, bottom velocity, and D85 were selected as the variables to use for habitat preference and WUA computations.

Patterns in total habitat availability varied considerably by site, however, utilization patterns were reasonably consistent. At Four Mile Bar, depths ranging from 0.5-1.25 m were utilized at a rate considerably higher than their overall availability (Fig. 3.1a). Differences between utilization and availability were much subtler with respect to near-bottom velocity and D85. Depths of 0.75-1.25 m were utilized disproportionately relative to their availability at Ferry Swale and there was also strong preferential use of near-bottom velocities ranging from 0.6-0.8 m/sec (Fig. 3.1b). There also appeared to be preferential use of substrates with

D85 values of 20-30 mm. Increased utilization at depths of 0.6 m and 1.2 m was apparent at Powerline Bar (Fig. 3.1c). This is the only case where a bi-modal response in habitat preference was observed and where the Beta distribution failed to capture the habitat relationship. We had to manually alter the Beta distribution for the Powerline Bar depth-utilization curve to provide the fit presented in Fig. 3.1c. At Powerline Bar, we also observed increased utilization at near-bottom velocities of 0.4-0.6 m/sec and for D85's of 20-35 mm.

Spawning habitat preference was somewhat consistent across sites but differences were apparent (Fig. 3.2). In general, depths of 0.5-1.25 m were preferentially utilized (preference > 1). A wider range in preferred near-bottom velocities was observed at Four Mile Bar (0.2 – 0.75 m/sec) relative to Powerline Bar (0.3 – 0.7 m/sec) and there was a preference for higher velocities at Ferry Swale (0.5-1.2 m/sec). Preferential use of particle sizes ranged from 20-30 mm at Ferry Swale and 10-40 mm at Powerline Bar. There was little evidence of preferential use of substrate at Four Mile Bar with the exception that areas with very fine (D85 < 5 mm) or large particles (D85 > 45 mm) were avoided. Differences in preference among sites and among variables within-a-site generally reflected the patterns seen in the discriminant function analysis; Particle size tended to be a relatively unimportant variable at most sites; Depth was an important variable at Powerline and Four Mile Bars; Velocity was a very important variable at Ferry Swale and moderately important at Powerline Bar.

Habitat preference relationships were determined from the ratio of utilization to total habitat availability. The site boundaries of our study sites were delineated based on geomorphic features (gravel bars, pool tail-out, etc.). When comparing preference relationships among sites it is important to realize that site boundaries, which control the distribution of total habitat availability, will affect the preference relationships. It is therefore important to examinee utilization (Fig. 3.3) and availability (Fig. 3.4) relationships when commenting on differences in habitat preference among sites. For example, we saw a noticeable difference in preference for D85 between Four Mile and Powerline Bars (Fig. 3.2c) even though utilization was almost identical (Fig. 3.3c). Differences in the availability of D85 among these sites (Fig. 3.4c) were therefore the cause for differences in preference. It would be wrong to conclude that the preference curve for D85 at Four Mile Bar suggests that

substrate is not an important component of spawning habitat. The correct inference is that D85 is not an important determinant for spawning at Four Mile Bar because the distribution of the material at this site matches the pattern of utilization. The same reasoning explains differences in near-bottom velocity preference between Ferry Swale and Four Mile Bar. The lack of strong preference for near bottom velocity at Four Mile Bar is driven by the fact that the distribution of velocities (Fig. 3.4b) nearly matches the utilization pattern. The availability of highly utilized velocity and substrate conditions at Four Mile Bar is probably a good part of the reason why it is the largest spawning site in the Lee's Ferry reach (Table 2.3).

Spatial patterns in predicted habitat preference at the redd-forming discharges for Four Mile Bare, Ferry Swale, and Powerline Bars were compared to redd locations (Fig. 3.5). The good correspondence between high preference and redd density is not an independent test of the models predictive ability since these same redd locations were used in the calculation of the preference models in the first place. However, one interesting characteristic of the maps are the areas that showed relative high preference coupled with low redd density. This pattern was statistically reflected in the discriminant function analysis through the large number of false-positives (incorrectly determination that a cell contained a redd when it did not). As previously mentioned, this could indicate either underutilization of spawning habitat or incomplete model specification. Highly preferred habitat with low redd densities tended to occur at the downstream ends of the gravel bars of all three sites. Many salmonid species have been observed to preferentially spawn where stream water down-wells into the gravel bed (Kondolf 2000). Down-welling will often be greater at the upstream side of gravel bars where the hydraulic gradient is largest. Upstream portions of the gravel bars may have been preferentially used relative to downstream areas with similar habitat conditions due to the this factor. The spatial pattern in model error may in part reflect failure to include a variable which accounts for variation in down-welling across the bar surface.

Increased discharge resulted in higher total spawning habitat availability at Four Mile and Powerline Bars where suitable spawning habitat was located at higher stages (Fig. 3.5). Increased discharge reduced spawning habitat availability at Ferry Swale where the majority of habitat was located in deeper water. At Four Mile Bar, the total wetted area increased by a

factor of 2 as discharge was increased from 5 – 20 kcfs (Table 3.2) while weighted useable area increased by almost five-fold. At Powerline Bar, total wetted area across this same discharge range increased by 1.4-fold while WUA increased over 9-fold. Increasing discharge at these high elevation gravel bars resulted in a disproportionate increase in spawning habitat availability. More importantly, as discharge increased, the proportion of spawning habitat at higher elevations also increased (Fig. 3.5a and c). Predictions of WUA by stage at the redd-forming discharge of 20 kcfs provided closely matched the observed vertical distribution of redds during the Mar. survey. While this is not an independent test of the model, it is comforting that the vertical distribution of WUA predicted by the models matches the pattern in redd hypsometry. Ferry Swale represented a deep-water redd site where all spawning habitat was below the 5 kcfs stage. At this site we saw little increase in total wetted area with increasing discharge (1.2-fold) and a very large decrease in WUA (4.6-fold). Higher discharges may therefore suppress spawning at deep-water redd sites. In support of this hypothesis, we saw over a 2-fold increase in the number of new redds at Ferry Swale between the Mar. and Apr. surveys (Table 2.5) when maximum daily flows were reduced from 20 to 12 kcfs. Increases in the number of new redds at the other sites over this same time period were considerably lower and ranged from 0.9 to 1.3-fold.

3.3 Conclusions from Spawning Habitat Preference Study

The rainbow trout spawning habitat preference component of this study represents a significant effort relative to the magnitude of habitat use studies conducted in most other river systems. We estimated habitat preference at 3 large sites and characterized depth and velocity fields at four levels of discharge. In other studies, depth and velocity fields are usually estimated using a multi-dimensional calibrated to a single level of discharge. The use of an underwater video camera to quantify particle size on the bed represents a significant improvement relative to other habitat studies where particle size is almost always roughly determined based on uncalibrated visual categorization.

Depths of 0.5 – 1.5 m, velocities of 0.3 – 1 m/sec, and D85 values of 15-45 mm are preferred by rainbow trout spawning in the Lee's Ferry reach. These statistics are reasonably close to the depth (0.3 – 0.8 m) and average velocity (0.3 – 1.0 m/sec) ranges reviewed in Montgomery and Tinning (1993). The D50 estimates of spawning areas in the Lee's Ferry reach reported by Kondolf et al. (1989) and Angradi et al. (1992) of 10 mm and 46 mm, respectively, bound the range of D85 values of sediments that were utilized for spawning in our study. It is important to note that the range of spawning depths we observed in the habitat component of our study underestimates the maximum depth where spawning was observed. In the system-wide redd survey we found many deep-water redd sites (Table 2.3) where the depth of redd locations was 1-2 m and we observed some redds in water greater than 3 m deep. Two inferences can be made from these observations: 1) the depth preference curves we developed from a limited number of sites are not representative of all spawning sites in the Lee's Ferry reach; or b) depth is not the physical variable that trout are using to select locations for spawning. It is possible that locations on gravel bars with shallow depth often have appropriate velocities or grain sizes and/or tend to be in areas where down-welling is greatest.

The spawning habitat preference models developed for the Lee's Ferry reach were useful for evaluating the extent to which increased discharge during the Jan. - Mar. experimental flow period altered the elevations where spawning occurred. Weighted useable area computations showed that higher discharges increased total spawning habitat availability at sites that had available spawning habitat at higher stages such as Four Mile and Powerline Bars, and reduced spawning habitat availability at deep-water redd sites such as Ferry Swale. The model also showed that the stage of spawning at Four Mile and Powerline Bars was increased under higher discharge. Such changes in spawning habitat availability would likely increase the proportion of redds that would be dessicated and the duration of exposure resulting from flow fluctuations. The redd hypsometry study showed that there was a high proportion of redds excavated in deep-water that would not be dewatered at flows as low as 5 kcfs. The large decline in spawning habitat availability at Ferry Swale under high discharge suggests that spawning at deep-water sites could be suppressed through maintenance of high flows. In support of this, we noted a large increase in the number of redds at Ferry Swale after

the maximum daily flows were reduced from 20 to 12 kcfs on Apr. 1 (Fig. 2.5 for Ferry Swale). We are uncertain whether this increase in spawning activity was the result of the flow change effecting spawning habitat availability, or was a normal occurrence driven by seasonal trends in spawn timing. Maintaining high fluctuating flows until the end of Apr. following the peak of spawning would help resolve this uncertainty. In short, there is a large proportion of redds that are formed at stages below 5 kcfs (40-50%) in the Lee's Ferry reach, and we are uncertain about the effectiveness of using high flows to reduce this proportion.

Results from our spawning habitat preference study must be interpreted with caution. We developed preference curves for each site based on a single discharge. When we predicted WUA as a function of discharge we assumed that the preference relationships were stationary with respect to discharge. Other studies have shown that habitat availability-discharge relationships do not always meet this assumption (e.g., Pert and Erman 1994). In many WUA studies there is often an implicit assumption that changes in habitat availability have some type of population-level effect. We have not evaluated whether reductions in spawning habitat availability reduce the total egg deposition in the Lee's Ferry reach or the survival of eggs and alevins. We have avoided this issue by using WUA to determine how discharge potentially influences the stage where spawning occurs. This has relevance for designing flow regimes that are more effective at increasing the percentage of redds which are potentially exposed due to fluctuating flows. We make no claims regarding the linkage between WUA predictions and impacts on recruitment of young trout. These impacts must be assessed through direct measurements such as the redd hypsometry and fry survival components of this study.

The extent of rainbow trout spawning in the mainstem below Lee's Ferry is currently unknown, but is highly relevant for evaluating alternate methods for reducing trout populations in Grand Canyon. Extensive mainstem spawning in Grand Canyon would imply that the source of rainbow trout in Grand Canyon is mostly local and can therefore be controlled by mechanical removal. On the other hand, if the amount of mainstem spawning is very limited, rainbow trout in Grand Canyon must originate from juveniles or adults emigrating from the Lee's Ferry reach. In this case, reducing rainbow trout abundance in Grand Canyon will require continuous mechanical removal efforts or a reduction in the

population above Lee's Ferry. A redd and spawning habitat survey in Grand Canyon will be conducted early-Apr., 2004. Documentation of extensive mainstem spawning in Grand Canyon usurps the need to apply the preference model to downstream locations. However, the model will be useful if water clarity is poor and limits our ability to conduct a thorough redd survey. In this situation, a failure to observe redds may simply reflect poor sampling efficiency. Predictions of habitat availability at downstream locations will then be useful in deciding whether the absence of redds is a due to sampling limitations or lack of suitable habitat. In addition, the utilization curves will be helpful for focusing downstream redd survey efforts.

4.0 Fry Hatch Timing, Recruitment, and Mortality

The increased daily flow fluctuations of the Jan.-Mar., 2003 experimental hydrograph were in part designed to increase the mortality of young-of-year (YoY) rainbow trout. YoY stream-dwelling salmonids prefer near-shore habitats that are typically low-velocity and shallow areas with abundant cover (Montgomery and Tinning 1993). Daily variation in discharge will result in lateral shoreline movement that can cause stranding of juvenile fish, or lead to sub-lethal impacts related to increased stress levels, predation risk, energy expenditure, or reduced feeding opportunities (Cushman 1985). Published data on the impacts of sub-lethal effects of fluctuating flows are limited and must be inferred from studies on habitat use and physiological stress. Vehenan et al. (2002) observed that juvenile brown trout used higher nose velocities with increasing water flow and did not fully compensate for increased energy expenditures by changing microposition. Shirvell (1994) reported that fish initially responded to increased flow by moving closer to the streambed and then, if necessary, by moving laterally to seek out appropriate velocity conditions. Flodmark (2002) showed that daily variation in discharge did not seem to affect fish stress levels when peaking was done frequently.

In contrast to the lack of data on sub-lethal effects of daily variation in discharge on juvenile fish, there are many observations of direct impacts caused by stranding. Factors that control the extent of stranding at a given site include riverbank profile, substrate type, fish size and age, species, time of day, exposure frequency, season, and temperature. The extent of stranding appears to be highest in low-angle habitats with abundant cover (Halleraker et al. 2003). Small brown trout YoY (ca. 50 mm) have been shown to be more vulnerable to stranding than larger juveniles (75-90 mm). Stranding rates tended to increase at lower water temperatures and were highest if the flow reductions occurred during daylight hours (Bradford et al. 1995, Saltveit et al. 2003). A decrease in the down-ramping rate from 60 cm/hr. to 10 cm/hr was shown to reduce stranding of brown trout YoY by 50% (Halleraker et al. 2003). For reference, the down-ramp rate in the Lee's Ferry reach during the Jan.-Mar., 2003 experimental flow period was approximately 15 cm/hr. Stranding rates have also been shown

to increase following a long habituation time at steady flows (Halleraker et al. 2003). Stranding of small juveniles (ca. 50 mm) may be difficult to observe in the field. A 1-hr. search of a 75 m^2 area by two technicians found less than 40% of the total fish known to be stranded in an enclosed area (Saltveit et al. 2003).

Measuring the effect of fluctuating flows on factors that have direct impacts on regulating population size, such as survival and recruitment, is challenging. In this study, we measured changes in length-frequency and relative abundance of YoY rainbow trout over the summer and fall through monthly sampling. We also analyzed the microstructure of otoliths from a subsample of fish to establish a length-age relationship. The combined data were used to define the seasonal timing and magnitude of hatch that can be used to better-define the window for future flow regimes targeted at reducing YoY survival. Estimates of seasonal trends in hatching inferred from fry surveys were compared to estimates of the timing of egg deposition from redd surveys to evaluate the effectiveness of flows targeted at reducing egg survival. For example, the failure of eggs deposited early in the spawning season, when fluctuating flows were increased, to show-up as fry in subsequent months, would indicate that the fluctuating flows reduced egg or alevin survival relative to rates that occurred under normal operations later in the year. Finally, length-frequency data and information on size-at-age was used to estimate the apparent survival rate of YoY in their first ½ year of life when they are likely most vulnerable to flow effects. The term 'apparent' is used because the survival rate that is estimated is not the true survival rate, but an index of the rate that depends on a number of factors including: size-dependent migration of fish out of the sampling area; gear-dependent size-vulnerability relationships; size-based differences in the distribution of fish among habitat types; and the distribution of effort across habitat and gear types. As we have no reason to believe that any of these factors would change over the sampling period or among years, differences in the apparent survival rate through time provide an index of the change in the true survival rate. Changes in the apparent survival rate within-season and across years can be compared to operational changes from Glen Canyon Dam to improve our understanding of how fluctuating flows can be used to regulate rainbow trout abundance.

4.1 Sampling and Analytical Methods for Young-of-Year Study

The YoY study in 2003 consisted of three major components. Field survey methods are described in Section 4.1.1. Analysis of otolith microstructure was used to estimate YoY age and make inferences on effects of fluctuating flows on growth. Methodologies for this analysis are described in Section 4.1.2. Estimates of recruitment and survival rate were based on a model combining ageing and field survey data. The model and related analytical methods are described in Section 4.1.3.

4.1.1 Methods for Young-of-Year Field Surveys

Rainbow trout YoY were sampled from twenty randomly selected 30 m sites on a near-monthly basis from Jun.-Oct., 2003 (Table 2.2). Limited sampling efforts conducted in Apr. and May were used to refine capture techniques and provide fish for development of daily ageing methods. Site selection was limited to potential fry habitat and included low angle cobble bars and vegetated or sandy shorelines as well as one low angle talus shoreline site. We initially avoided sites comprised of steep talus shorelines as we felt they would not be used by young fry and were challenging to sample by backpack electrofishing at night. We added 6 steeper talus shoreline sites in the Sep. and Oct. sample periods to account for some very noticeable changes in fish distribution and density. We performed most analyses on both sets of sites and refer to them as the "Original 20"and "Original 20 + 6" sets.

Upon arrival at a site, a 30-meter length was measured with a survey tape and the upstream and downstream limits were marked with fluorescent glow sticks. Starting at the downstream end of the site, two fisheries technicians systematically worked their way upstream catching all fish within 2.5 meters from the shoreline using a backpack electrofisher. Electrofisher settings were standardized at 100 Volts, a frequency of 80 Hz, and a pulse width of 8 msec. All sampling was conducted at night at the minimum discharge, which usually occurred between 23:00 – 6:00. A Q-beam spotlight (ca. 1 million candlepower) was used to illuminate the area in the vicinity of the anode. Every effort was taken to ensure that thoroughness and technique were consistent among sites and sample periods. On average, 10

minutes of electrofishing effort over a 15 minute period was required to fish a 30 m site. Upon completion of sampling at each site, the forklengths of all fish were measured to the nearest mm and the majority of fish were released at the downstream end of the site. A subsample of fish were retained for ageing.

The use of a boat electrofisher to sample YoY fish potentially has a number of advantages over backpack electrofishing. First, the increased power of a boat electrofisher (max. of 5000 Watts) relative to a backpack unit (max. of 600 Watts) increases the size and strength of the electric field and would therefore capture more fish per unit time. This in turn would increase the precision of length-frequency determinations. Second, a boat electrofisher is a more efficient, easier, and safer method for capturing YoY in steep shoreline habitats. This is particularly important for the 2004 study below Lee's Ferry where such habitat types are quite common. We therefore performed a small comparison of catch rates and size distributions of fish captured by boat and backpack electrofishers. On Oct. 26, 2003 we sampled 4 talus shorelines sites and two vegetated/sandy shorelines sites in the Lee's Ferry reach using both backpack and boat (Achilles) electrofishers. Each site was 75 m long with the lower 30 m and upper 45 m sections being sampled by backpack and boat electrofishers, respectively. All sampling was conducted at night (21:00 to 2:01) at near minimum flows.

4.1.2 Methods for Analysis of Otolith Microstructure for Ageing YoY Fish

A subsample of YoY fish captured on each trip were preserved in 95% ethanol and sent to a laboratory (www.mar.dfo-mpo.gc.ca/science/mfd/otolith/) for examination of otolith microstructure. The otoliths of teleost fish contain growth increments that are deposited with a daily periodicity (hence the term "daily ring"), thus providing precise age and growth information through much of the first year of life (Campana and Nielson 1985). Fish selected for ageing were randomly subsampled from the total catch on each survey using a length-stratified design: within each sample period 10 fish were selected at random from those available in each 10-mm length category. We sampled at non-random locations to meet the target sample size for each 10mm length category if we failed to meet the target based on the 20 randomly

selected sites. Approximately 25% of the total number of fish captured across sampling trips were aged.

The forklengths of preserved fish were measured in the laboratory prior to dissection. Both sagittal otoliths were removed from each fish and mounted individually on microscope slides in cyanoacrylate glue. Otoliths were polished close to the mid-plane, flipped and re-glued, then polished to the growth plane with 30 µm and 3 µm lapping film, as per established procedures (Stevenson and Campana 1992). All otoliths were examined at a magnification of 400-1250x under a compound microscope. Using the well-defined hatch check as a reference point, daily increments between the hatch check and edge were counted 2-4 times in at least one otolith of each pair (Campana 1992). The resulting count was recorded as the age from hatch to capture.

To determine otolith growth since the time of hatch, the otolith growth axis from the hatch check to the edge of the otolith was measured along the longitudinal axis. Measurements (± 1 µm) were made with an image analysis system working at a resolution of 1280 x 1024. A check and that may have corresponded to emergence was occasionally observed; however, the interpretation of this check was often ambiguous, so increment counts and otolith measurements between hatch and emergence, and between emergence and the edge, were only performed for a random subset of 50 otoliths.

A von Bertalanffy model was fit to the length - age data using a non-linear iterative search procedure. The form of the von Bertalanffy model was,

(4.1) $$L_{iage} = L_{\infty} * 1 - e^{-K*(iage - t_0)} + \nu$$

where L_{iage} is the predicted forklength (of preserved fish measured in the laboratory) at age *iage* (days from hatch), K is the Brody growth coefficient (a measure of the rate at which growth rate declines with age), L_{∞} is the asymptotic length, t_0 is the predicted age at which fish length is zero, and ν is a normally distributed error term with a standard deviation σ_{fl}. The seasonal trend in egg hatch was estimated by predicting the age of each fish that was captured

from Apr. – Oct. sample periods (n=991) based on their forklengths measured in the field. Age was subtracted from the date of capture to estimate the date of hatch. A random subsample of 90 fish were measured in the field, preserved individually in 95% ethanol for 1 month, the ca. time between preservation and otolith extraction, and then re-measured in the laboratory. The correlation between preserved and live forklengths was extremely high (r^2 = 0.997) and shrinkage of preserved fish averaged only 1%. We therefore did not bother to account for the effects of shrinkage when back-calculating age based on forklengths measured in the field.

A striped pattern in increments was observed on the otoliths of many individuals. This visual pattern was identified from the presence of atypical daily increments (different appearance, usually light in color) formed every 7 days. For all otoliths, the presence or absence of the striping pattern was recorded. The number of otoliths where the presence of a striping was ambiguous was also recorded. To determine if the 7-day striping pattern was associated with periodic growth, a random sample of otoliths (n=15) containing clear striping patterns were examined and digitally photographed at a microscopic magnification of 600x under oil immersion. Given the 1280 x 1024 resolution of the image analysis system, measurement accuracy was ~ 0.1 µm. The width of individual daily increments was measured as the distance between the midpoints of adjacent D zones (terminology of Kalish et al. 1995). Measurements were made perpendicular to the local growth axis, beginning at the D zone just medial to the white stripe, and proceeding distally. Increment sequences were measured only if every increment of the 7-day striping cycle was clearly defined.

The validity of daily increment counts as accurate age indicators in young fish is well established (Campana and Neilson 1985). However, to insure accuracy in this application, we compared estimates of age derived from otoliths for a small sample of hatchery YoY where age was precisely known. As part of a normal hatchery operation, wild spawning rainbow trout were removed from their natal stream (Blackwater River, BC) and spawned in a B.C. hatchery on May 13, 2003. Eggs were reared under constant temperature (7 C) and moved to a feeding trough (10 C) at swim-up. Fish were sampled from the trough at 31 and 84 days after hatching and preserved in 95% ethanol. Otoliths from these fish were removed and the known

number of days from hatch to sampling was compared to the estimates derived from the daily ring counts between the hatch check and the otolith edge. This was a blind-analysis as the age of fish was unknown to the technicians at the time they examined the otoliths.

4.1.3 Methods to Analyze Catch and Age Data

A stock synthesis model was used to estimate seasonal trends in the number of fry-at-hatch (hereafter referred to as fry recruitment) and the apparent mortality rate from the length-frequency and ageing data. The model predicted the number of fish alive for 45 weekly cohorts ($N_{iage,t}$) from Jan. through Oct. based on the equation,

$$N_{iage,t} = N_{iage-1,t-1} * e^{-M} \tag{4.2}$$

where, t is the number of weeks from start of the simulation, *iage* is the age of a fish in weeks from hatch, and M is the instantaneous mortality rate. The weekly survival rate, S is equal to e^{-M}. Mortality was represented by a single parameter under the assumption that it was constant over weeks and across ages, or was represented by a vector of parameter values for more complex models that accounted for changing mortality over time or with age (e.g., $M_{iage,t}$).

To model age-specific differences in mortality, fish size (predicted from eqn. 4.1) was used in the allometric relationship between natural mortality and body length (Lorenzen 2000),

$$M_l = M_r * (\frac{l}{l_r})^c \tag{4.3}$$

where M_l is the instantaneous mortality rate at forklength l, M_r is the mortality rate at reference forklength l_r, and c is the allometric exponent of the mortality-length relationship. We assumed that c = -1 following Lorenzen's (2000) analysis based on stocking experiments of salmonids of various sizes, Note that c = 0 can be used to simulate the case where mortality

does not change with size ($M_r = M_l$). The reference forklength was assumed to be 50 mm and M_r (or $M_{r,t}$ for the variable survival-over-time model) was estimated from the data.

The recruitment of fish to each weekly cohort of the YoY population, which is equivalent to the number of eggs that hatch per week ($N_{1,t}$ from eqn. 4.2), was estimated using three alternate methods:

1) Time-independent recruitment estimates for all 45 weeks of the simulation period;
2) time-dependent estimates of weekly recruitment based on the assumption that the seasonal trend in weekly recruitment can be approximated using a beta distribution; and
3) back-calculation of the shape of the seasonal trend in recruitment from the combined catch and length-at-age data (see Section 4.1.2) with the overall magnitude of recruitment estimated by the stock synthesis model. To derive the shape of the seasonal trend, the back-calculated egg hatch trend over time was fit using a Beta distribution.

The beta-distribution used to model seasonal recruitment trends for methods 2) and 3) was,

$$R_t = R_{\max} \int_{t-1}^{t} \theta_t^{(\alpha r - 1)} \left(1 - \theta_t\right)^{(\beta r - 1)} dt \,, \tag{4.4}$$

where R_{max} is the maximum number of eggs hatching per week over the entire simulation period, and αr and βr are parameters of the Beta distribution that define the timing of hatch. θ_t represents the proportional date of hatch and ranges from 1/45 on the first possible week of hatch (beginning on Jan. 1) to 1 on the last week T (beginning on Oct. 29), that is $\theta_t = t/T$.

The age-frequency computed by the model for each week based on recruitment and survival estimates was translated into a corresponding set of weekly length-frequencies based on the von Bertalanffy growth model parameterized from the otolith microstructure analysis (eqn. 4.1). The error term in the von Bertalanffy (σ_{fl}) model was used to predict the length-

frequency distribution for each weekly age. Within a cohort, the number of fish in a particular length bin was comprised of fish from a range of weekly ages.

We assumed that vulnerability to capture was a sigmoid saturating function of fish size,

(4.5) $$V_{fl} = \frac{fl^s}{FL_h + fl^s}$$

where, *fl* specifies the 5 mm increment forklength category, V_{fl} is the forklength-dependent relative vulnerability (0-1), Fl_h is the size at which the fish are half as vulnerable as larger, fully vulnerable fish, and '*s*' is a "steepness" parameter for the function (higher values of '*s*' imply a "knife edge" change in vulnerability near size Fl_h). Parameters for this function (Fl_h = 30 and *s*=10) were estimated based on observations of the numbers of fish that evaded capture. The model was parameterized so that fish below 20 mm were completely invulnerable, 30 mm fish had a vulnerability of 50%, and 40 mm fish were completely vulnerable. Vulnerability parameters were assumed to be constant across sampling periods. The simulated length-frequency was translated into an observed length-frequency by multiplying the predicted numbers of fish in each 5 mm forklength category by their assumed vulnerabilities.

The model was fit to the Jun. – Oct. 2003 length-frequency data by estimating the apparent mortality rate(s) and weekly recruitment parameters. We assumed the error in the model followed a Poisson distribution (Hilborn and Mangel 1997),

(4.6) $$P\left(k_{ifl,t} \middle| R_{iwk}, M\right) = \frac{e^{-p_{ifl,t}N_t}\left(p_{ifl,t}N_t\right)^{k_t}}{k_{ifl,t}!}$$

Eqn. 4.6 computes the probability of the recruitment (R_{iwk}) and mortality rate(s) (M) parameter estimates based on the observation of catching *k* fish in the *ifl*th 5-mm length category on week *t.* The total catch for week *t* (N_t) and the proportion of the total catch in length category *ifl* ($p_{ifl,t}$) in that week were predicted by the model as a function of the parameter estimates. A

non-linear iterative search procedure (Solver as implemented in EXCEL) was used to minimize the sum of the negative log-likelihoods of eqn. 4.6 across all length categories and sample periods. The log-likelihood, Ln(L), for a single length category and period is,

(4.7) $$\ln(L) = -p_{ifl,t} N_t + k_{ifl,t} (\ln(p_{ifl,t}) + \ln(N_t))$$

Six alternate models were fit to the observed length-frequency data based on different assumptions regarding recruitment and survival dynamics. Three different models were used to simulate the weekly recruitment of hatching fry (time independent weekly values, time-dependent weekly values modeled using a Beta distribution, and the back-calculated fry recruitment pattern where only the overall magnitude of recruitment is estimated by the stock synthesis model). The weekly mortality rate was either held constant over the simulation period or could vary by month. The simplest model consisted of 1 parameters defining recruitment and one parameter defining the overall weekly survival rate. The most complex model consisted of 45 weekly recruitment estimates and 10 individual monthly survival estimates (n=55). The stock synthesis model was fit to the length-frequency data collected from the 20 original sample sites only, which were predominantly low angle cobble bars and vegetated or sandy shorelines. We did not include data from the additional six talus shoreline sites sampled during the last two sample periods. The data suggest an ontogenetic habitat shift from low angle habitats to talus shorelines (see Section 4.2.1) as YoY grow. Including data from these additional six sites would introduce bias into estimates of recruitment and survival due to changes in sampling.

We used a likelihood ratio test to evaluate the statistical reliability of increasingly complex models. Twice the difference between the log-likelihood values from two different models has a Chi-square distribution with the degrees of freedom equal to the difference in the number of parameters between models (Hilborn and Mangel 1997). A more complex model would be considered to be significantly better than a simpler model if twice the difference in log-likelihoods among models exceeded the threshold Chi-square value at the specified Type I error level (e.g., $\alpha = 0.05$).

As we did not attempt to estimate an overall catchability for the Lee's Ferry reach when fitting the model, the sum of the predicted recruitment rates over the simulation period represents the number of hatched eggs required to fit the sample catch. A reach-wide YoY population estimate could be derived by scaling-up the abundance of fish at any age by a factor that accounts for both the proportion of the total habitat that was sampled as well as the proportion of fish in the sampled areas that were not caught. As we did not use a multi-pass depletion approach in enclosed areas to capture fish, we have no way of estimating the latter proportion and therefore do not present estimates of reach-wide YoY population size.

4.2 Results from Young-of-Year Sampling and Analysis

4.2.1 Results from Young-of Year Field Survey

Our initial efforts to capture fry by backpack electrofishing during the Apr. and May sample periods were not very successful. We fished during night and day, but always at relatively high flows (e.g. 8:00 – 22:00). In Apr., the few fry we were able to capture were very small (< 30 mm) and always located in the immediate vicinity of submerged redds. At this time we assumed that our lack of success at capturing fry was because very few fry had emerged. Based on our observation that very few redds were present during our pilot redd survey conducted in late Jan., this was a reasonable assumption, as there would be a minimum two month lag between the time of spawning and the time when we could capture emerging fry assuming 30 days spawn-to-hatch and an additional 30 days for emergence. Our May redd survey was conducted over the Memorial Day long-weekend when flows were held steady at 8 kcfs for aerial photography. Test sampling for YoY during steady flows revealed that many small fry were present, and we obtained a sufficient sample for otolith analysis. We decided to perform representative fry sampling at 20 random locations immediately following the long-weekend when flows returned to normal operations for that month (7.5-13.5 kcfs) as we suspected that flow and daily flow variation could effect catchability, and we wanted catchability in May to be comparable with subsequent sample periods. In spite of considerable effort, we were unable to catch fry on May 27 when discharge was increased to ca. 13 kcfs. At

this point we realized that fry must not be following the waters edge on a diurnal basis as discharge was increased, but instead must have been holding near the minimum daily stage (7.4 kcfs in May). All future sampling was therefore conducted at night at the daily minimum flow. Fish collected in Apr. and May were useful for ageing purposes, but mean size and abundance estimates derived from these fish cannot be compared with those in subsequent months because of differences in sampling methodology.

As expected, fish size increased over the summer and fall while density generally declined (Table 4.1). Talus shorelines had much higher densities compared to lower angle habitats (cobble bars and vegetated/sandy shorelines) and tended to attract or support slightly larger fish. A considerable reduction in density and the percentage of sites with fish present was evident between the late-Jul. and early-Sep. sampling periods in low angle habitats.

The longitudinal distribution of fry across sites showed a strong seasonal pattern (Fig. 4.1). Highest densities were observed at the most upstream sites during the Jun. sample period. In Jul., densities in the upper portion of the Lee's Ferry reach were somewhat reduced and higher densities were observed at the lower end of the reach. This could be indicative of either earlier spawning at upstream locations (Fig. 2.3) or downstream dispersal. By the Sep. sample period fry distribution based on the original 20 sites (i.e., low angle habitats) was essentially limited to the lower 2.5 miles of the Lee's Ferry reach. We added an additional 6 talus shoreline sites to our sampling program beginning in Sep. when we observed the dramatic decline in fish numbers in low angle habitats. When we include these additional sites in the analysis (Fig. 4.1b), fry were present in the upper river in Sept., but only in steeper talus shoreline habitats. The Oct. spatial distribution of YoY was very similar to that observed in Sept. The monthly length-frequency samples from the 20 original sites for Jun., Jul., Sept., and Oct. had modes of 25-30 mm, 40-45 mm, 55-60 mm, and 65-70 mm, respectively (Fig. 4.2).

The boat electrofisher was generally more efficient at capturing YoY relative to the backpack electrofisher, but differences depended on habitat type and fish size (Table 4.2). A 45 m site, on average, took ca. 14 minutes to sample using 700 seconds of backpack

electrofishing effort, In contrast, the same site sampled by a boat electrofisher took about half as long to sample in terms of both time (6 minutes) and electrofishing effort (350 seconds). At sites that were fully accessible to the boat (3.5 Mile, 4 Mile, 7 Mile, near Waterholes Canyon), the boat electrofisher caught 2- to 6-fold more fish compared to the backpack electrofisher. At sites that were very shallow where only ca. 50-75% of the site was accessible to the boat (6 and 9 Mile), catches with the backpack electrofisher were equal or higher compared to the boat electrofisher. Catches were also higher with the backpack electrofisher at a site with a sandy/vegetated bottom as the hand-held anode was very effective at 'straining' stunned fish from submerged vegetation and algae. Average fish size captured with the boat electrofisher was consistently larger by ca. 10 mm at all locations except one site (9 Mile) that was only partially accessible to the boat.

4.2.2 Results from Analysis of Otolith Microstructure

The otoliths of 266 YoY rainbow trout captured between Apr. – Oct. sample periods were extracted and successful age determinations were made for 237 of these fish. Age determinations were not possible for 29 fish due to difficulties encountered during preparation (otolith cracking or chipping) or for larger fish where counting increments became difficult to distinguish. Age estimation in fish > 50 mm of length was noticeably more difficult than for smaller fish, and fish >80 mm were very difficult to age reliably. For that reason, some ages for larger fish were not obtained, and replicate age estimates for larger fish were more variable than those for smaller fish. In contrast, the precision of otolith radius measurements was unaffected by fish size.

Hatch checks were clearly evident on all otoliths (Fig. 4.3). Emergence checks tended to be subtler and could not always be identified, thus age was determined relative to the hatch date. A major white band was observed in more than half (54%) of the total number of otoliths examined. The white band was often characterized by narrowing growth increments of low visual contrast, which increased in width and contrast immediately distal to the band. A prominent check was often, but not always, associated with the band. The band was present in all collection months, but was usually seen only in fish above 30 mm in length. Bands near

the edge of the otolith were difficult to identify because of their position. The position and age of formation of the band was measured in 52 fish from various sample periods and size categories. The age from hatch at which the white band was formed averaged 39 days and was highly variable (95% confidence limits of +/- 20 days). The average size of fish at the time the major white-band was formed, determined from length back-calculation using the best-fit von Bertalanffy relationship (eqn. 4.1), was 25 mm (+/- 7 mm). The width of the band averaged 3-10 days. In the Lee's Ferry reach, fish between 25 and 28 mm often showed remnants of a yolk sac. Rainbow trout require two to six weeks to emerge following hatch (Moyle 2002, McEwan and Jackson 1996). The average number of days between hatch and the formation of the major white band corresponds to the upper-end of emergence time requirements from the literature. The white band could therefore represent the transition period between yolk-sac absorption and first-feeding.

There was little error in the estimation of days from hatch based on a blind-test using hatchery fish of known age (Fig. 4.4). The estimated age of hatchery fish averaging 28 mm (n=11) in length sampled 31 days after hatch on Jul. 24, 2003 ranged from 30-36 days with an average of 32 days. The estimated age from hatch for fish averaging 52 mm in length (n=10) sampled 84 days after hatch on Sep. 15, 2003 ranged from 73-89 days with an average of 82 days. The precision of the daily age from hatch was ca. +/- 7 days for larger fish and +/- 2 days for smaller fish.

There was a very strong relationship between forklength and daily age from hatch (Fig. 4.5). The best-fit von Bertalanffy relationship had parameters K=0.0035 (per day), L_{∞}= 150 (mm), and t_0 = -14.06 (days) and explained over 87% of the variation in forklength (n = 237). No seasonal trend in mean size-at-age was apparent. The absolute amount of variation in size-at-age increased with age but the relative variation remained constant (CV = 11%). YoY less than 80 mm grew on average 2.2 mm/week, equivalent to 10.3 mm/month or 0.3 mm/day. Very young fish 5-10 weeks from hatch grew ca. 3 mm/week while older fish 30-35 weeks from hatch grew at ca. ½ this rate.

In 2003 the majority of hatching occurred between mid-Mar. and late-May with a peak in late-Apr (Fig. 4.6). A spawn-timing curve was derived from the hatch-timing curve by assuming a 30-day egg incubation time. Incubation time was estimated based on intergravel temperature measurements from the Lee's Ferry reach in 2003 and literature values on the required number of thermal units from fertilization to hatch (Table 4.3). The peak of this fry-derived spawn-timing curve was close to the peak spawn of the curve derived from the redd count data (Fig. 4.7). The redd-based spawn-timing curve fit to the Feb. – May redd survey data suggests that there was considerably more spawning in Jun. and Jul. than implied by the fry-derived curve. This could indicate either: a) considerably higher egg or fry mortality for fish spawned later in the year, or b) overestimation of the late-spawning component based the redd data. While we observed many redds during our late-May survey, little spawning activity was seen. When we fit the spawn-timing curve to the observed redd count data with the assumption that spawning was complete by the end of May (Fig. 2.8a), the fry- and redd-derived spawn-timing curves are in closer agreement. However, because the modified spawn-timing curve is based on anecdotal information, we cannot determine which of the two hypotheses is more likely.

A weekly striping pattern was evident in at least 51% (131) of the 255 otoliths that were examined (Fig. 4.8). The striping pattern was ambiguous in 14% of the otoliths (36). In general, striping was most evident in the middle and outer sections of the otolith, and in larger individuals. However, since the striping pattern was only obvious when several consecutive cycles were present, it is probable that additional otoliths from smaller fish had the pattern, but could not be identified. Of the 15 daily increment sequences measured in striped otoliths, all but 3 spanned more than 1 week. The atypical increment formed every 7 days tended to be 25% wider (3.12 microns) compared to the other increments (2.51 microns) when averaged across all striping cycles and fish, and the difference was statistically significant (Table 4.4). Within fish, the average increment width for the atypical bands was larger than the average width of the other increments in 14 of 15 cases, and the differences were often statistically significant when sample size for atypical increments was adequate.

4.2.3 Results from Stock Synthesis Model

The stock synthesis model was able to provide good fits to the observed monthly length-frequency distributions (Fig. 4.9). Increasingly complex models that allowed time-independent weekly recruitment and/or variable survival rates across months explained the most variation in the data. The most likely estimate of the weekly survival rate ranged from 0.88 to 0.90 across alternate recruitment models when the survival rate was assumed to be constant over the simulation period (Table 4.5). All constant-survival models tended to over predict the number of fish present in the 45-75 mm length categories on the Sept. sample period (Fig. 4.9). The extent of this discrepancy decreased with increasingly complex recruitment models because a more dynamic recruitment pattern could help compensate for an apparently anomalously low survival rate that occurred between the late Jul. and early Sep. samples. All recruitment models showed a large decrease in the survival rate between the Jul. and Sep. sample periods when survival rate was allowed to vary by month (Table 4.5). We cannot determine if the seasonal trend in survival rate, or the discrepancy between observations and predictions in Sep. under the constant-survival model, are the result of increased mortality between late-Jul. and early-Sep., or alternately, displacement from low angle habitats in Aug./earl-Sep. followed by recolonization of these habitats in Oct.

The time-independent recruitment model did not result in a statistically significant ($\alpha = 0.05$) improvement in fit relative to the model where recruitment was simulated using the best-fit Beta distribution (Table 4.5) when survival rate was held constant. However, for the constant-survival model, the weekly recruitment model produced a significantly better fit compared to the back-calculated recruitment model ($p<0.001$). There were no statistically significant improvements among increasingly complex recruitment models when survival rate was allowed to vary by month. Inflexibility in recruitment dynamics associated with simpler models could be compensated by the variable survival rate, resulting in little difference in likelihoods (Table 4.5). Thus, recruitment rates and survival are confounded when survival rates are allowed to vary over time. Within recruitment models, allowing survival rate to vary by month always resulted in a statistically significant improvement in fit ($p < 0.005$) relative to the models where survival rate was held constant.

The constant weekly survival estimate was very precisely defined and its precision was not dependent on the form of the recruitment model. 95% confidence limits were 0.88 +/- 0.015 for time-independent and best-fit Beta distribution recruitment models (Fig. 4.10). The shape of the likelihood profiles for these two models was virtually identical even though the absolute value of the likelihoods for the more complex model was lower. As confidence limits are based on the difference between the minimum negative log likelihood and other values, identical shapes of the likelihood profiles for the two recruitment models meant that confidence limits were also identical. Survival rate and recruitment would have been completely confounded if only one length-frequency sample was collected. With multiple sampling episodes, survival rate had to explain differences in the same weekly cohorts through time and was therefore somewhat independent of the estimated recruitment rates. For example, estimates of very large recruitment values would force the model to estimate a low survival rate to fit the length-frequency data from the first sample period. The low survival rate would then under predict the abundance of these fish as they recruited to larger size classes in the next sample period and would therefore be considered improbable.

Predictions of seasonal recruitment trends were dependent on the flexibility in the recruitment model. When survival rate was held constant, the time-independent weekly recruitment model predicted a strong recruitment peak in early May (Fig. 4.11) to produce the strong cohort of 25-35 mm fish captured during the late Jun. sample period (Fig. 4.2). The length-age model predicted that it took 8 weeks to reach 30 mm from hatch, which was the length of time between the early May recruitment peak and the late-Jun. sample period. The time-dependent best-fit Beta distribution recruitment model produced a recruitment trend that was essentially a smoother version of the time-independent one with a slightly earlier date of peak hatch. The back-calculated recruitment trend produced a peak hatch near the same date as the time-independent weekly model. The fixed shape of the back-calculated model produced lower recruitment rates in Mar. and Apr. relative to other recruitment models that in turn resulted in a slightly higher estimate for the constant survival rate (Table 4.5). When survival rate was allowed to vary, recruitment trends could not be estimated reliably as they were completely confounded with survival rates.

4.3 Conclusions from Analysis of Young-of-Year Data

The stock synthesis model applied to length-frequency data from monthly sampling provided a very accurate estimate of the apparent weekly survival rate for YoY rainbow trout in the Lee's Ferry reach. Increasing variation in size-at-age for older age groups tends to 'smear' year-to-year variation in recruitment and survival estimates developed from annual length-frequency datasets. In this application, the relationship between length and age derived from analysis of otolith microstructure was very precise and the model was applied over a relatively short time period (10 months). This minimized the typical 'smearing' problems associated with many length-frequency analyses and led to a precise estimate of the weekly survival rate. The sampling and analytical approach can therefore be used to estimate apparent survival rates in subsequent years under different GCD operations as a means for evaluating the effectiveness of flows targeted at reducing survival rates of rainbow trout YoY. The methodology will likely be able to detect smaller effects induced by dam operations than the current adult monitoring program that is subject to greater smearing effects. The YoY methodology also produces a signal in the same year as the experimental treatment. In contrast, 2-3 years are required before recruitment and survival effects on YoY manifest themselves in the adult population.

The constant-survival rate model over-predicted the abundance of most size classes of YoY during the early-Sep. sampling period. This suggests that the survival rate between the late-Jul. and early-Sep. trips was somewhat lower than the average rate for the rest of the summer, or that there was a displacement of fish from low angle habitats between these two periods. A key flaw in our sampling design was poor representation of steeper shoreline habitats during early sampling periods. We did not anticipate that YoY trout would utilize these habitats in their first 6 months of life. Without a consistent representation of these habitats across all sampling periods, we were not able to determine if the dramatic change in density in low angle cobble bars observed in early-Sep. was the result of mortality or migration to steeper shorelines. We plan on remedying this flaw in the 2004 YoY sampling

program by using a combination of backpack and boat electrofishing in low angle and steeper habitats, respectively. We have shown that backpack shocking was most effective in very shallow habitats utilized by the smallest component of the YoY population. Boat electrofishing was more efficient in deeper habitats such as steeper talus shorelines, but tended to select for larger fish. As both gear types must be used to efficiently sample all habitat types, it is critical that they are consistently applied over sample periods in terms of the proportion of sites sampled by each method and the habitat types where they are utilized.

The dramatic change in YoY density in low angle cobble bar habitats between the late-Jul. to early-Sep. sample periods could have been caused by the large change in the minimum flow from 10 to 5 kcfs that occurred after the labor-day weekend (Table 2.2). There is a considerable body of literature documenting the effects of short-term changes in flow on stranding of juvenile salmonids. Stranding rates are highest for very young fish and in low angle complex habitats such as the cobble bars and vegetated shorelines. Low angle habitats (vegetated shorelines associated with sand bars, debris fans, and cobble bars) constitute over 55% of the useable shoreline length in the Lee's Ferry reach (cliff areas excluded), with steeper talus shorelines making up the remaining 45% (Steve Mietz, GCMRC GIS database, Flagstaff, AZ., unpublished data). Imposing a large mortality event in low angle habitats by sudden changes in the minimum flow could therefore cause a considerable impact to the population as a whole. Stranding rates have also been shown to be highest following a long habituation period at one flow regime (Halleraker et al. 2003). It is possible that YoY in low angle habitats were habituated to a 10 kcfs minimum over the summer and therefore very susceptible to stranding when the minimum flow was changed to 5 kcfs after the labor-day weekend.

The literature suggests that typical daily fluctuations in flow are unlikely to have a direct mortality impact on YoY rainbow trout in the Lee's Ferry reach, but our data almost certainly suggest that there is an impact on growth rate. Sampling observations showed that YoY do not follow the diurnal rise and fall of the waters edge but instead reside near the stage of the daily minimum flow. It is very likely that the larger width of atypical increments on the otolith that occurred with a periodicity of exactly 7 days (+ 50%) were caused by steady low

flows on Sunday. We know of no other physical event that occurred with a periodicity of exactly 7 days over the study period. Changes in increment width or visual contrast in otolith microstructure can be induced by short-term temperature fluctuations (Campana and Nielsen 1985). It is possible that water temperature at the stages where the majority of YoY are residing was higher on Sundays than other days during the week as water depth would be much shallower and velocities would be slower. Shoreline-offshore temperature gradients have been documented during long periods of steady flow in Grand Canyon (B. Vernieu, Grand Canyon Monitoring and Research Center, unpublished data). It is also possible that increased growth of YoY during Sunday-steady low flows was the result of increased feeding opportunities or reduced energy expenditure. YoY must have been residing very close to the substrate to maintain their position at the daily minimum flow elevation during the day when flows were high. This positioning would likely reduce their ability to forage or increase their energetic costs. The fact that we observed no lag effect in the otolith microstructure, that is, only 1 increment per week was affected by steady low flows, could suggest that the effect was an instantaneous one associated with temperature, rather than a smoothed effect associated with increased feeding opportunities or reduced energy expenditure. We plan on deploying continuously recording temperature loggers at increasing distance from the shoreline in the Lee's Ferry reach for brief periods over the spring and summer in 2004. The presence of increased temperatures on Sunday at elevations where YoY reside, relative to temperatures at these elevations on other days of the week, would support the temperature hypothesis.

5.0 Preliminary Recommendations for the Design of Future Experimental Flow Regimes and Monitoring of their Effects

The 2003 study of the effects of fluctuating flows on the early life stages of rainbow trout in the Lee's Ferry reach provided some useful information with respect to designing and monitoring future flow regimes. As we conducted no work in Grand Canyon in 2003, our recommendations apply only to the Lee's Ferry reach. However, since the objective of the increased fluctuating flow experiment was to reduce the population of rainbow trout in Grand Canyon, our recommendations may be of limited value. On the other hand, if the processes we observed in the Lee's Ferry reach are a good model for those in Grand Canyon, or if the source of rainbow trout in Grand Canyon is from juveniles and adults emigrating from the Lee's Ferry reach, the recommendations we provide are of interest.

Fluctuating flows targeted at increasing egg-to-alevin mortality should be conducted over a four-month period between Feb. and May to coincide with the majority of spawning activity. We estimated that 50 - 60% of redd excavation in 2003 occurred after Mar. 31. Terminating high flows after this date probably increased the number of redds excavated at lower stages where temperature and exposure impacts would be less severe. We do not recommend delaying the timing of the morning increase in discharge as was done in 2003 when lost hydropower revenue costs are considered. Significant temperature-induced mortality can be achieved by implementing low steady flows every Sunday. This strategy will result in lethal or sub-optimal temperatures occurring once per week above the Sunday minimum flow elevation by about mid-Mar. The downside of this strategy is that the Sunday low flows will likely increase the extent of spawning at stages below the minimum flow. An earlier rise in discharge will also increase the error in redd surveys which should be conducted at minimum flows during daylight hours. To limit these effects, steady low flows could be conducted every second week. We therefore recommend a bi-weekly steady low flow of 5 kcfs over one or two days, coupled with fluctuating flows up to 20 kcfs from Feb. through May, as the most effective means of reducing egg and alevin survival rates in the Lee's Ferry reach.

The spawning habitat preference models developed for the Lee's Ferry reach were useful for evaluating the extent to which increased discharge during the Jan. - Mar. experimental flow period altered the stages where spawning occurred. Weighted useable area computations showed that higher discharges increased total spawning habitat availability at sites that had available spawning habitat at higher stages such as Four Mile and Powerline Bars, and reduced spawning habitat availability at deep-water redd sites such as Ferry Swale. The model also showed that the stage of spawning at Four Mile and Powerline Bars was increased under higher discharge. Such changes in spawning habitat availability would likely increase the proportion of redds that would be desiccated and the duration of exposure resulting from flow fluctuations. The redd hypsometry study showed that there was a high proportion of redds excavated in deep-water that would not be dewatered at flows as low as 5 kcfs. The large decline in spawning habitat availability at Ferry Swale under high discharge suggests that spawning at deep-water sites could be suppressed through maintenance of high flows. We noted an increase in spawning at Ferry Swale when flows were reduced on Apr. 1, but we are uncertain whether this increase was the result of the flow change effecting spawning habitat availability, or was a normal occurrence driven by seasonal trends in spawn timing. In summary, the high discharges implemented in Jan.-Mar. 2003 were successful at increasing the stages of spawning at a limited of number sites (thus increasing mortality exposure), but the efficacy of these flows for reducing the large proportion of redds that are formed at stages below 5 kcfs (40-50%) is highly uncertain. The ultimate test would be to measure redd hypsometry in subsequent years under normal operations and compare the results with hypsometry measured under the experimental flow regimes. Maintaining higher flows for the duration of the spawning period (Jan. – May) would improve this comparison as well as the effectiveness of the flow regime.

A number of preliminary flow recommendations can be made based on results from the 2003 Young-of-Year survey results:

1. **Fluctuating Flows Targeting YoY Rainbow Trout Should Be Implemented from Apr. through July.** In 2003, very few fry or alevins were present during the Jan.-Mar. period when flows fluctuated from 5-20 kcfs. Literature and experimental studies in the Lee's Ferry reach (Montgomery and Tinning 1993) demonstrate that post-hatch stages of rainbow trout are the most sensitive to fluctuating flows. The timing of increased fluctuations targeted at fry should therefore begin on the date when a significant proportion of the eggs begin to hatch, which in 2003, was approximately Apr. 1. The negative effects of fluctuating flows will likely attenuate as YoY grow and migrate to steeper shoreline habitats. Increased fluctuating flows could probably be terminated by the end of Jul. if necessary. The 2004 study will provide a clearer picture of the ontogenetic habitat shift from low angle habitats to steeper shoreline that occurs over the summer and therefore provide better resolution on when enhanced fluctuating flows can be terminated.

2. **Summer Steady Flows are Beneficial to YoY Rainbow Trout.** The weekly striping pattern in otolith microstructure that we observed suggests that steady low flows, such as those conducted during the summer of 2000, almost certainly enhance the growth of YoY rainbow trout. Increased growth could lead to increased survival and higher abundance. In support of this hypothesis, preliminary analysis of rainbow trout length-frequency data from Grand Canyon shows the presence of a very strong cohort from the 2000 brood year when the low steady flow experiment was conducted (S. Rogers, AGF, Flagstaff, AZ., unpublished data).

3. **Sudden Reductions in the Minimum Daily Flow Have the Potential to Strand or Displace Many YoY Rainbow Trout.** Fluctuating flows, when implemented on a very regular basis, likely do not displace or strand large numbers of YoY rainbow trout in the Lee's Ferry reach. However, the dramatic decline in the density of fish in low angle habitats that we observed following the labor-day weekend in 2003, suggests

that large and sudden reductions in the daily minimum flow (e.g., 10 to 5 kcfs) may achieve this objective. The stranding literature suggests that the most effective 'stranding flow' would consist of high steady flows (e.g. 15-20 kcfs) for a few days to allow sufficient time for YoY to habituate by moving to the waters edge associated with the high flow. A sudden drop in flow (e.g. to 5-8 kcfs) using an unrestricted ramping rate would likely strand a large number of young fish. Such a flow should be conducted in Jun. when the majority of YoY have already hatched but are still small and have not migrated in large numbers to less vulnerable steeper habitats. Better documentation of the ontogenetic habitat shift from low angle to steeper shorelines in 2004 will be useful for defining the best time to conduct stranding flows. Conducting fry surveys before and after a flow change could assess their effects.

If managers must choose between flows targeted at reducing the survival rate of incubating stages vs. those targeted at fry that have already emerged, our preliminary opinion is that the latter choice would be better. We base this opinion both on the effectiveness of using flow to reduce survival as well as our ability to monitor these effects:

1. **Uncertainty in Altering Spawning Stages.** It will take at least a few more intensive years of study, coupled with experimental flows, to determine if deep-water spawning can be minimized by high discharge. If it can't, it is likely that redd dewatering will only effect a small component of the overall spawn and therefore not be that effective in reducing rainbow trout recruitment. Even if the Jan.-Mar. 2003 flow regime did limit deep-water spawning, recall that our estimate of the total egg deposition loss due to Glen Canyon Dam operations in 2003 ranged from 30 - 40%, with only about half of this mortality being a direct consequence of the enhanced fluctuating flows in Jan.-Mar. It seems unlikely that an additional mortality on eggs and alevins of 15-20% would have a significant impact on adult abundance when post-emergent density-dependent processes are considered.

2. **Density Dependence.** There are many opportunities for density dependent processes to compensate for the reduced production of emergent fry due to exposure of redds. In

comparison, reducing the survival of fry over the summer through flow fluctuations would occur after some, if not the majority, of density dependence.

3. **Fluctuating Flows Likely Have a Larger Impact on Fry that Have Already Emerged than on Incubating Stages.** This statement is supported by many studies that show considerable tolerance for egg stages of rainbow trout to prolonged periods of exposure, including field experiments in the Lee's Ferry reach (Montgomery and Tinning 1993). The stranding literature clearly demonstrates the impacts of certain types of fluctuating flows on young salmonids. The large change in density and distribution of fry in the Lee's Ferry reach following the flow change in early-Sep. suggests that stranding could be an efficient method for reducing fry production. 'Stranding-flows' would likely be effective even if implemented on a bi-weekly or monthly basis. Relative to increased fluctuating flows implemented on a continuous basis, periodic stranding-flows would likely have less of an impact on other resources such as recreation.

4. **Measuring the Effects in the Lee's Ferry Reach.** Uncertainty in estimates of egg and alevin mortality derived from redd counts is higher than the uncertainty associated with estimating summer fry survival. Identification of redds is a somewhat subjective process and error increases at deep-water sites. Even if the resulting redd hypsometry derived from the redd counts is accurate, we can only infer mortality rates based on exposure periods and intergravel temperatures. This inference could be improved by in-situ incubations studies as performed by Montgomery and Tinning (1993), but only at higher stages. We will likely never be able to evaluate the survival of incubating stages at deep-water sites that constitute a large component of the total production. In contrast, the precision and inferences of apparent fry survival estimates seem much better. In addition, information on changes in density, habitat use, and growth provided from the fry sampling improves our understanding of dam operations on survival and growth of young trout.

5. **Measuring the Effects in Grand Canyon.** Accurate redd counts in Grand Canyon will very likely be much more difficult to achieve than in the Lee's Ferry reach. Reduced water clarity will limit our ability to detect deep-water redds. It is important to conduct redd surveys at the minimum flow to maximize the proportion of redds that are exposed or in shallow water where they can be more easily identified. In lower Marble Canyon, the minimum flows occur mostly at night so we will be forced to conduct surveys either during the day at high flows or during the night. Preliminary mainstem redd surveys conducted at night in Grand Canyon (L. Coggins, GCMRC, Pers. Comm..) did not observe any spawning activity at higher stages that were exposed during minimum flows. If most of the mainstem spawning in Grand Canyon is in deep water, redd count estimates will be more uncertain relative to the Lee's Ferry reach. If water clarity is low at the time of the surveys, the data could be very inconclusive. In contrast, fry sampling will be no more difficult downstream, excluding logistic costs, than in the Lee's Ferry reach.

The objective of work in FY04 is to continue with the redd hypsometry and fry surveys in both the Lee's Ferry reach and in Grand Canyon. While we did not conduct any work in Grand Canyon in 2003, our gut-feeling based on observations in the Lee's Ferry reach is that increased fluctuations in flow will have a smaller effect on early life stages in Grand Canyon relative to the Lee's Ferry reach. If there is considerable mainstem spawning downstream of Lee's Ferry, it is likely at lower stages. Many fisheries biologists have traveled through Marble Canyon and it is unlikely they would have missed large spawning sites located at higher stages. Thus, if there are many redds in the mainstem of Grand Canyon, it is unlikely that many will be dewatered through fluctuating flows. With regards to fry that have emerged from the gravel, it is likely that the impacts of fluctuating flows on growth and survival are less severe in steeper shoreline habitats than in low angle cobble bars and vegetated shorelines. This is supported by the dramatic change in the density of fry in low angle habitats that we observed in the Lee's Ferry reach following the early-Sep. flow. As there is a higher proportion of steeper shoreline habitat downstream of Lee's Ferry, it follows that impacts from fluctuating flows will be less severe. These hypotheses are highly

speculative and we hope our work in FY04 will provide data to help evaluate them more rigorously.

6.0 References

Angradi, T.R., Clarkson, R.W., Kinsolving, D.A., Kubly, D.M., and S.A. Morgensen. 1992. Glen Canyon Dam and the Colorado River: Responses of the aquatic biota to dam operations.

Report prepared by Arizona Game and Fish Department for Glen Canyon Environmental Studies.

Becker, C.D., D.A. Neitzel, and D.H. Fickeisen. 1982. Effects of dewatering on Chinook salmon redds: Tolerance of four developmental phases to daily dewaterings. Transactions of the American Fisheries Society 111:624-637.

Bovee, K.D. 1982. A guide to stream habitat analysis using the Instream Flow Incremental Methodology. Instream Flow Inf. Pap. 12. U.S. Fish Wildl. Serv. FWS-OBS 82/26.

Bradford, M.J. Taylor, G.C., Allan, A., and P.S. Higgins. 1995. An experimental study of the stranding of Coho Salmon and Rainbow Trout during rapid flow decreases under winder conditions. North Amer. J. Fish. Manag. 15: 473-479.

Campana, S.E. 1992. Measurement and interpretation of the microstructure of fish otoliths. P. 59-71. In: D.K. Stevenson and S.E. Campana [eds]. Otolith microstructure examination and analysis. Can. Spec. Publ. Fish. Aquat. Sci. 117.

Campana, S. E. and J.D. Neilson. 1985. Microstructure of fish otoliths. Can. J. Fish. Aquat. Sci. 42:1014-1032.

Chapman, D.W., Weitkamp, D. E., Welsh, T.L., Dell, M.B., and T.H. Schadt. 1986. Effects of river flow on the distribution of chinook salmon (Onchoynhus-thawytscha) redds. Transactions of the American Fisheries Society. 115(4):537-547.

Crisp, D.T. 1981. A desk study of the relationship between temperature and hatching time for the eggs of five species of salmonid fishes. Freshwater Biology 11:361-368.

Cushman, R.M. 1985. Review of ecological effects of rapidly varying flows downstream from hydroelectric facilities. North American Journal of Fisheries Management 5:330-339.

Flodmark, L.E.W., Urke, H.A., Halleraker, J.H., Arnekleiv, J.V., Vøllestad, L.A. & Poléo, A.B.S. 2002. Cortisol and glucose response in juvenile brown trout subjected to a fluctuating flow regime in an artificial stream. Journal of Fish Biology 60:238-248.

Foster, D. 2002. Fly fishing Lee's Ferry, Arizona. The complete guide to fishing and boating the Colorado River below Glen Canyon Dam. Nononsense Fly Fishing Guidebooks, Sisters, Oregon.

Gordon, N.D., T.A. McMahon, and B.L. Finlayson. 1994. Stream hydrology: an introduction for ecologists. John Wiley and Sons, New York.

Halleraker, J.H., Saltveit, J.J., Harby, A., Arnekleiv, J.V., Fjesdstad, H.P., and B. Kohler. Factors influencing stranding of wild juvenile brown trout (Salmo Trutta) during rapid and frequent flow decreases in artificial stream. Riv. Res. Applic. 19: 589-603.

Hilborn, R., Bue, B.G., and S. Sharr. 1999. Estimating spawning escapements from periodic counts: a comparison of methods. Can J. Fish. Aquat. Sci. 56: 888-896.

Hilborn, R., and M. Mangel. 1997. The ecological detective: Confronting models with Data. Princeton University Press, Princeton, NJ.

Irvine, J.R., and T.C. Nelson. 1995. Proceedings of the 1994 salmon escapement workshop plus an annotated bibliography on escapement estimation. Can. Manuscr. Rep. Fish. Aquat. Sci. No. 2305.

Kalish, J. M., Beamish, R. J., Brothers, E. B., Casselman, J. M., Francis, R. I. C. C., Mosegaard, H., Panfili, J., Prince, E. D., Thresher, R. E., Wilson, C. A., and Wright, P. J. 1995. Glossary for otolith studies. P. 723-729. In: Secor, D. H., J.M. Dean, and S.E. Campana. Recent Developments in Fish Otolith Research. University of South Carolina Press. Columbia, S.C.

Kondolf, G.M. 2000. Assessing salmonid spawning gravel quality. Trans. Am. Fish. Soc. 129:262-281.

Kondolf, G.M., and M.G. Wolman. 1993. The sizes of salmonid spawning gravels. Water Resources Research, 29:2275-2285.

Kondolf. G.M., S.S. Cook, H.R. Maddux and W.R. Persons. 1989. Spawning gravels of rainbow trout in the Grand Canyon, Arizona. Journal of the Arizona Nevada Academy of Science, 23:19-28.

Korman, J., Ahrens, R.N.M., Higgins, P.S., and Walters, C.J. 2002. Effects of observer efficiency, arrival timing, and survey life on estimates of escapement for steelhead trout (O*ncorhynchus mykiss*) derived from repeat mark-recapture experiments. Can. J. Fish. Aquat. Sci. 59: 1116-1131.

Leopold, L.B. 1994. A view of the river. Harvard University Press, Cambridge, Massachusetts. 294 pp.

McEwan, D. and T.A. Jackson. 1996. Steelhead restoration and management plan for California. Department of Fish and Game.

McKinney, T., Speas, D.W., Rogers, R.S., and W.R. Persons. 1999. Rainbow trout in the Lee's Ferry recreational fishery below Glen Canyon Dam, Arizona, following

establishment of minimum flow requirements. Report prepared for Grand Canyon Monitoring and Research Center by Arizona Game and Fish Department.

Montgomery, W. L. and K. Tinning. 1993. Impact of fluctuating water levels on early life history of rainbow trout (Draft). Report prepared for Glen Canyon Environmental Studies.

Moyle, P. 2002. Inland fishes of California, 2nd Ed. University of California Press, Berkeley, CA.

Pert. E.J., and D.C. Erman. 1994. Habitat use by adult rainbow trout under moderate artificial fluctuations in flow. Trans. Am. Fish. Soc. 123: 913-923.

Piper, R.G., McElwain, I.B., Orme, L.E., McCraren, J.P., L.G. Fowler, and J.R. Leonard. 1986. Fish Hatchery Management. American Fisheries Society. 517 pp.

Raleigh, R. F., T. Hickman, R. C. Solomon, and P. C. Nelson. 1984. Habitat suitability information: rainbow trout. U.S. Fish and Wildlife Service, Division of Biological Services (FWS/OBS-82d/10.60). Washington, DC.

Reiser, D.W., and R.G. White. 1983. Effects of complete redd dewatering on salmonid egg-hatching success and development of juveniles. Transactions of the American Fisheries Society. 112:532-540.

Randle, T.J., and E.L. Pemberton. 1987. Results and analysis of STARS modeling efforts of the Colorado River in Grand Canyon. U.S. Department of Interior, Bureau of Reclamation. NTIS No. PB88-183421/AS.

Saltveith, S.J., Halleraker, J.H., Arnekleiv, J.V., and A. Harby. 2001. Field experiments on stranding in juvenile Atlantic Salmon (Salmo Salar) and Brown Trout (Salmo Trutta)

during rapid flow decreases caused by hydropeaking. Regu. Rivers: Res. Mgmt. 17: 609-622.

Shirvell, C.S. 1994. Effect of changes in streamflow on the microhabitat use and movements of sympatric juvenile coho salmon and chinook salmon in a natural stream. Can. J. Fish. Aquat. Sci. 51: 1644-1652.

Stevenson, D.K. and S.E. Campana [ed]. 1992. Otolith microstructure examination and analysis. Can. Spec. Publ. Fish. Aquat. Sci. 117: 130 pp.

Systat, 1997. Statistics. SPSS Inc.

Vehanen, T., Bjerke, P.P. Heggenes, J., Huusko, A., and A. Maki-Petays. 2000. Effect of fluctuating flow and temperature on cover type selection and behaviour by juvenile brown trout in artificial flumes. J. Fish. Bio. 56: 923-937.

Wiele S. M. and E.R. Griffin. 1997. Modifications to a one-dimensional model of unsteady flow in the Colorado River through the Grand Canyon. U.S. Geological Survey Water Resources Investigation Report 97-4046.

Table 2.1. Summary of survival experiments conducted by Montgomery and Tinning (1993) in the laboratory and the Lee's Ferry reach. All experimental results were conducted at water temperatures < 11 C except the one experiment that is noted.

Experimental Results				
			Survival Rate (%)	
	Exposure (hrs)	Duration (days)	Eggs	Alevins
	3	26	100	100
	3 (>11 C)	26	100	40
	6	16		50
	12	16	100	12.5
	15	13	10	0
Field Results				
			Survival Rate (%)	
Stage (kcfs)	Exposure (hrs)	Duration (days)		Alevins
1	0	22		72
5	6	22		32
10	10	22		0
15	15	22		0

Table 2.2. Sampling Schedule for 2003 Lee's Ferry redd and fry surveys. The discharge column shows the typical daily flow range for the month.

Month	Date	Daily Discharge Range (kcfs)	Trip Type
Jan.	23	5.0 - 20.1	Pilot Redd
Feb.	10-15	5.0 - 20.2	Redd
Mar.	8-12	5.0 - 20.1	Redd
Apr.	8-11	6.5 - 12.1	Redd and Pilot Fry
May	24-26	7.4 - 12.4	Redd and Pilot Fry
Jun.	25-26	10.0 - 16.8	Fry
Jul.	26-27	10.1 - 17.3	Fry
Aug.		10.2 - 17.4	No trip
Sept.	8-9	5.0 - 9.8	Fry
Oct	24-26	4.9 - 9.8	Fry

Table 2.3. Peak redd counts at intensive sites and those surveyed using the rapid assessment technique (RAT). The hypsometry column specifies the elevation of the majority of redds at each site ('deep' = redds mostly below 5 kcfs stage; '> 5 kcfs' = redds mostly above 5 kcfs stage). Note that peak counts among sites could occur in different survey months.

ID	Site Name	River Mile	Site Type	Hypsometry	Peak Count
1	Dam Island (top-center)	-15.3	RAT	>5 kcfs	4
2	Dam Island (River-Right)	-15.0	RAT	>5 kcfs	13
3	Dam Island (Deep)	-14.9	RAT	Deep	16
4	Pumphouse Bar	-14.5	Intensive	>5 kcfs	26
5	D/S End of Pumphouse on River-Right	-14.4	RAT	Deep	14
6	Powerline	-13.8	Intensive	>5 kcfs	105
7	Center of channel upstream of Honey Draw	-13.4	RAT	Deep	52
8	Tire Bar	-13.2	RAT	>5 kcfs	19
9	Catchings Bar	-12.7	RAT	Deep	2
10	Center of channel at U/S end of Slough	-12.4	RAT	Deep	68
11	Prop Bar @ Stranding Pool	-11.8	RAT	>5 kcfs	7
12	Ferry Swale	-11.1	Intensive	Deep	96
13	Petroglpyh Bar on RL	-10.2	RAT	Deep	4
14	Duck Island Main	-10.0	RAT	Deep	48
15	Duck Island Inside Channel at D/S end	-9.9	RAT	>5 kcfs	62
16	Downstream of Duck Island in Center Channel	-9.3	RAT	Deep	4
17	8 Mile Bar	-9.0	RAT	Deep	37
18	7.5 Mile Bar in center of channel	-8.8	RAT	Deep	4
19	7.5 Mile Bar on River-Left	-8.2	RAT	>5 kcfs	49
20	6 Mile Bar on RL	-5.8	RAT	>5 kcfs	6
21	Cliff on RR Upstream of FM	-4.3	RAT	Deep	34
22	Four Mile Bar	-4.0	Intensive	>5 kcfs	372
23	Water Holes	-3.9	RAT	>5 kcfs	12
24	3.5 Mile Bar	-3.0	RAT	Deep	98
25	Fall Ck.	-2.5	RAT	>5 kcfs	4
	Total				1156

Table 2.4. Combined redd counts from intensive and rapid assessment technique surveys by discharge elevation and survey period. The percentage of redds above 5, 8 and 12 kcfs is also shown.

Discharge (kcfs)	Mar.	Apr.	May
<=5	288	459	332
5-8	152	143	217
8-12	125	106	118
12-15	163	152	134
15-20	29	76	77
Total	757	936	878
% > 5	62	51	62
% > 8	42	36	37
% > 12	25	24	24

Table 2.5. Summary of spatial analysis of redd count data to determine redd survey life. The number of $1m^2$ grid cells containing redds were summed into the following 3 categories: New = a redd was present in a cell in the second month (e.g. Mar.) but not in the first (e.g., Feb.); Faded = a cell where a redd was present in the first month but not in the second month; Old =a cell where a redd was present in both the first and second months. The number of cells which contained redds ("Present") is simply the sum of the cells in the "New" and "Old" columns. The column labeled Redd Count is the actual number of redds counted on each survey. PH, PL, FS, and FM refer to Pumphouse Bar, Powerline Bar, Ferry Swale, and Four Mile Bar, respectively.

		# of $1m^2$ Cells				
Site	**Period**	**New**	**Faded**	**Old**	**Present**	**Redd Count**
PH	Feb				15	15
	Feb-Mar	19	9	6	25	26
	Mar-Apr	17	19	6	23	23
	Apr-May	3	22	1	4	4
PL	Feb				42	43
	Feb-Mar	72	16	26	98	101
	Mar-Apr	88	81	17	105	105
	Apr-May	18	84	21	39	41
FS	Feb				20	20
	Feb-Mar	34	20	0	34	36
	Mar-Apr	76	34	0	76	88
	Apr-May	59	73	3	62	96
FM	Feb				171	174
	Feb-Mar	162	109	62	224	230
	Mar-Apr	214	150	74	288	293
	Apr-May	212	150	138	350	371

Table 2.6. Statistics used to estimate survey life at four sites based on a spatial analysis of redd data. Survey life (in units of weeks) was computed based on the ratio of the integral of the number of redds present over the entire survey period (redd-weeks) to the number of new redds excavated over the same period. Survey life calculations were made assuming no redd superimposition (top), or that 100% of cells classified as "Old" redds were actually new redds that were superimposed on top of existing redds. PH, PL, FS, and FM refer to Pumphouse Bar, Powerline Bar, Ferry Swale, and Four Mile Bar, respectively.

.

Site	New Redds	AUC (Redd-Wks.)	Survey Life (Wks.)
No Superimposition			
PH	39	265.1	6.8
PL	178	1161.2	6.5
FS	169	783.4	4.6
FM	588	3919.4	6.7
Avg.			6.2
100% Superimposition on Old Redds			
PH	52	265.1	5.1
PL	242	1161.2	4.8
FS	172	783.4	4.6
FM	862	3919.4	4.5
Avg.			4.7

Table 2.7. Maximum intergravel daily temperatures on Sunday at Four Mile and Powerline Bars. Values are means of two temperature loggers at each elevation per site.

		Four Mile Bar				Powerline Bar			
		Elevation (kcfs)				Elevation (kcfs)			
Month	**Day**	**18**	**15**	**10**	**5**	**18**	**15**	**10**	**5**
Feb	16	15	13	13	9	8	9	9	10
	23	14	13	12	10	8	8	9	10
Mar	2	16	14	15	10	8	9	9	10
	9	17	15	16	12	8	8	8	10
	16	18	16	17	12	11	10	10	10
	23	22	20	21	14	10	9	9	10
	30	20	18	21	14	12	9	9	10
Apr	6	17	15	16	10	17	14	15	11
	13	28	26	27	11	27	21	21	12
	20	24	22	24	11	26	20	20	12
	27	30	27	29	12	29	23	22	12
May	4	28	25	26	11	26	21	21	12
	11	31	28	30	12	30	23	24	12
	18	32	28	28	12	31	25	24	12

Table 2.8. Timing of inundation and exposure of various stages in the Lee's Ferry reach, Jan.-Apr, 2003.

Jan. – Mar., 2003

Stage (kcfs)	*Hour* Dried-Out	Hour Wetted	Hours Exposed
5			0
6	1:30	9:00	7.5
8	0:30	9:30	9
10	23:30	10:00	10.5
12	23:00	10:30	11.5
15	22:00	11:00	13
20	20:00	12:00	17

Apr., 2003

Monday - Saturday

Stage (kcfs)	Hour Dried-Out	Hour Wetted	Hours Exposed
5			0
6			0
8	0:00	5:30	5.5
10	22:00	7:00	9
12	21:00	11:00	14
15			24
20			24

Sunday

Stage (kcfs)	Hour Dried-Out	Hour Wetted	Hours Exposed
5			0
6			0
>=8			24

Table 3.1. Particle size categories (b-axis diameter) used to characterize grain size of gravel bars in the Lee's Ferry reach, 2003.

Size Category (mm)	Substrate Type
<1	Sand and Finer
1-2	
2-4	
4-6	
6-8	
8-10	
10-12	
12-14	
14-16	
16-20	
20-24	Small Gravel
24-28	
28-32	
32-40	
40-48	Medium Gravel
48-64	Large Gravel
64-128	Small Cobble
>128	Larger Cobble and Boulder

Table 3.2. Number of elevation, substrate, depth, and velocity observations (Points) collected at Four Mile Bar (FM), Ferry Swale (FS), Powerline Bar (PL), and Pumphouse Bar (PH). Depth and velocity observations were collected at 5, 8, 12, and 20 kcfs. The total area of each study site by discharge is also shown (Area m^2).

Site	Observation Type	Elevation	Substrate	Depth and Velocity			
				5	8	12	20
FM	Points	1868	196	187	348	246	460
	Area (m^2)			12,966	16,864	21,948	28,352
FS	Points	679	136	177	232	141	129
	Area (m^2)			17,818	20,160	21,241	21,328
PL	Points	734	64	52	124	93	257
	Area (m^2)			7,831	8,790	9,705	11,510
PH	Points	335	22	90	79	46	66
	Area (m^2)				Not Computed		
Grand Total Points		3616	418	506	783	526	912

Table 3.3. Grain size characteristics of surficial substrate (top) at Four Mile Bar (FM), Ferry Swale (FS), Powerline Bar (PL), and Pumphouse Bar (PH). N refers to the number of habitat locations where statistics were computed, with each location consisting of 10-15 measurements. D15, D50, and D85 refer to the grain size where 15%, 50%, and 85% of the sample is finer. The average statistical values across the number of location samples are shown. Grain size statistics for depth-integrated samples collected in the top 15 cm of gravel bars are shown in the lower table.

Surface Samples

Statistic	FM	FS	PL
N	196	136	64
Average D15	7.45	6.13	4.96
Average D50	18.67	12.53	19.10
Average D85	36.83	21.05	46.56
Average Geometric Mean (DG)	15.52	10.46	13.41
Average Geometric Standard Deviation (SG)	2.55	2.58	4.73
Average Skewness (SK)	-0.16	-0.18	-0.23

Integrated 0-15 cm Samples

'Data for lower table to be provided by GCMRC

Statistic	FM	FS	PL
N			
Average D15			
Average D50			
Average D85			
Average Geometric Mean (DG)			
Average Geometric Standard Deviation (SG)			
Average Skewness (SK)			

Table 3.4. Correlations (r^2) among grain size statistics (surface only) at 3 locations in the Lee's Ferry reach. D15, D50, and D85 refer to the grain size where 15%, 50%, and 85% of the sample is finer, respectively. DG, SG, and SK, refer to the geometric mean, geometric standard deviation (sorting index), and skeweness, respectively.

All Sites

	D15	D50	D85	DG	SG
D50	0.38				
D85	0.18	0.61			
DG	0.78	0.62	0.59		
SG	0.25	0.01	0.06	0.09	
SK	0.05	0.07	0.00	0.04	0.12

Four Mile Bar

	D15	D50	D85	DG	SG
D50	0.35				
D85	0.24	0.70			
DG	0.81	0.61	0.64		
SG	0.18	0.04	0.10	0.04	
SK	0.08	0.08	0.00	0.05	0.12

F erry Swale

	D15	D50	D85	DG	SG
D50	0.59				
D85	0.32	0.74			
DG	0.86	0.76	0.65		
SG	0.28	0.00	0.01	0.15	
SK	0.03	0.04	0.00	0.02	0.11

Powerline Bar

	D15	D50	D85	DG	SG
D50	0.26				
D85	0.13	0.33			
DG	0.77	0.41	0.54		
SG	0.52	0.01	0.00	0.30	
SK	0.11	0.16	0.01	0.09	0.16

Table 3.5. Summary statistics and classification tables from the discriminant function analysis predicting the presence of redds within grid cells based on the habitat characteristics depth, near-bottom velocity, and particle size characteristics D50, D85, and SG (geometric standard deviation which provides a sorting index). The F-to-Remove statistic determines the relative importance of variables included in the disrciminant function.

Powerline Bar

Canonical correlation		0.59				
	F-to-Remove				Predicted	
				Non-Redd	Redd	
Depth	62		Non-Redd	72	23	95
Vel	6.0	Observed	Redd	8	96	104
D50	0.43					
D85	1.0				% Correct	84
SG	0.0					

Ferry Swale

Canonical correlation		0.62				
	F-to-Remove				Predicted	
				Non-Redd	Redd	
Depth	22.1		Non-Redd	39	18	57
Vel	29.9	Observed	Redd	5	47	52
D50	0.8					
D85	1.4				% Correct	79
SG	2.7					

Four Mile Bar

Canonical correlation		0.46				
	F-to-Remove				Predicted	
				Non-Redd	Redd	
Depth	79.9		Non-Redd	146	74	220
Vel	0.3	Observed	Redd	29	184	213
D50	1.0					
D85	6.4				% Correct	76
SG	0.3					

All Sites Combined

Canonical correlation		0.45				
	F-to-Remove				Predicted	
				Non-Redd	Redd	
Depth	155.5		Non-Redd	215	157	372
Vel	0.0	Observed	Redd	43	326	369
D50	0.0					
D85	6.4				% Correct	73
SG	0.3					

Table 4.1. Sample size, density, frequency of fish presence, and forklength of young-of-year rainbow trout in the Lee's Ferry reach in 2003 by habitat type and sample period. Statistics in parentheses for Sep. and Oct. are based on values from the original 20 sites sampled from Jun. – Sep. plus 6 additional talus shoreline sites sampled in Sep. and Oct only. Values not in parentheses are based on the original 20 sites only.

	Jun	Jul	Sep	Oct
# of Sites				
Cobble Bar	11	11	11	11
Veg./Sand	8	8	8	8
Talus	1	1	7	7
Total	20	20	26	26
Total Catch	294	240	49 (182)	83 (183)
Density (#/100 m)				
Cobble Bar	48	38	8	18
Veg./Sand	44	30	4	8
Talus	47	140	50 (69)	30 (52)
Average	46	40	9 (24)	15 (24)
% of Sites with Fish				
Cobble Bar	91	91	60	50
Veg./Sand	100	91	38	63
Talus	100	100	100 (100)	100 (100)
Total	95	90	53 (64)	58 (68)
Mean Forklength (mm)				
Cobble Bar	37	45	55	69
Veg./Sand	33	44	54	69
Talus	56	49	54 (61)	76 (75)
Average	37	45	55 (58)	70 (72)

Table 4.2. Comparison of catch-per-effort and mean size of rainbow trout YoY based on boat and backpack electrofishing at 6 sites in the Lee's Ferry reach, Oct. 2003.

Site	Fish/100 m		Mean Forklength (mm)	
	Back	Boat	Back	Boat
3.5 Mile	30	62	68	75
4 Mile	7	13	64	84
6 Mile	33	20	71	90
7 Mile	7	42	67	85
9 Mile	43	13	83	76
Waterholes	63	31	69	79

Average Effort for a 45 m site

	Back	Boat
Time (minutes)	14	6
Seconds Shocked	700	350
Seconds/meter	16	8

Table 4.3. Relationship between water temperature, accumulated thermal units (ATUs) and the number of days for rainbow trout eggs to hatch (top) from Piper et al. (1982). Prediction of hatch dates based on these relationships and specific spawn dates are also shown (lower). Temperature-driven statistics between spawn and hatch dates are based on intergravel measurements at Four Mile Bar at an elevation of 5 kcfs .

Temperature		ATUs (C)	Days to
F	C	to Hatch	Hatch
45	7.2	347	48
50	10.0	310	31
55	12.8	307	24

Spawn Date	Average Temperature over Incubation (C)	Predicted Hatch Date
Feb-01	9	Mar-10
Mar-01	9.5	Apr-02
Apr-01	10	May-02
May-01	10.5	May-30

Table 4.4. Summary statistics for the increment widths on otoliths from a sample of 15 fish where a weekly striping pattern was evident.

	# of Increments Measured		Average Width of Increments (microns)		Width Comparison	Statistical Probability that Width of Atypical Increment > Width of Typical Increment
Fish	Atypical	Typical	Atypical	Typical	Atypical > Typical	
All 15	38	227	3.12	2.51	Yes	0.000
1	1	6	2.55	2.35	Yes	
2	5	30	2.17	2.17		0.998
3	2	12	3.03	2.77	Yes	
4	4	24	2.37	2.18	Yes	0.219
5	3	18	2.60	2.10	Yes	0.167
6	5	30	2.73	2.38	Yes	0.030
7	4	24	2.58	2.36	Yes	0.455
8	2	12	3.72	3.00	Yes	0.003
9	3	18	4.03	2.75	Yes	0.000
10	2	12	5.00	3.01	Yes	0.287
11	1	6	4.13	2.39	Yes	
12	2	12	4.68	3.69	Yes	0.058
13	3	17	4.31	2.78	Yes	0.092
14	1	6	2.31	2.10	Yes	
15	1	6	2.98	2.83	Yes	

Table 4.5. Summary of stock synthesis model parameter estimates for alternate models that simulate weekly survival rate (constant over simulation or varying by month) and recruitment (independent weekly values, weekly values estimated from a 3-parameter Beta distribution, and weekly values estimated by fitting the magnitude parameter of the Beta distribution with shape parameters determined by back-calculation of hatch dates from catch data and length-age relationship). The "Parameters" row shows the number of recruitment and survival parameters (Recruitment + Survival) estimated by each model.

	Weekly	**Beta Best-fit**	***Beta* Back-calculated**
Constant Survival			
Parameters	45 + 1	3 + 1	1 + 1
Weekly Survival Rate	0.88	0.88	0.90
Negative Log Likelihood	145.28	167.37	194.1
Mar.-Jun. Recruitment	7,785	7,176	4,243
Monthly Survival			
Parameters	45+10	3+10	1+10
Jun. Weekly Survival	0.75	0.75	0.68
Jul. Weekly Survival	0.97	0.97	0.99
Aug. Weekly Survival	0.75	0.70	0.71
Sep. Weekly Survival	0.88	0.99	0.99
Negative Log Likelihood	132.87	134.13	134.78
Mar.-Jun. Recruitment	1,211	6,852	16,145

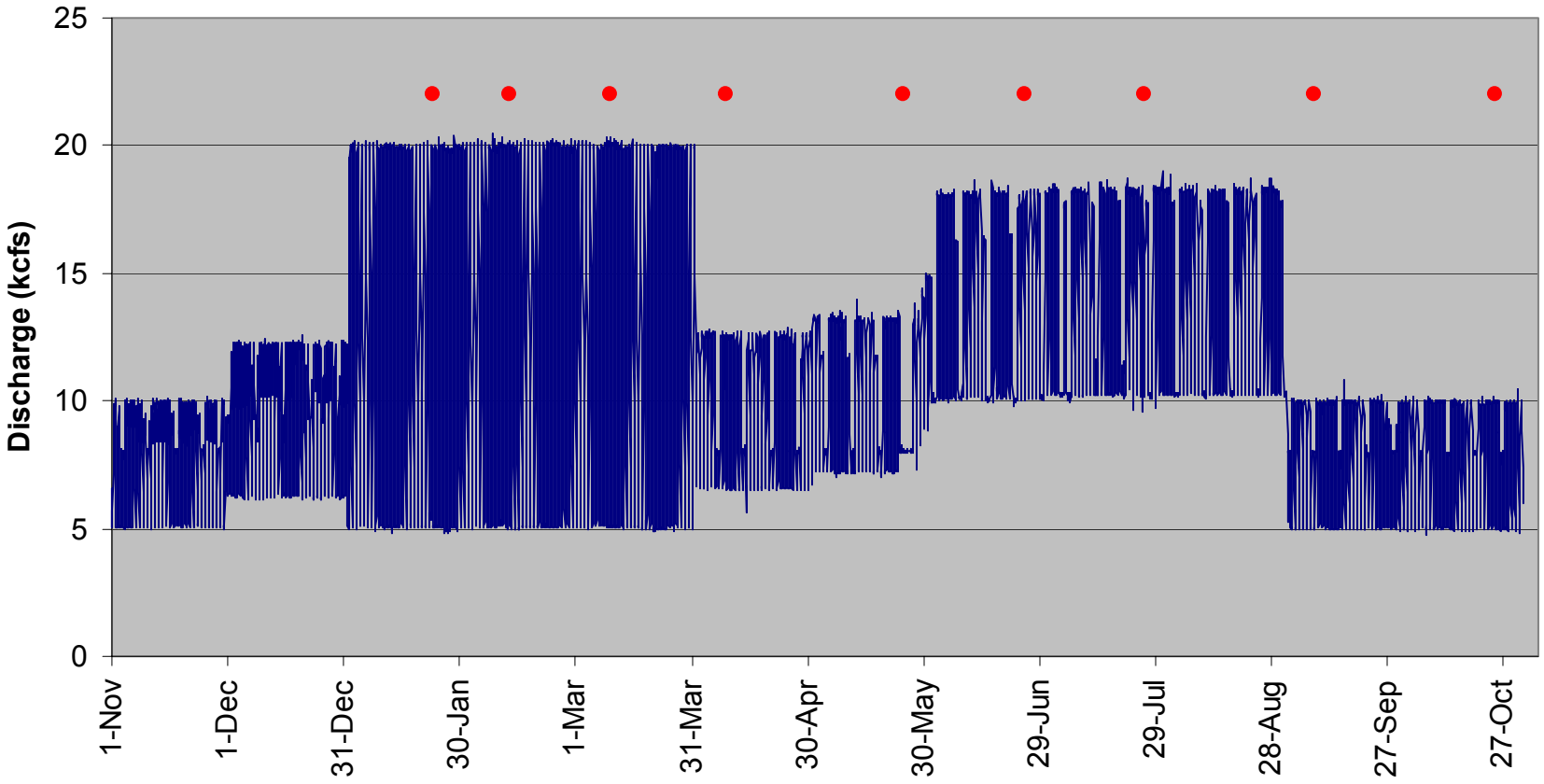

Figure 1.1. Hourly hydrograph for the 2003 water year from Glen Canyon Dam. Red circles denote sampling periods in this study.

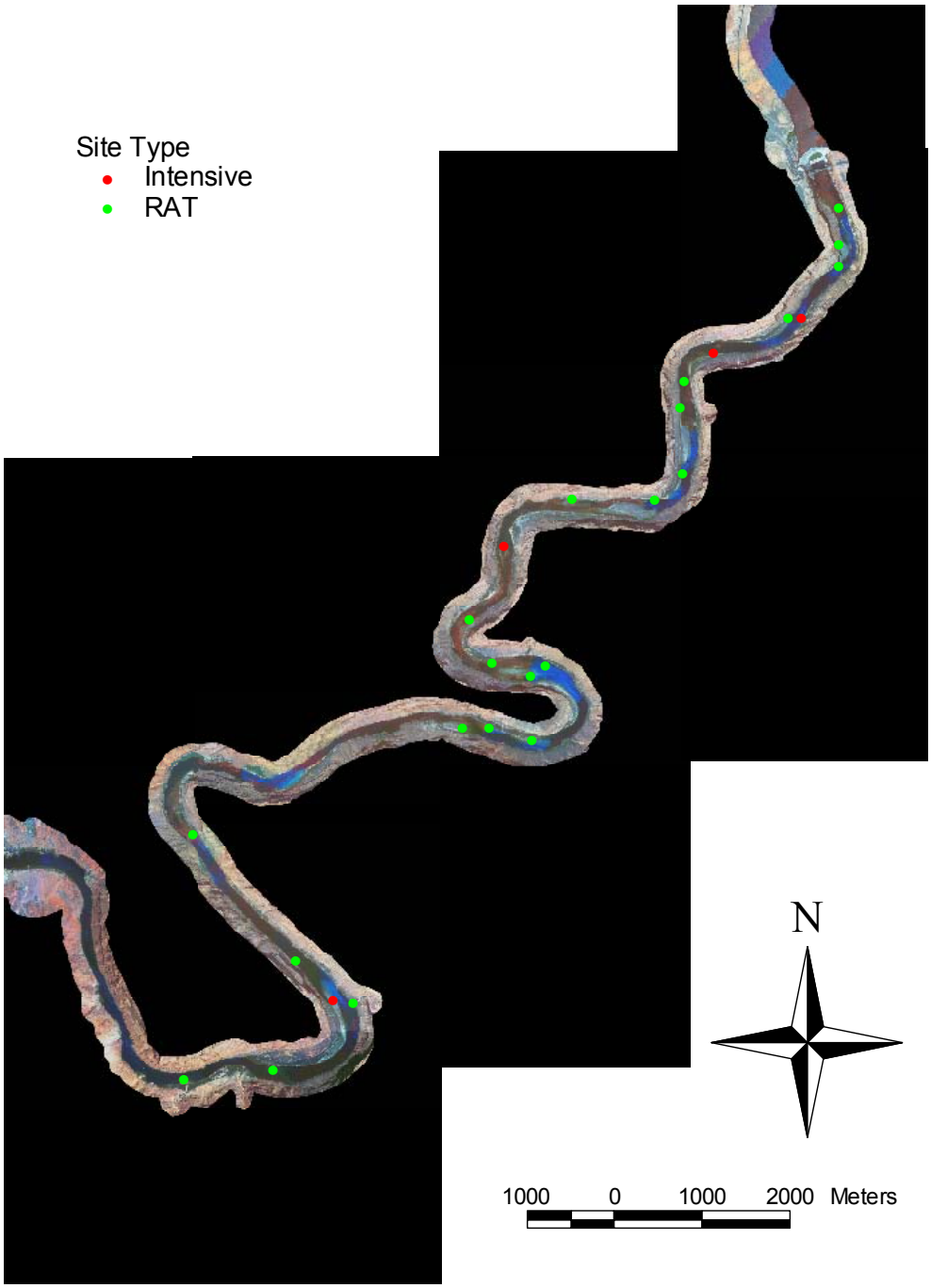

Figure 2.1. Map of the Lee's Ferry Reach showing locations of intensive (red) and rapid assessment technique (green) redd survey sites. Glen Canyon Dam can be seen near the top of the map. The intensive sampling sites Pumphouse Bar, Powerline Bar, Ferry Swale, and Four Mile Bar are located at increasing distances downstream from the dam.

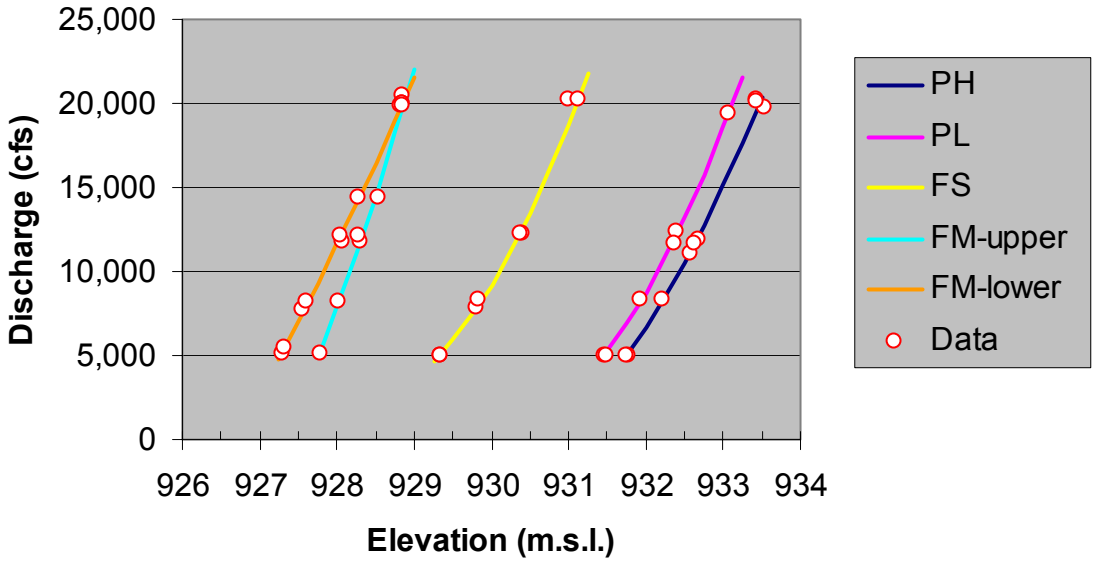

Figure 2.2. Stage-discharge data (circles) and best-fit relationships at Pumphouse Bar (PH), Powerline Bar (PL), Ferry Swale (FS), and Four Mile Bar (FM-upper, FM-lower).

a)

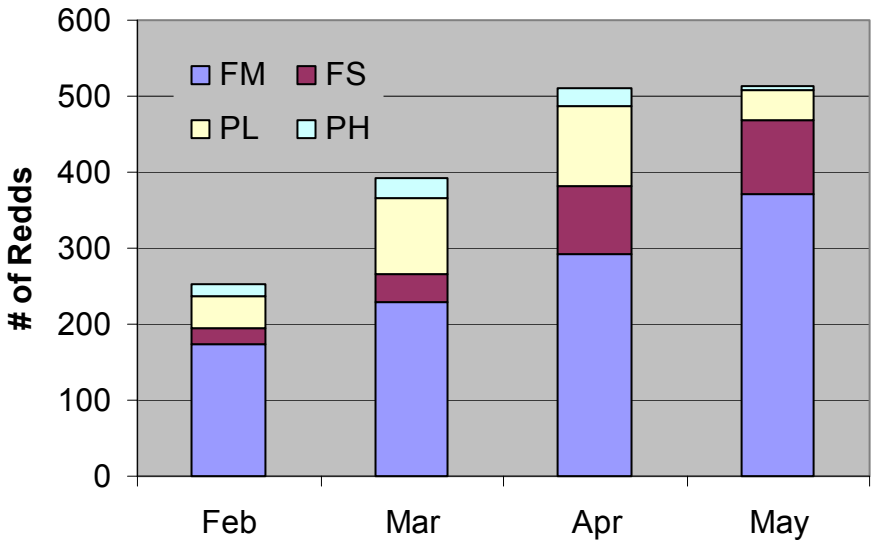

b)

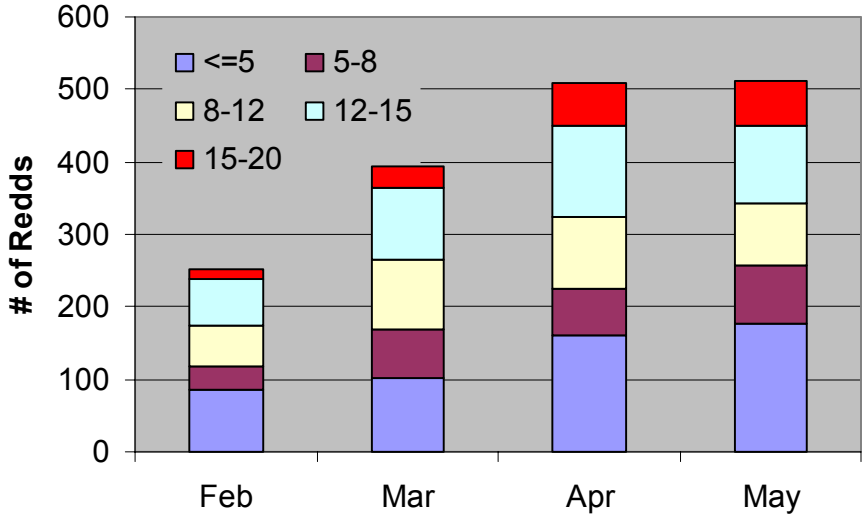

Figure 2.3. Distribution of redd counts across a) sample sites and b) elevation (in kcfs) at four intensively sampled sites.

a) Pumphouse Bar

Figure 2.4. Redd location and elevation at a) Pumphouse Bar, b) Powerline Bar, c) Ferry Swale, and d) Four Mile Bar across all four survey periods.

b) Powerline Bar

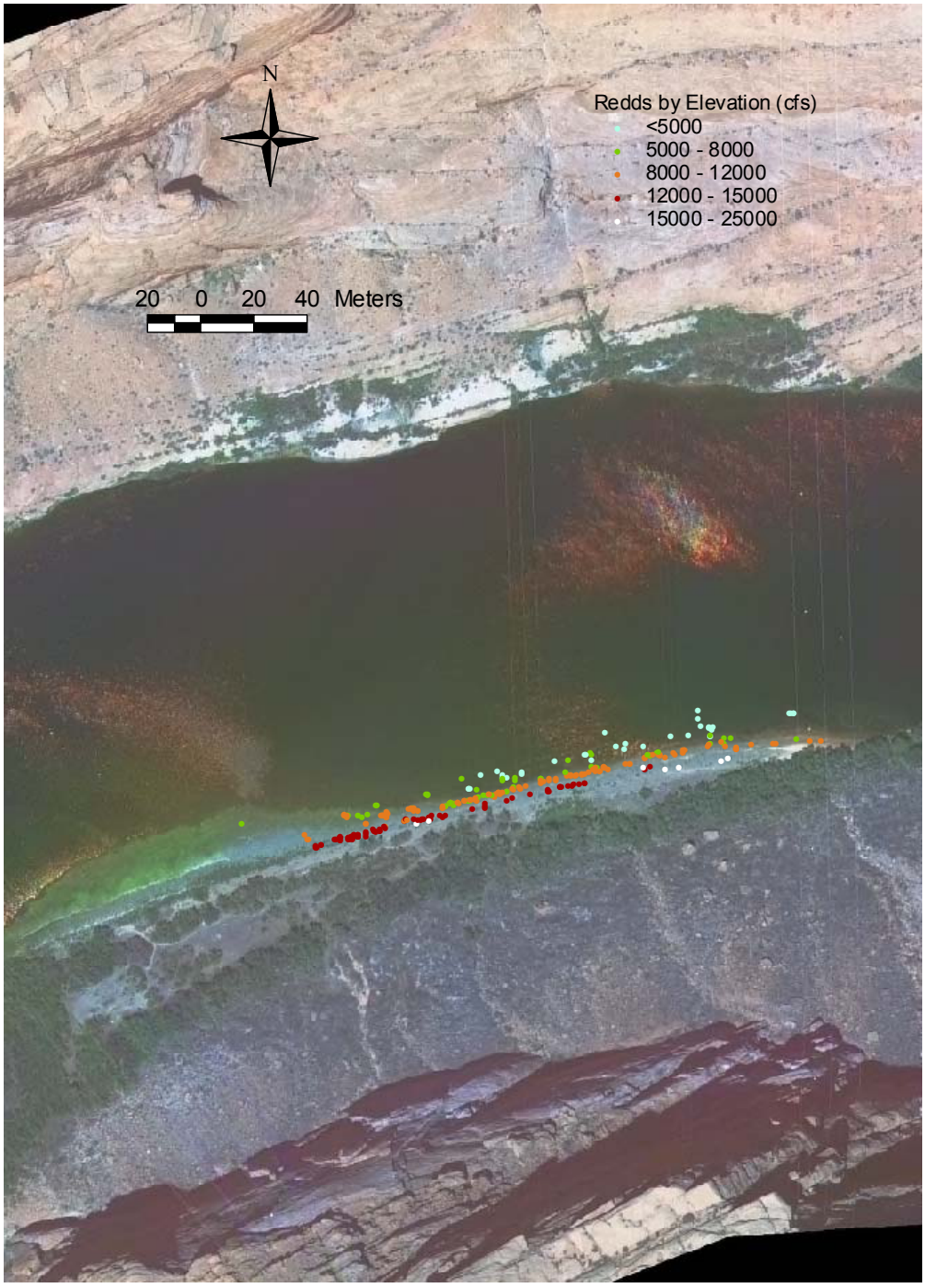

Figure 2.4. Con't.

c) Ferry Swale

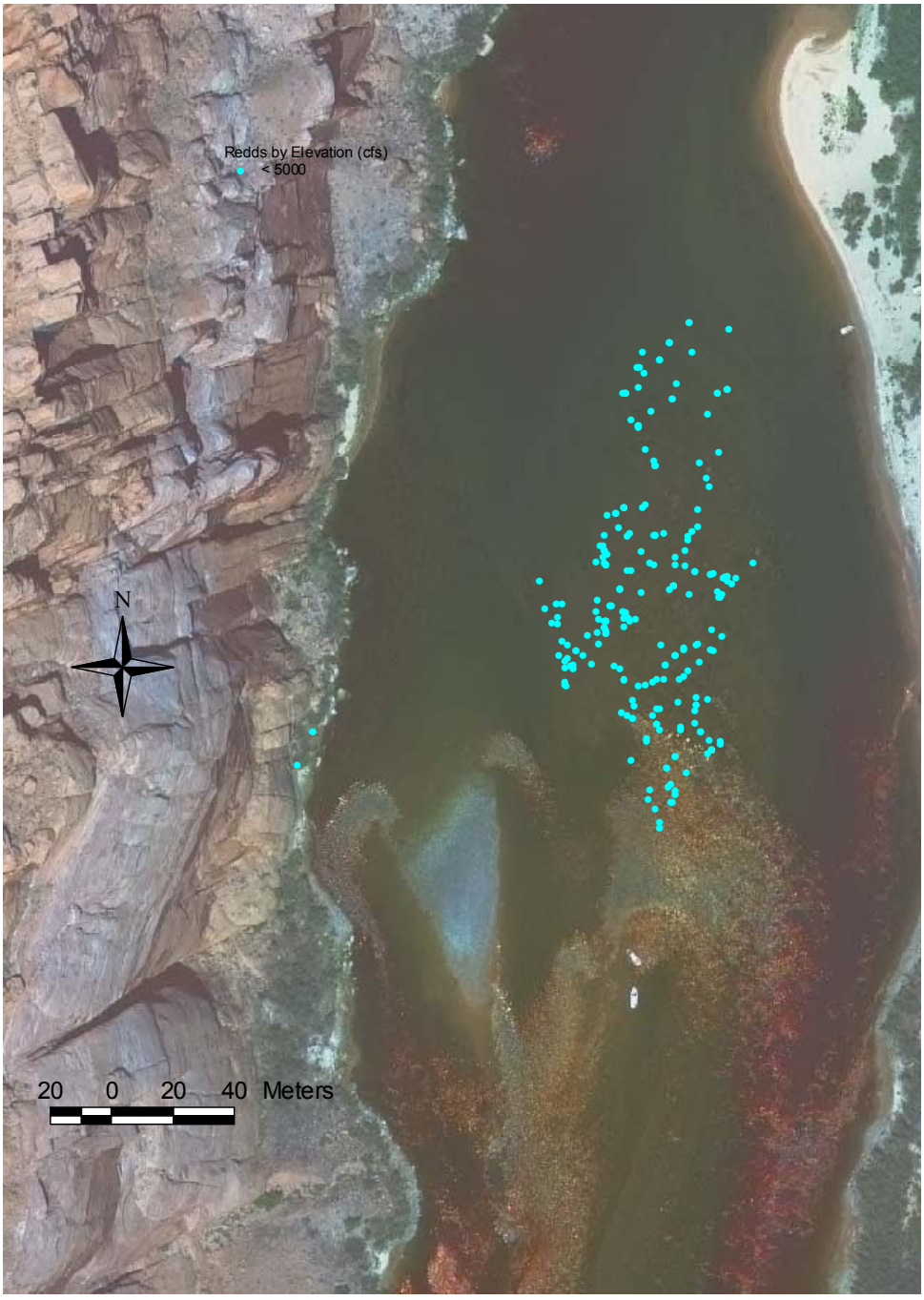

Figure 2.4. Con't

d) Four Mile Bar

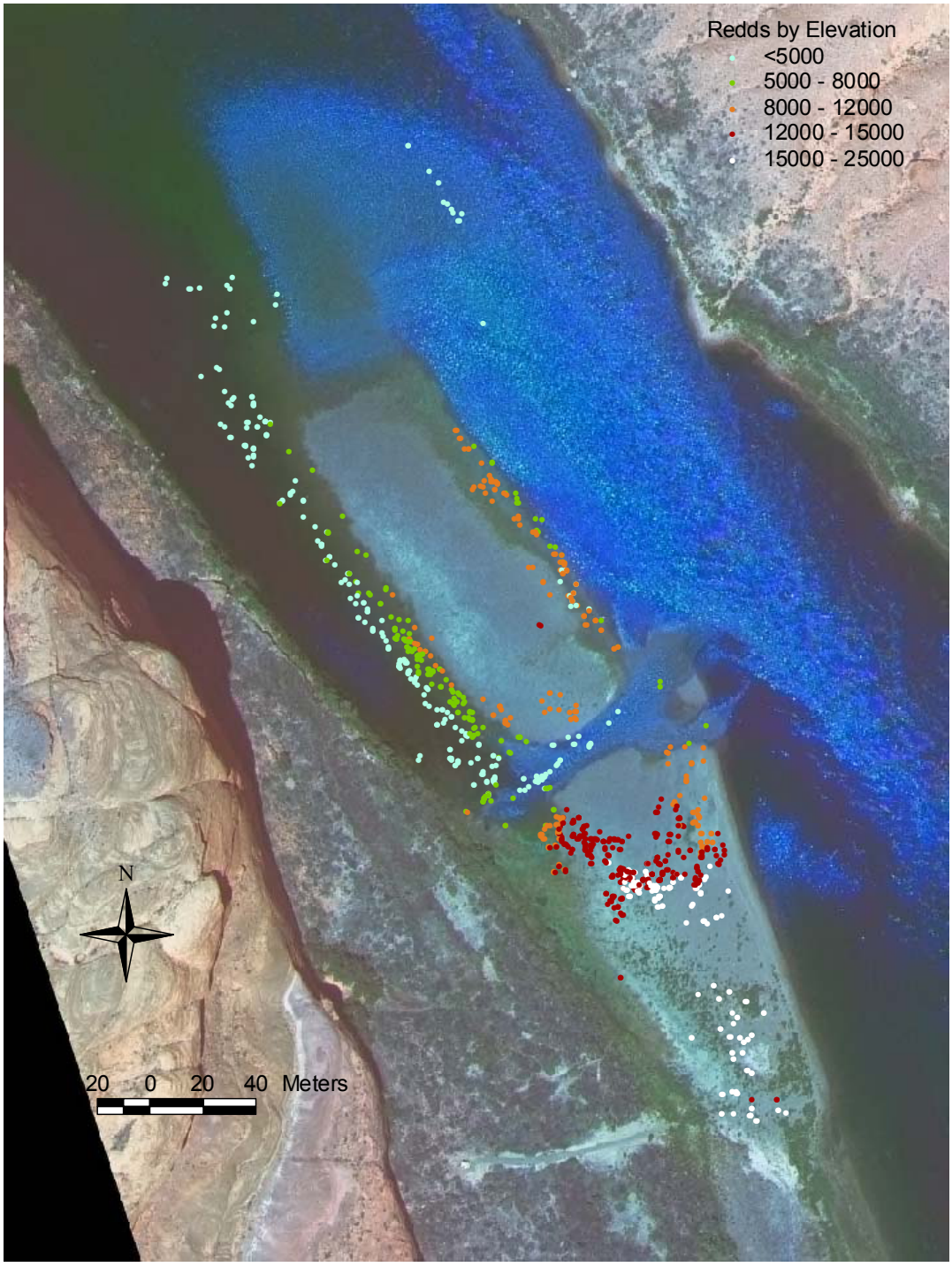

Figure 2.4. Con't

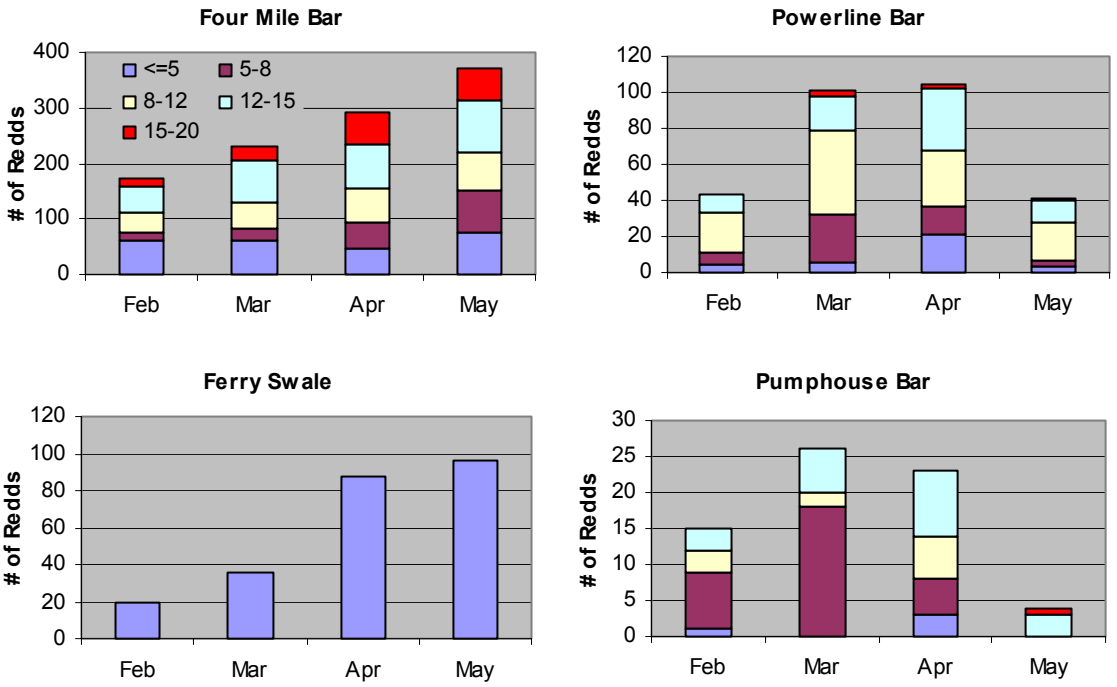

Figure 2.5. Summary of redd hyspometry (kcfs) at four intensive sites by survey period.

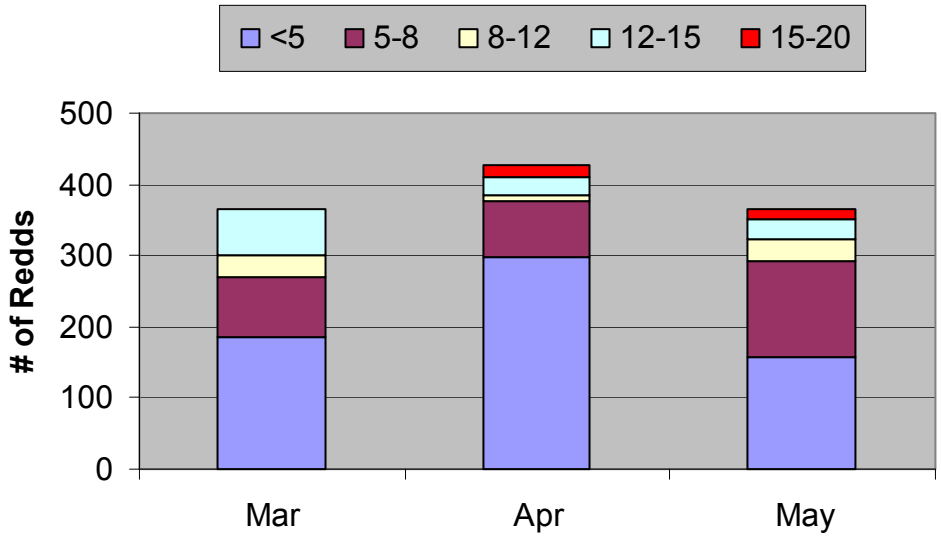

Figure 2.6. Redd hypsometry from the rapid assessment surveys.

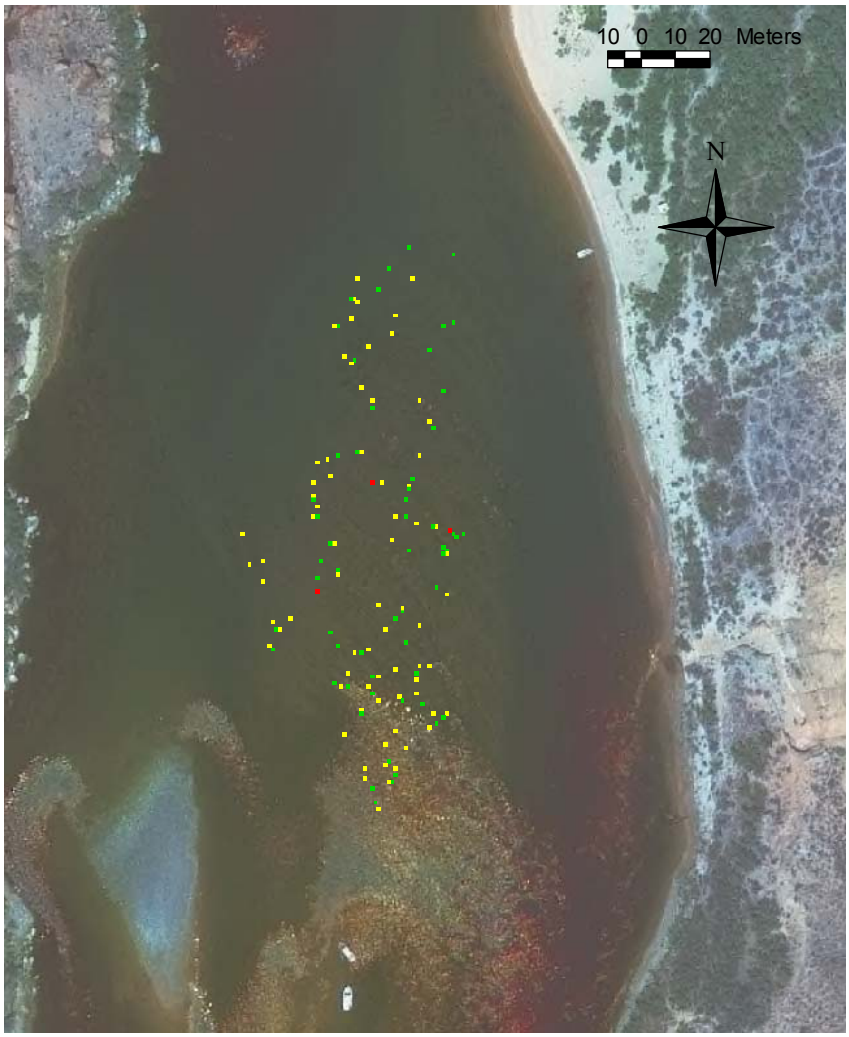

Figure 2.7. Example of 1 m^2 grid showing the change in the location of redds between Apr. and May survey periods at Ferry Swale. Green cells denote locations where a redd was present in May but not in Apr ("New" redds). Yellow cells denote locations where a redd was present in Apr. but not in May ("Faded" redds). Red cells denote locations where a redd was present in both Apr. and May("Old" redds). The total number of cells with redds in May is the sum of green and redd cells.

a)

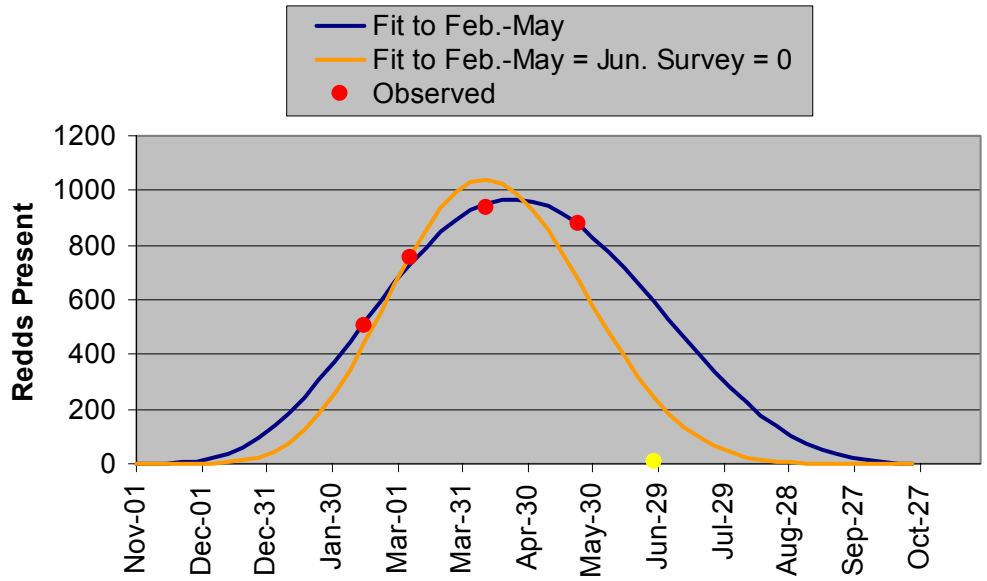

b)

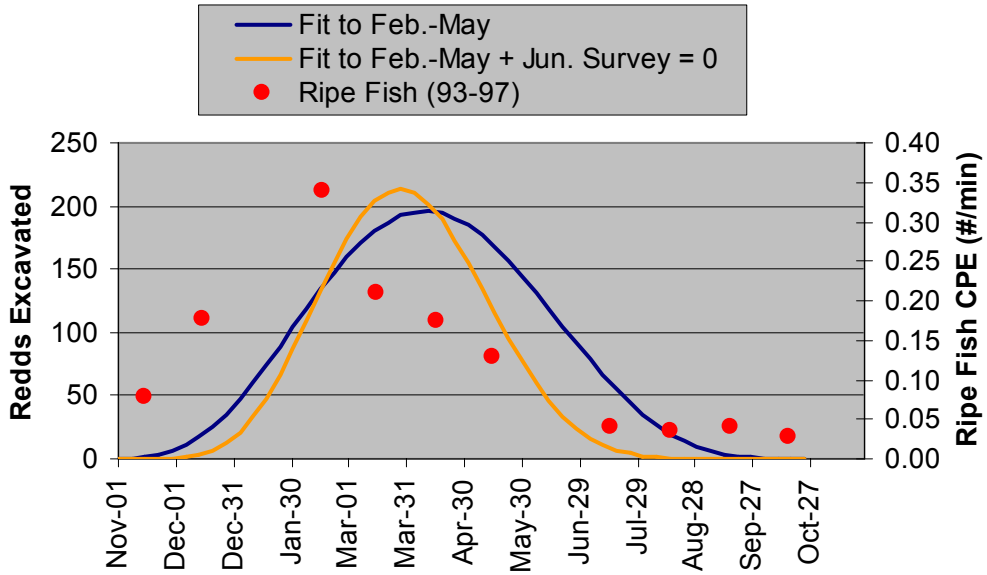

Figure 2.8. Observed and predicted numbers of redds present in 2003 assuming a survey life of 5 weeks and no redd superimposition (a). Predictions were made using the Feb-May redd count data only (redd dots and blue line), and using the same data but assuming no redds would be present by late Jun (redd + yellow dots). The corresponding spawn timing curves are shown in b) and are compared with the catch rate (CPE) of ripe fish from 1993-1997 (McKinney et al. 1999).

a)

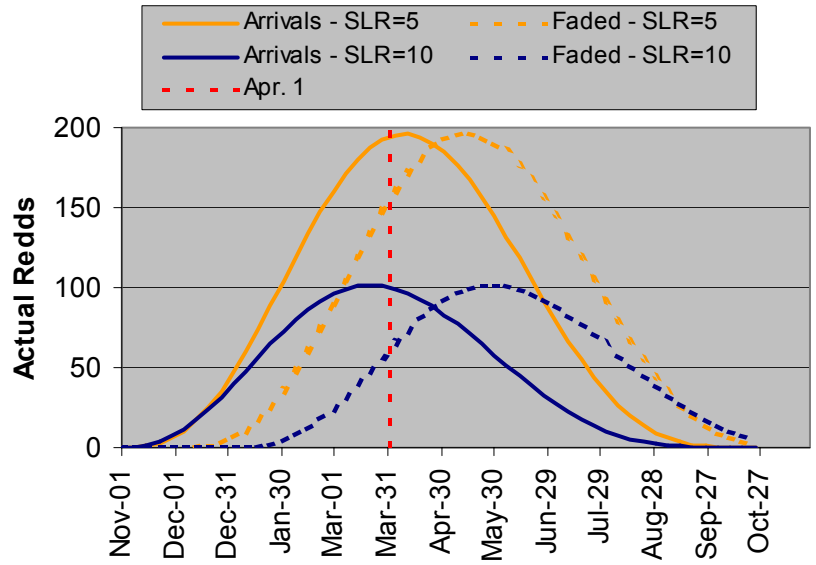

b)

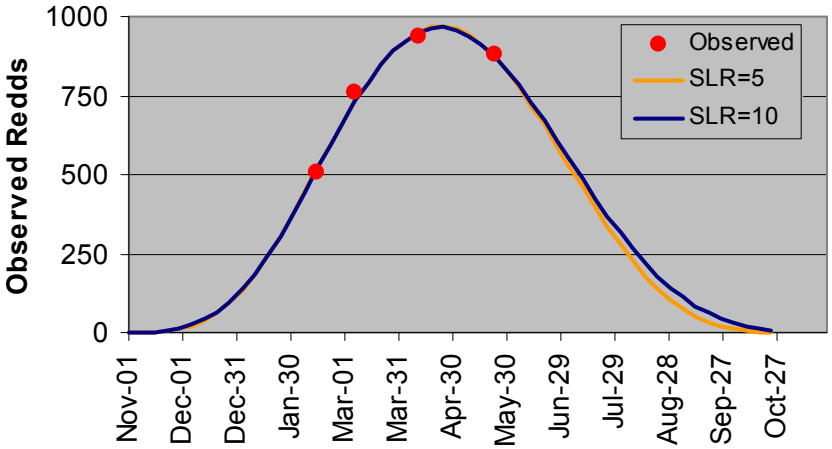

Figure 2.9. Timing of a) excavation of redds ("arrivals") and loss of redds due to fading ("faded") under two assumptions of survey life (SLR=5 and 10 weeks), and b) observed and predicted number of redds under these two assumptions. Red dots in b) are the observed redd counts. The total number of redds excavated, and the percentage of excavation prior to Apr. 1 for SLR = 5 and 10 was 4,175 (42%) and 2,143 (53%), respectively.

a)

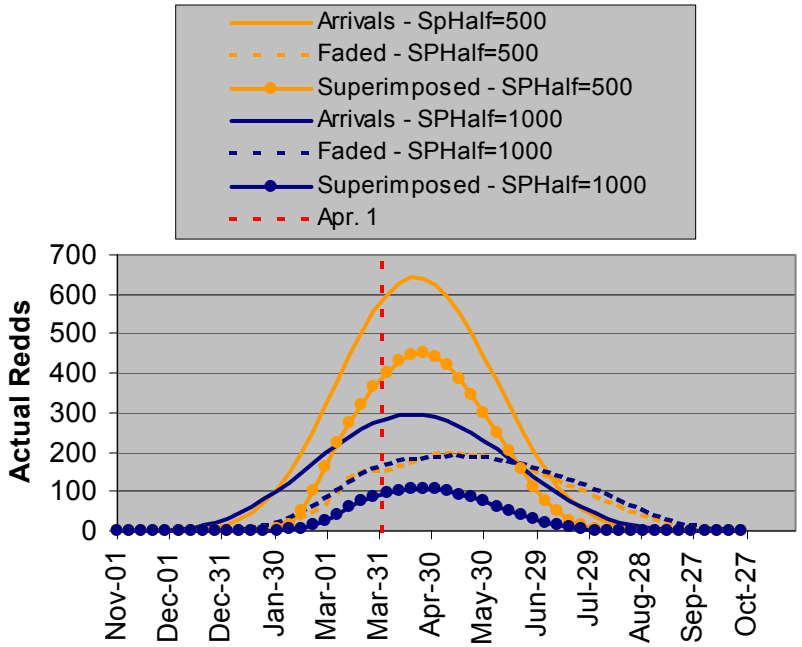

b)

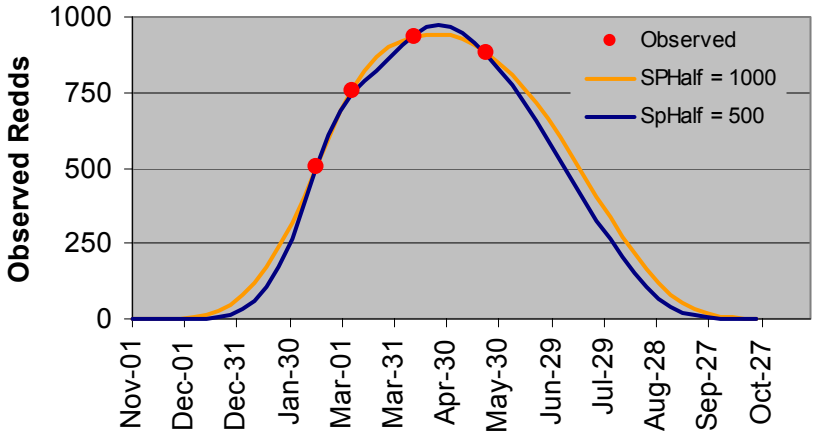

Figure 2.10. Timing of a) excavation of redds ("arrivals"), loss of redds due to fading ("faded"), and number of redds that are superimposed for two estimates of *SPHalf*, the number of redds present where the maximum superimposition rate is reduced to ½ of its maximum value (*SPHalf*=500 or 1000). The maximum superimposition rate (SPmax) and survey life (SLR) were set at 0.8 and 5 weeks, respectively. Predicted and observed redd numbers are shown in b).

a)

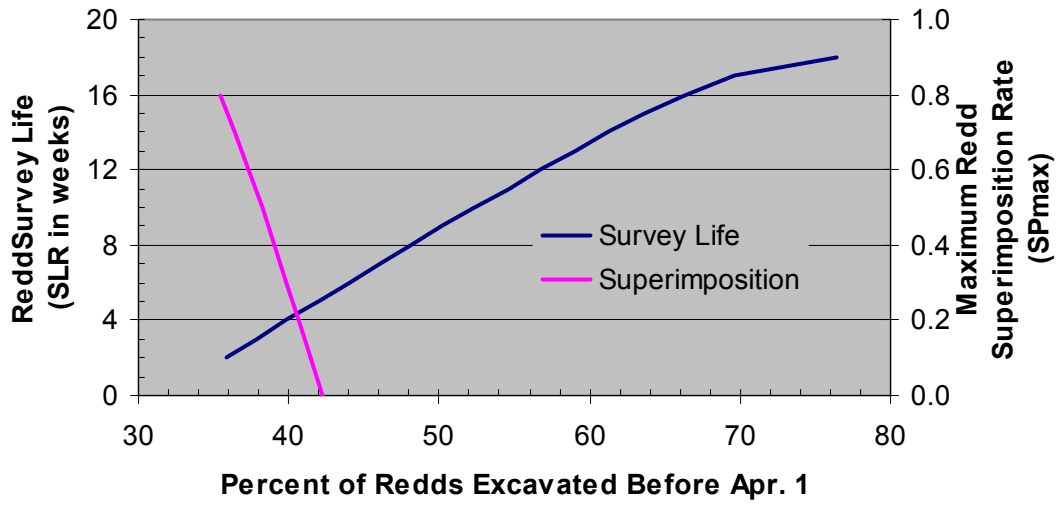

b)

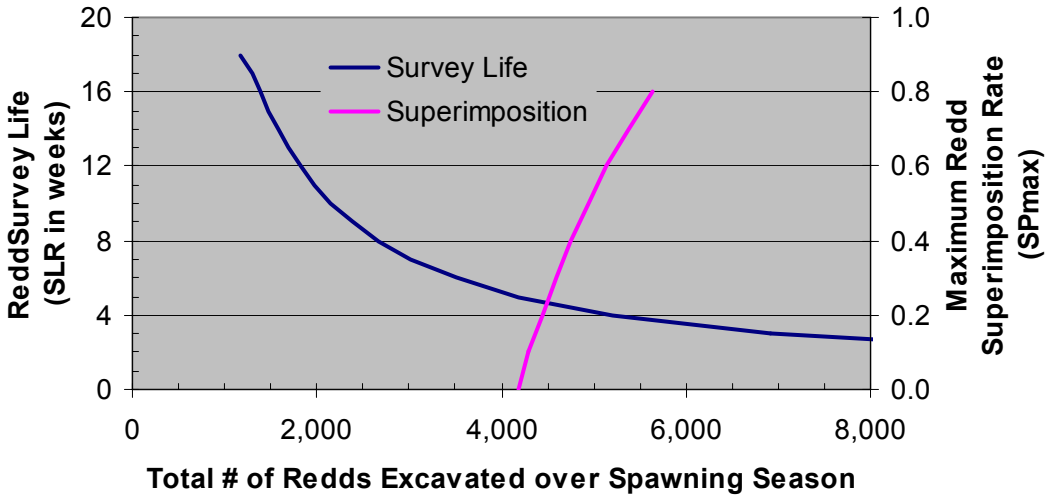

Figure 2.11. The effect of alternate assumptions about redd survey life (*SLR*) and the maximum rate of superimpostion (*SPmax*) on a) the percent of redds excavated prior to Apr. 1, and b) the total number of redds excavated over the spawning season. The superimposition rate was assumed to be 0 over the range of survey life values that were explored. Survey life was assumed to be 5 weeks over the range of superimposition rates that were explored. For the superimposition rate analysis, the number of redds present required to reduce the superimposition rate to ½ of its maximum value (*SPhalf*) was set at 1000.

a)

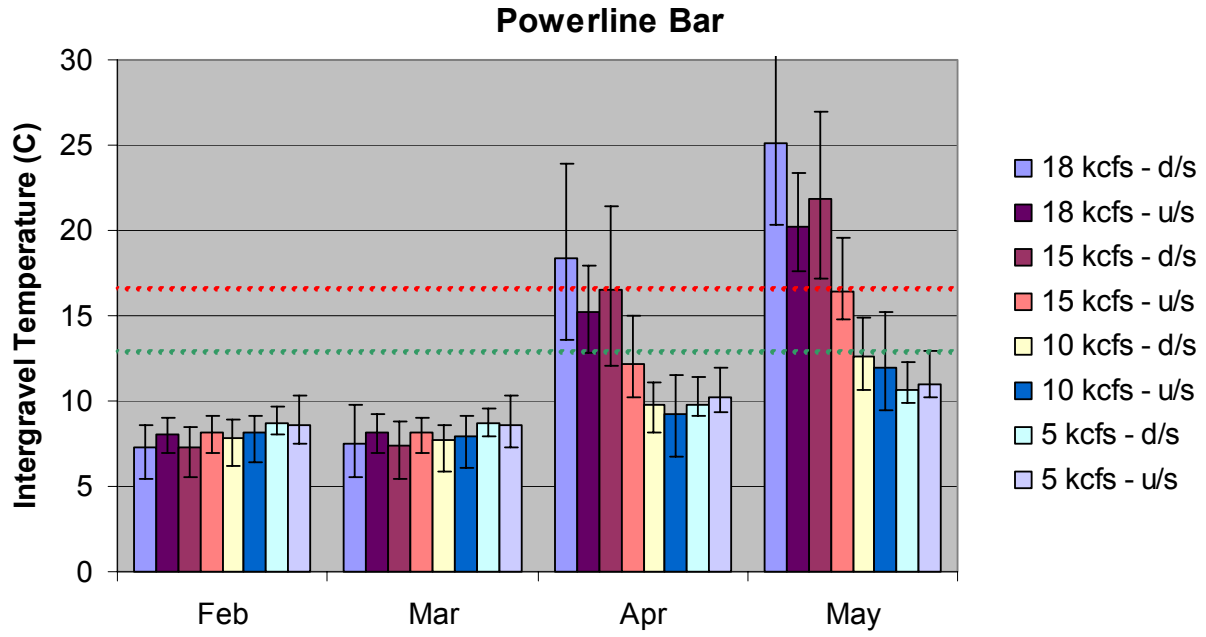

b)

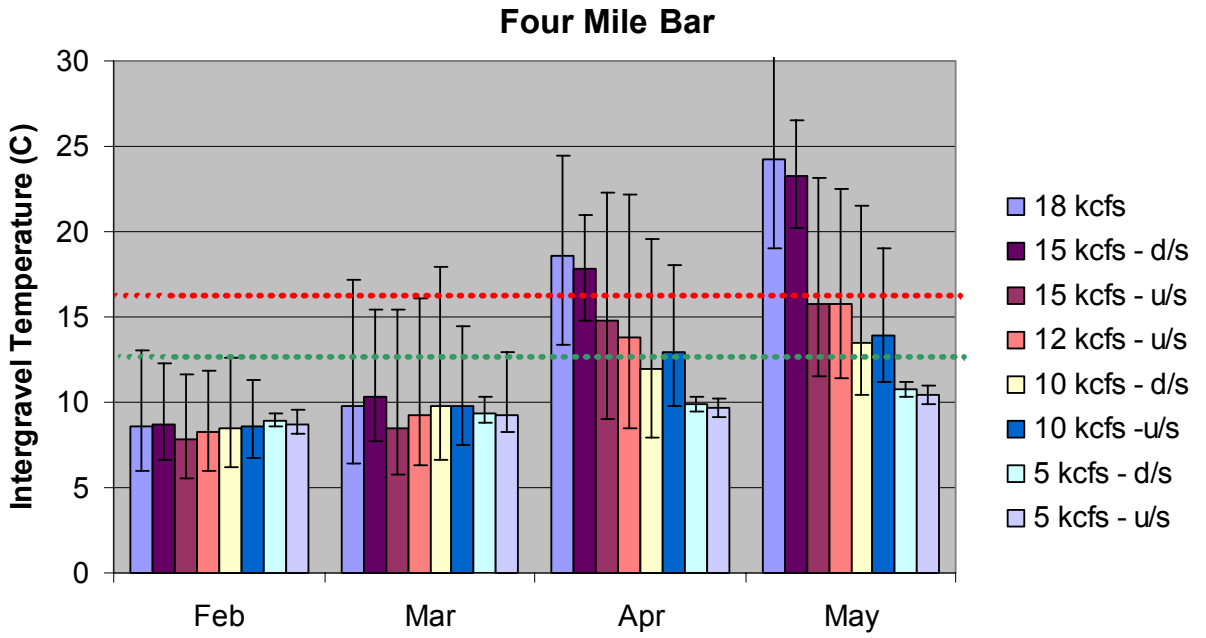

Figure 2.12. Intergravel temperatures at a) Powerline and b) Four Mile Bars at different elevations. Bar height represents the mean monthly temperature (based on hourly observations) with error bars denoting the average daily minimum and maximum values. Green and red lines denote the maximum recommended (13 C) and lethal temperature (16 C) limits for rainbow trout egg incubation, respectively.

a)

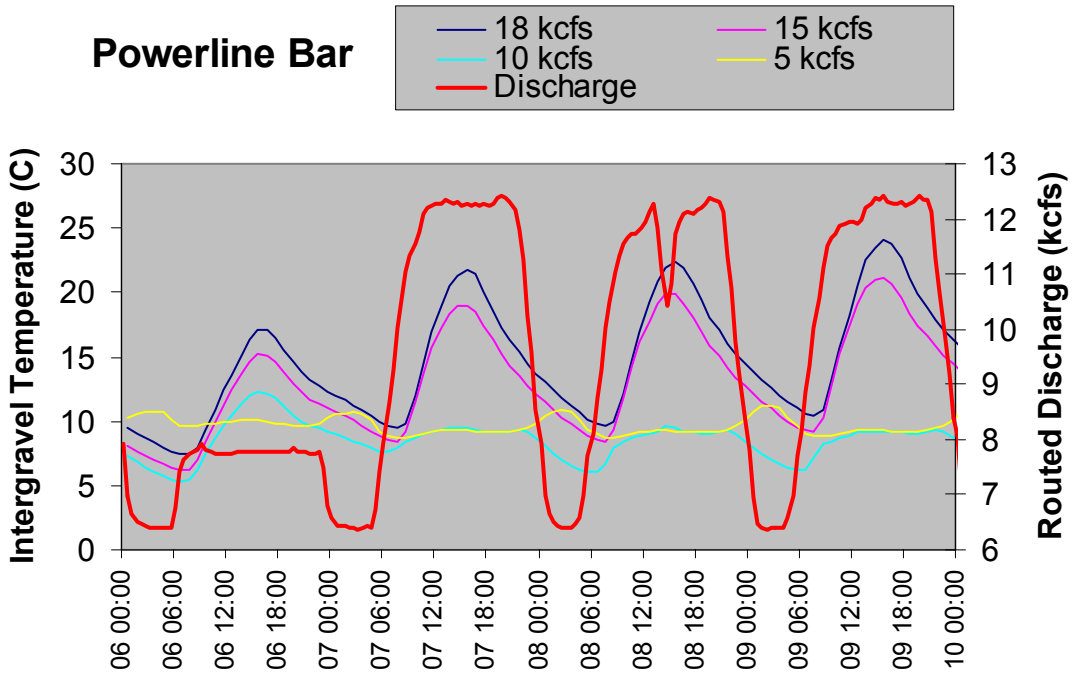

b)

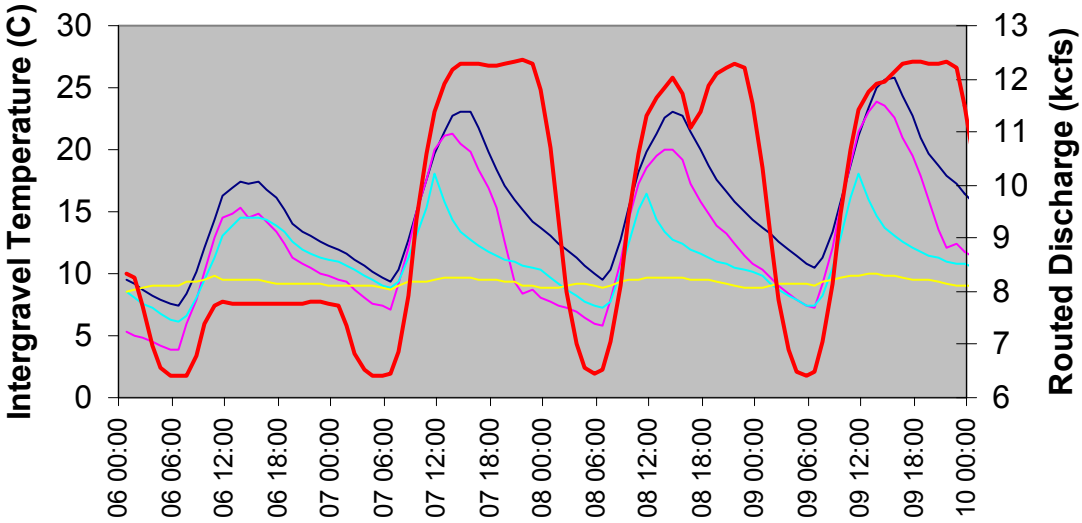

Figure 2.13. Comparison of intergravel thermographs and hydrographs (Apr. 6-9, 2003) at a) Powerline Bar and b) Four Mile Bar. The effect of differences in the timing of inundation on temperature at the 10 kcfs stage is clearly seen.

a)

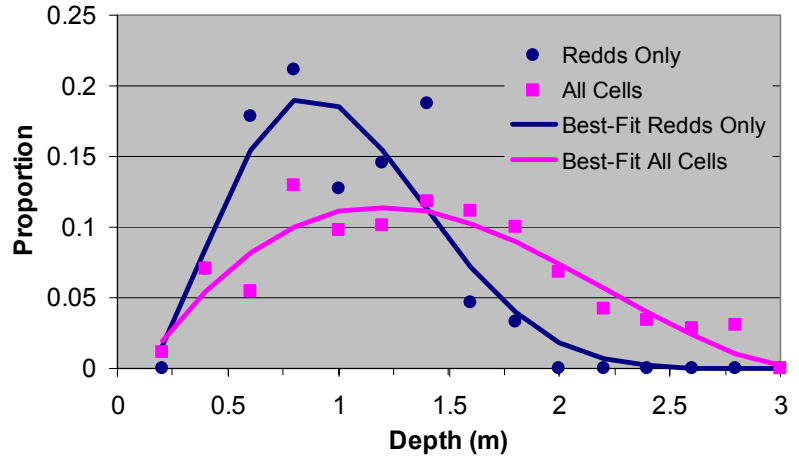

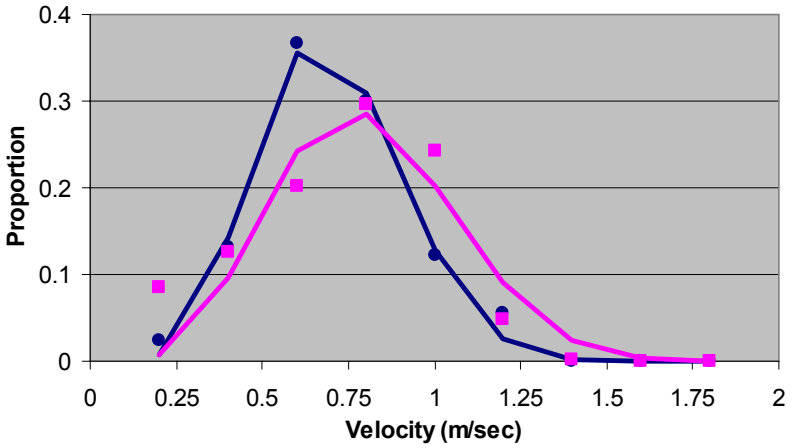

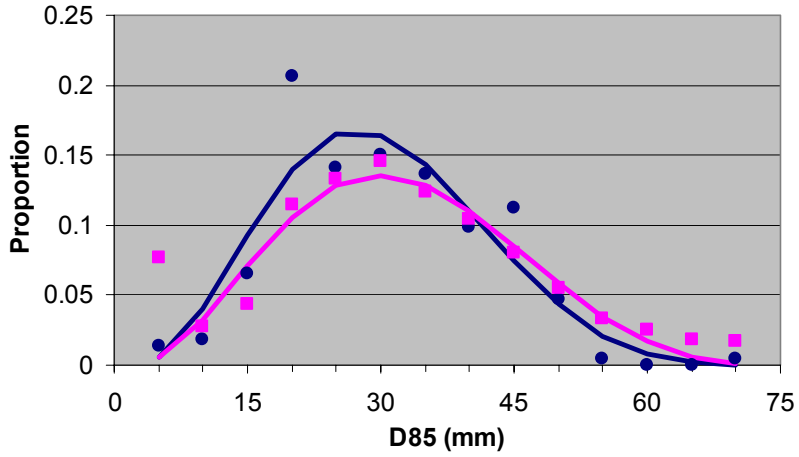

Figure 3.1. Proportion of all grid cells (magenta) across a range of depth, near-bottom velocity, and D85 categories at Four Mile Bar (a), Ferry Swale (b), and Powerline Bar (c) and proportions for cells in these categories where a redd was present during the Mar. survey (blue). Depth and velocity statistics are based on measurements taken at 20 kcfs at Four Mile and Powerline Bars, and at 5 kcfs at Ferry Swale, the assumed discharges when the Mar. redds were excavated at these sites.

b)

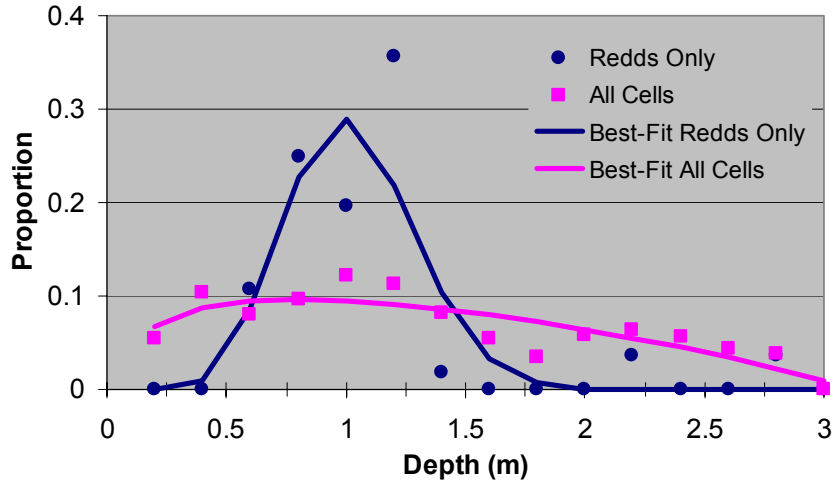

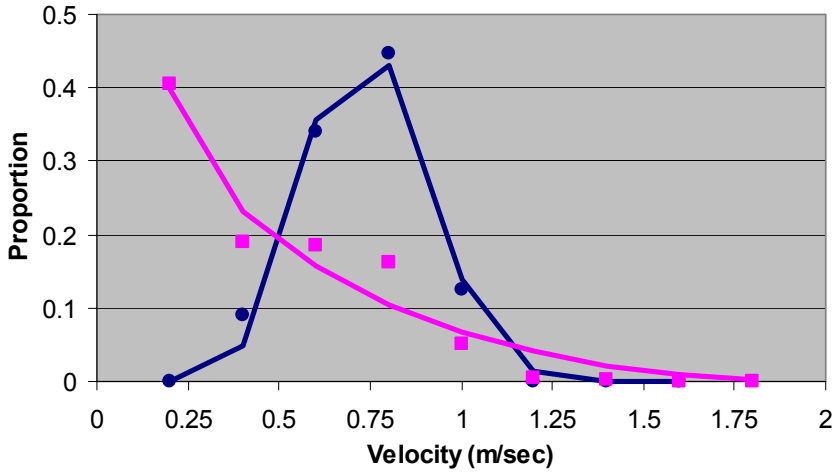

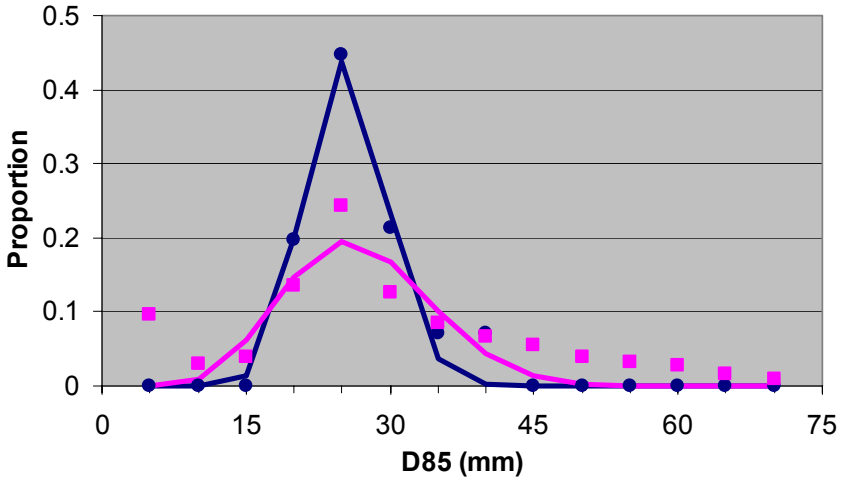

Figure 3.1. Con't (Ferry Swale).

c)

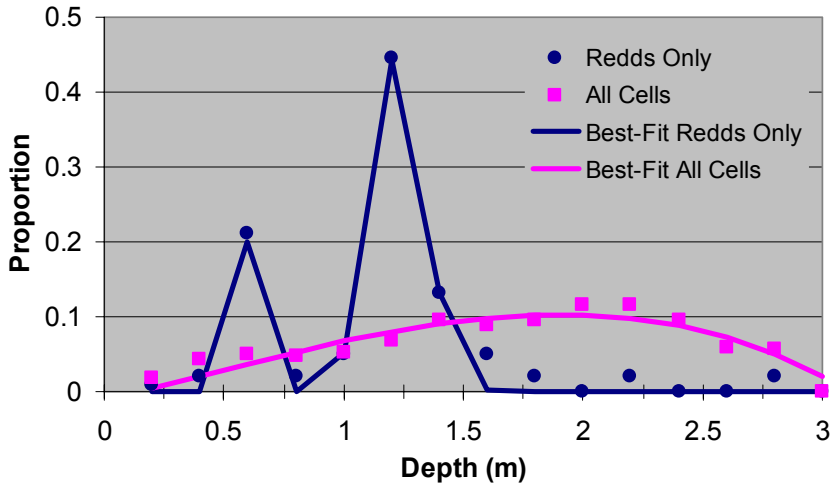

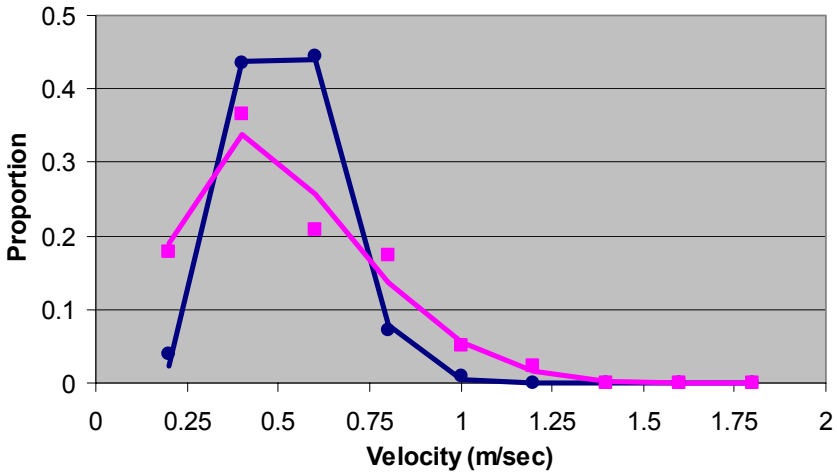

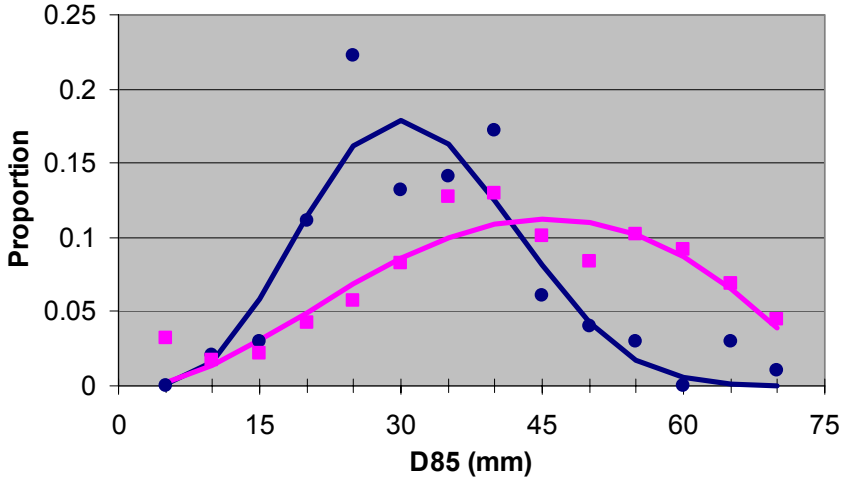

Figure 3.1. Con't (Powerline Bar).

a)

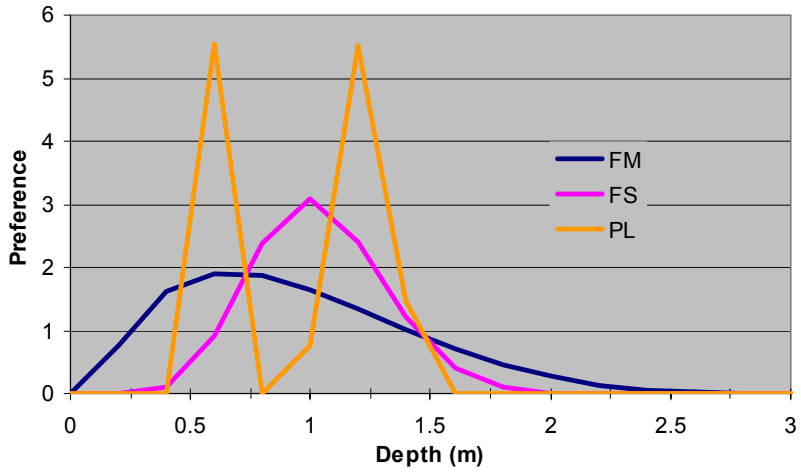

b)

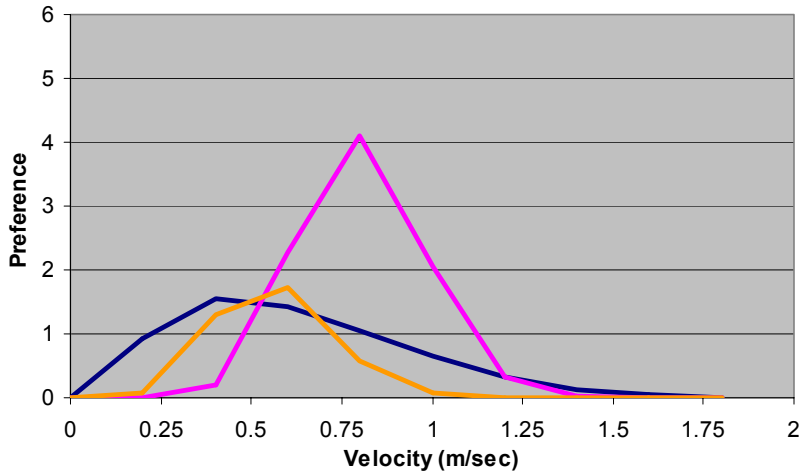

c)

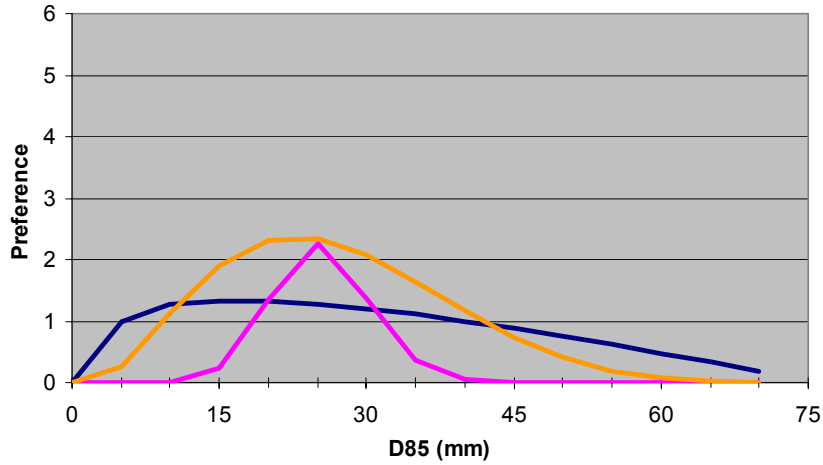

Figure 3.2. Comparisons of preference for a) depth, b) near-bottom velocity, and c) D85 at Four Mile Bar (FM), Ferry Swale (FS), and Powerline Bar (PL). Curves are the best-fit Beta distribution models fit to the ratio of "redd-only cells"- to "all cells".

a)

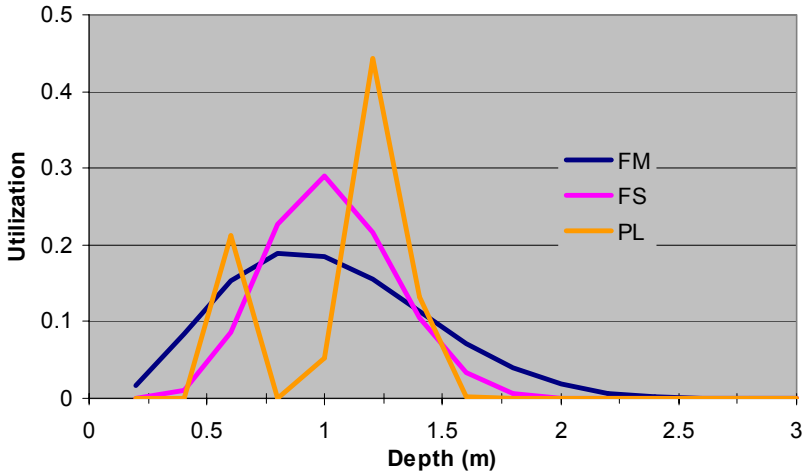

b)

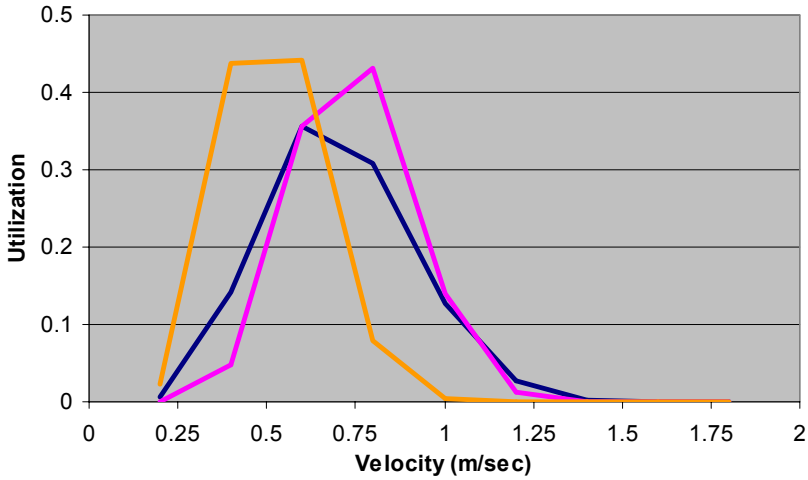

c)

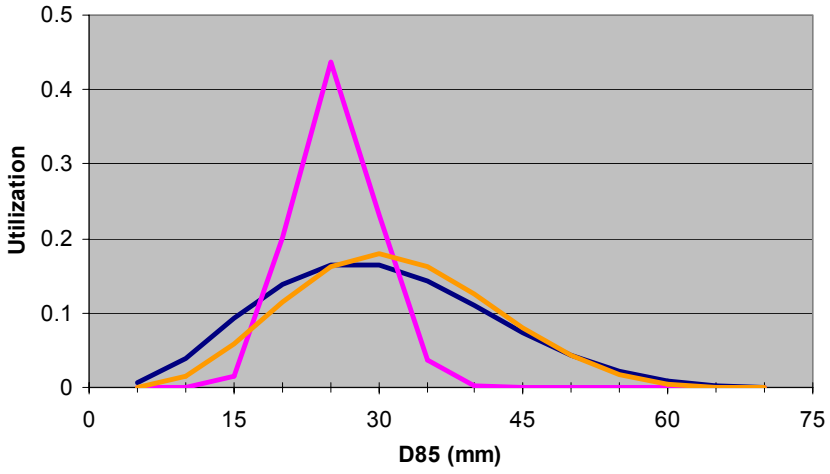

Figure 3.3. Comparisons of the spawning habitat utilization as a function of a) depth, b) near-bottom velocity, and c) D85 at Four Mile Bar (FM), Ferry Swale (FS), and Powerline Bar (PL). Curves are the best-fit Beta distribution models fit to data from "redd-only" grid cells at each site (blue lines in Fig. 3.1).

a)

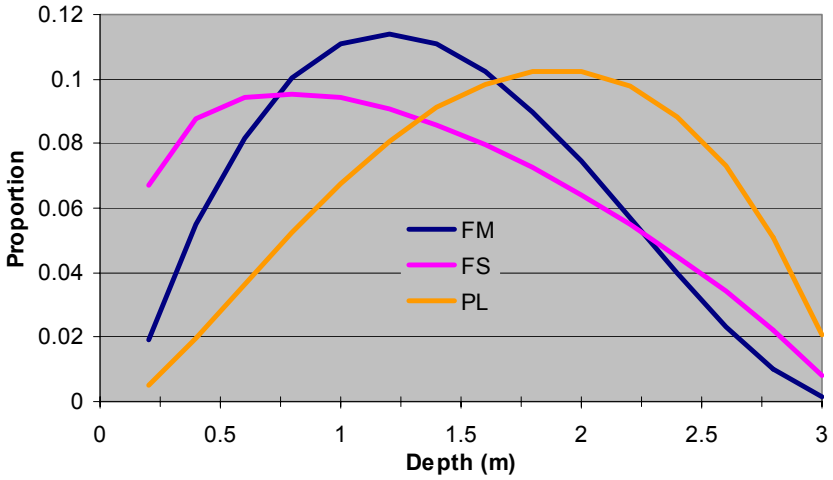

b)

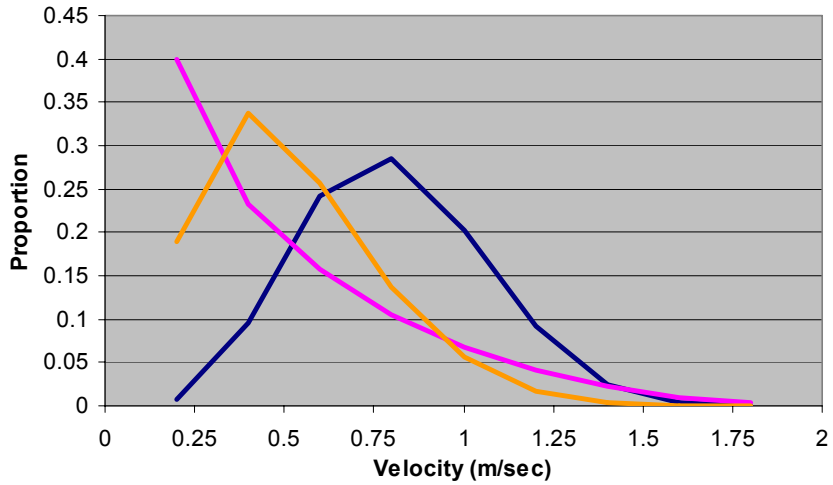

c)

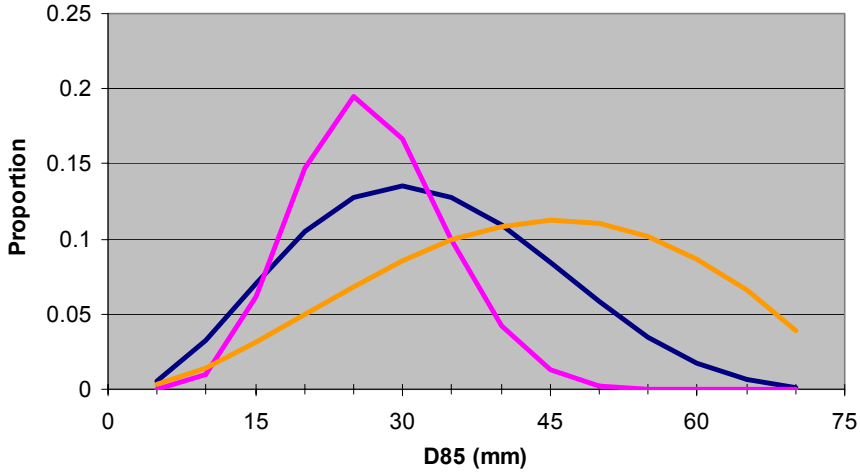

Figure 3.4. Comparisons of the availability of a) depth, b) near-bottom velocity, and c) D85 at Four Mile Bar (FM), Ferry Swale (FS), and Powerline Bar (PL). Curves are the best-fit Beta distribution models fit to data from all grid cells at each site (magenta lines in Fig. 3.1).

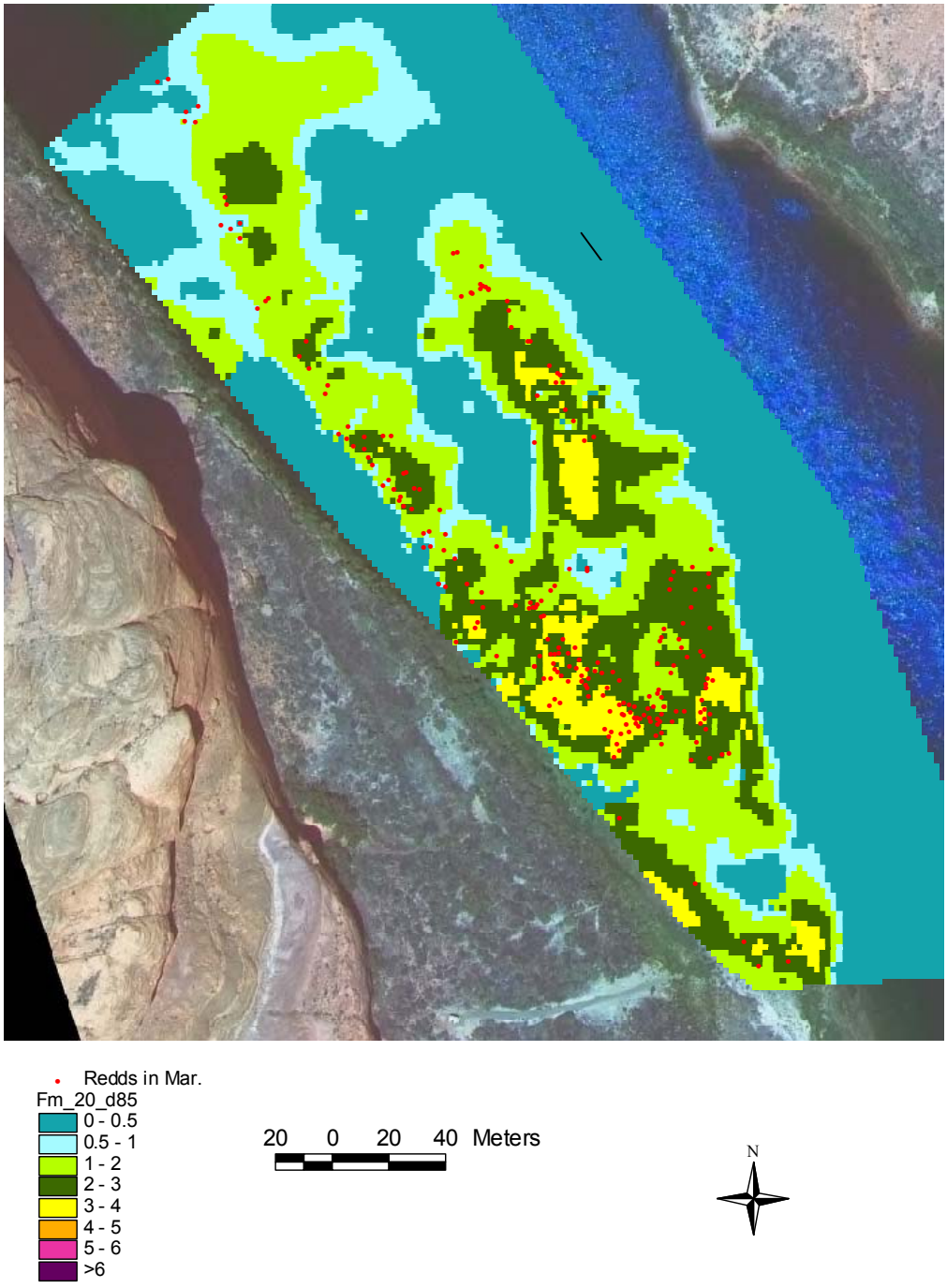

Figure 3.5. Maps of predicted habitat preference at Four Mile Bar at 20 kcfs (a) above), Ferry Swale at 5 kcfs (b), and Powerline Bar at 20 kcfs (c) based on the product of preferences for depth, bottom velocity, and D85. Location of redds during the Mar. survey, from which habitat preferences were developed, are also shown. The black arrow denotes the direction of water flow.

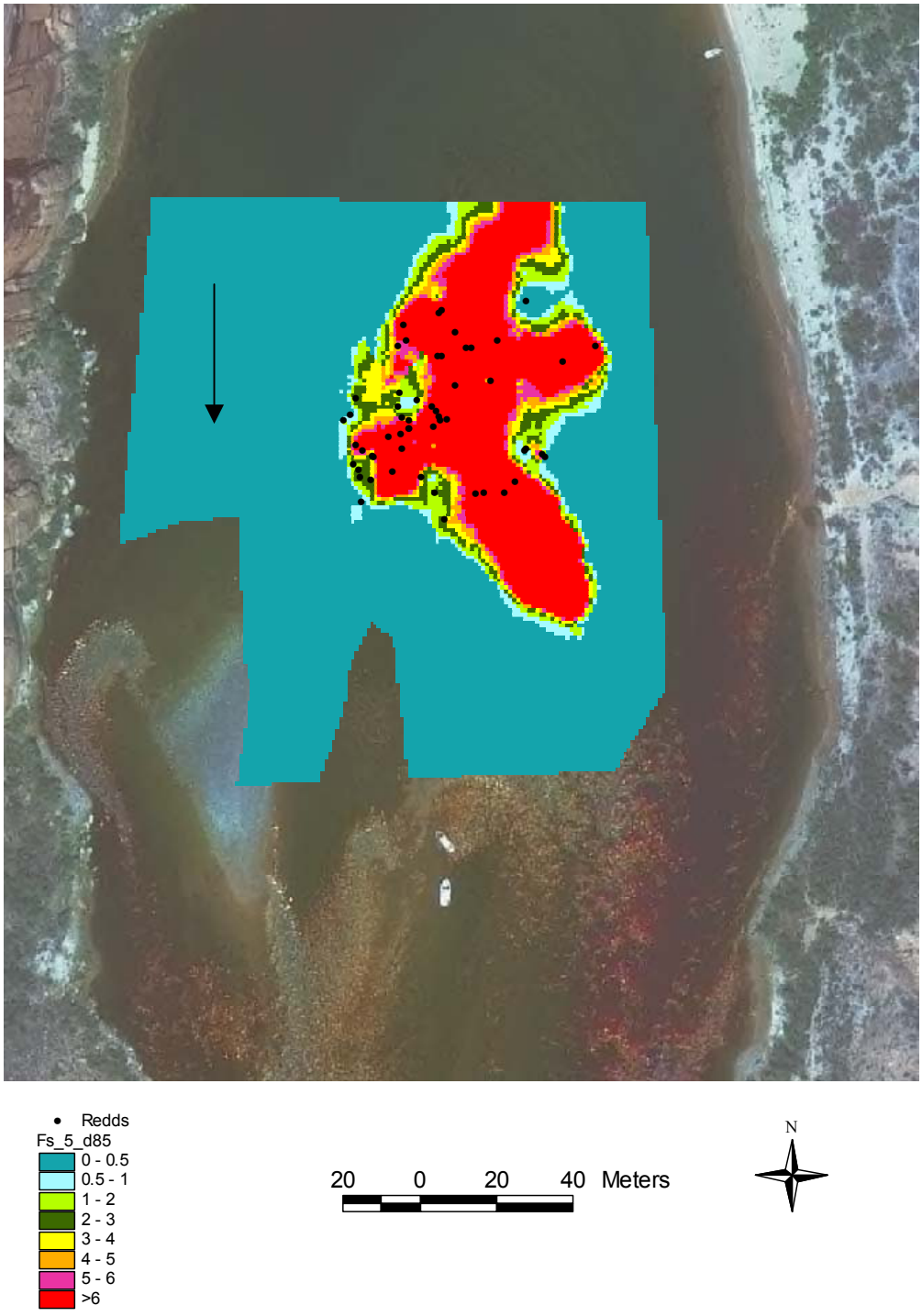

Figure 3.4. Con't (b) - Ferry Swale)

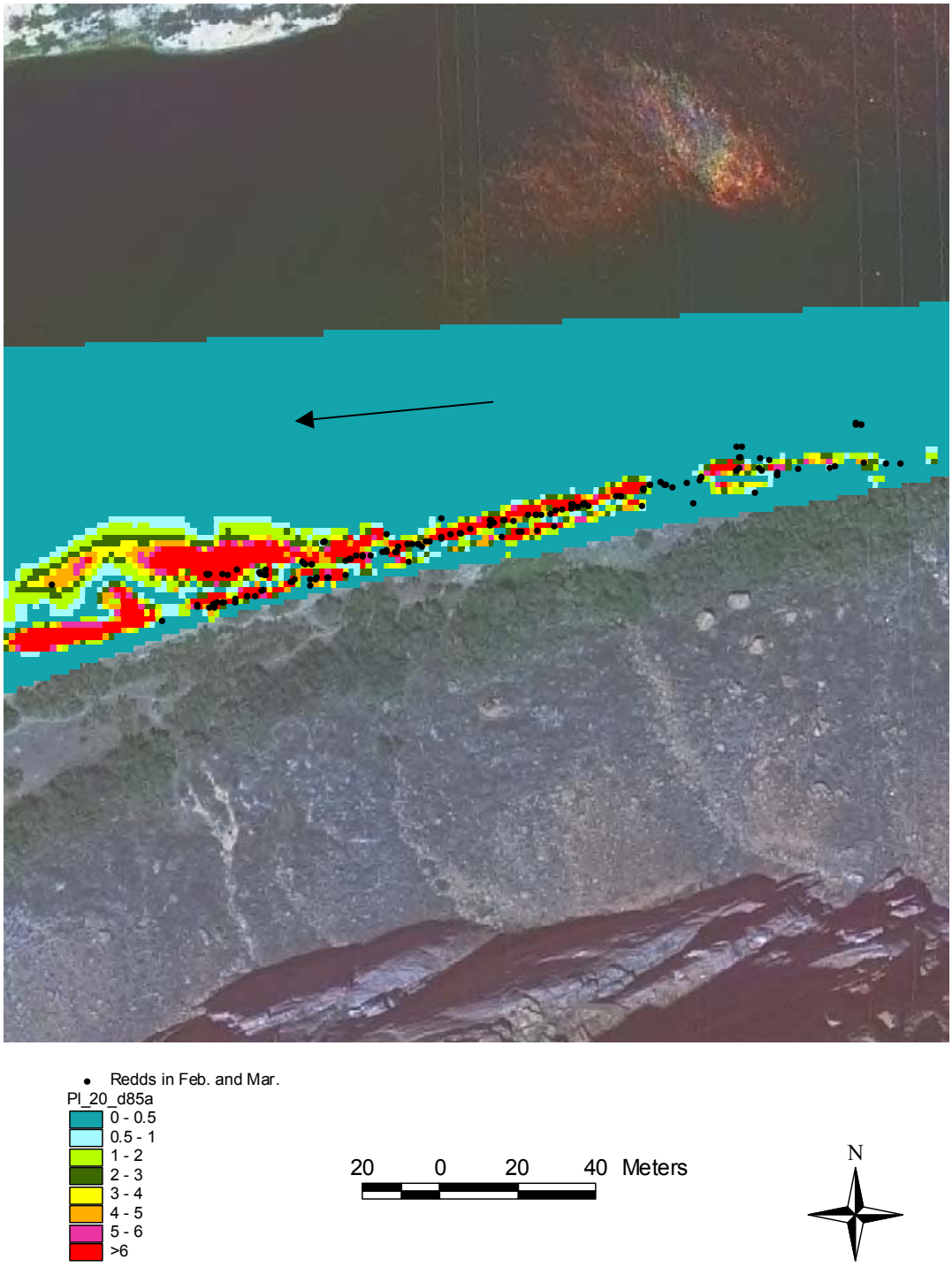

Figure 3.4. (c) Powerline Bar).

a)

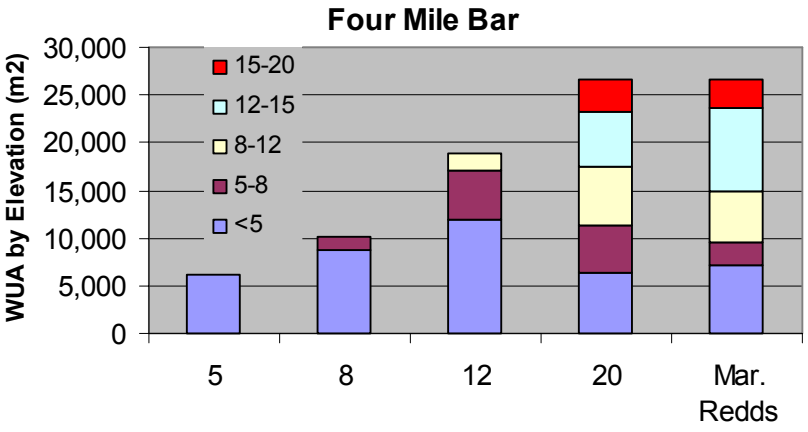

b)

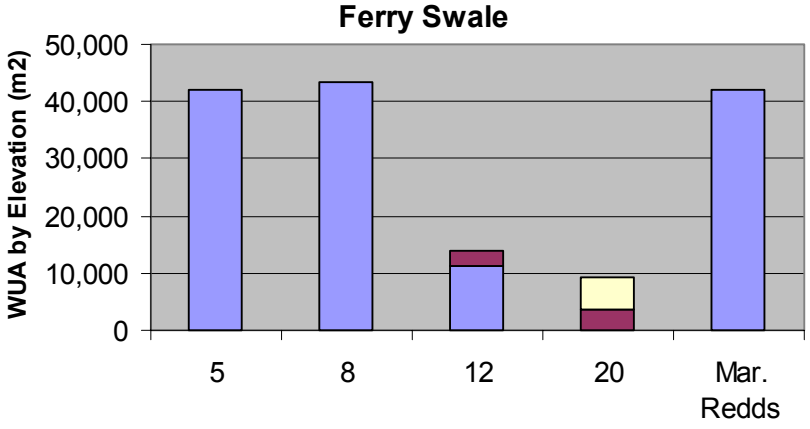

c)

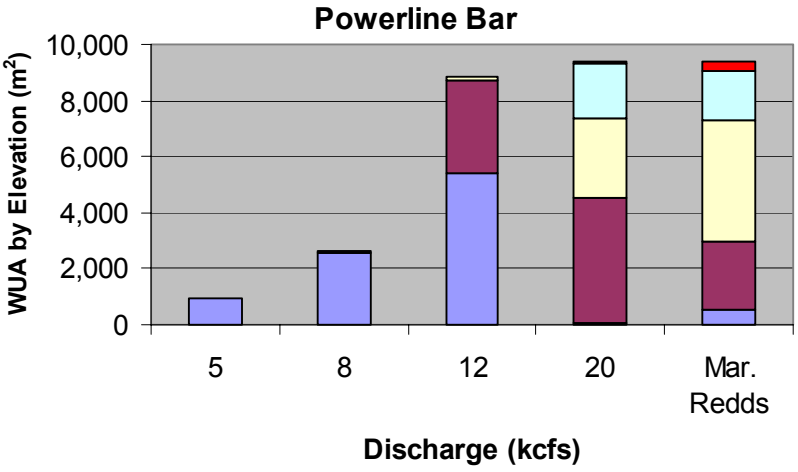

Figure 3.5. Predictions of Weighted Useable Area (WUA) at 5 stages (expressed in discharge units of kcfs) at four levels of discharge (x-axis) at a) Four Mile Bar, b) Ferry Swale, and c) Powerline Bar. The total WUA across stages is equivalent to the total bar height. Also shown is the distribution of redds over the same stages from the Mar. survey (from Fig. 2.5). The redd distributions should be compared to the distribution of WUA at 20 kcfs at Four Mile and Powerline Bars, and at 5 kcfs at Ferry Swale. These discharges are the assumed flows that the redds were created at.

a)

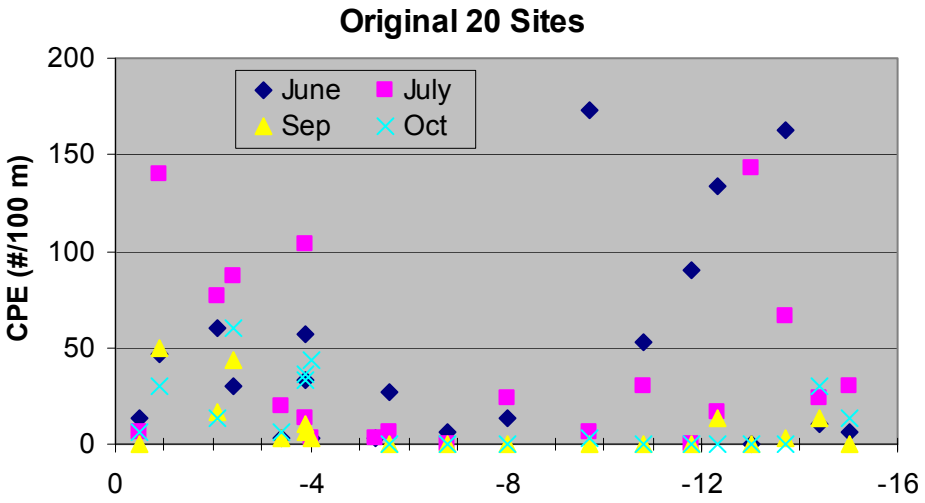

b)

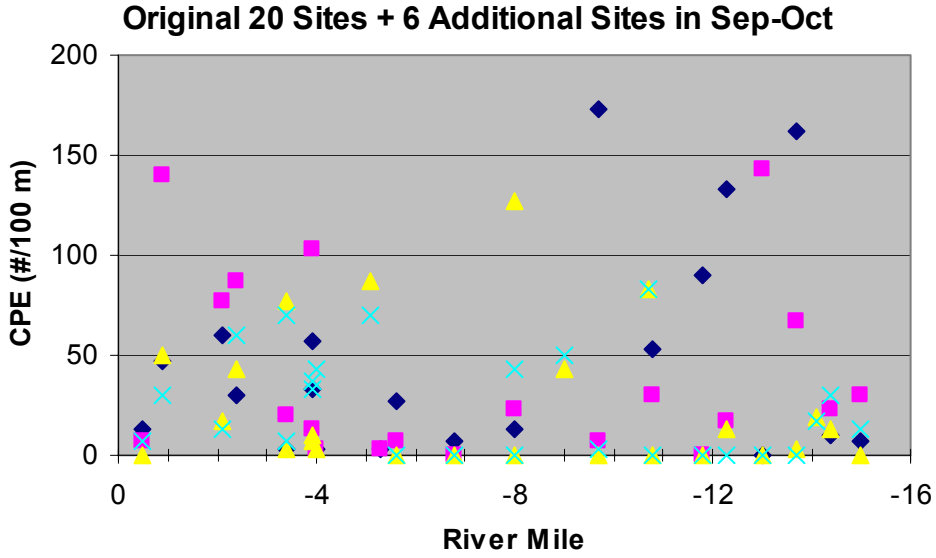

Figure 4.1. Density at the a) 20 original YoY sampling locations by river mile and b) the density at the original 20 sites plus an additional 6 talus shoreline sites sampled on the Sep. and Oct. sample trips. Glen Canyon Dam is located at river mile – 15.6 and Lee's Ferry is located at river mile 0.

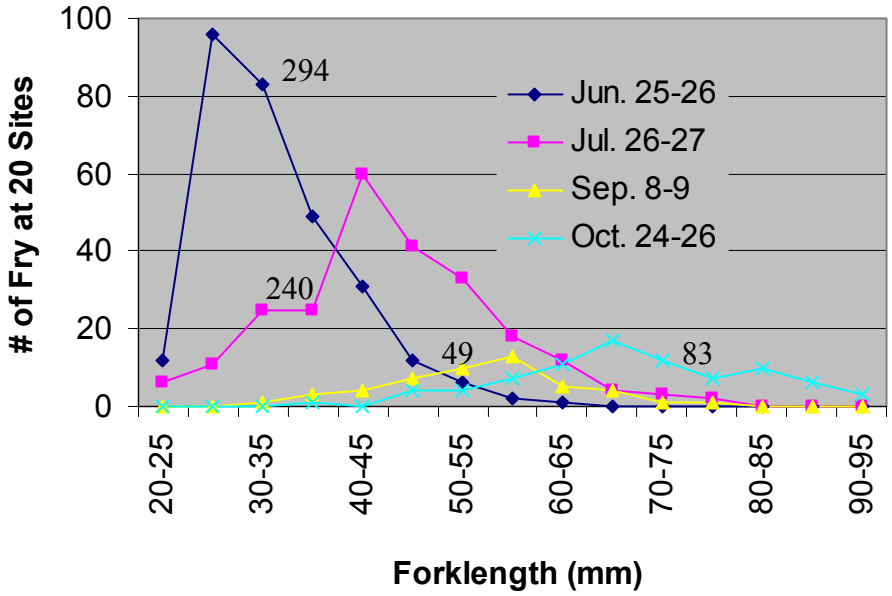

Figure 4.2. Observed length frequency of YoY rainbow trout at the original 20 sampling sites in the Lee's Ferry reach in 2003 over four sampling periods. Sample sizes for each length-frequency distribution are shown.

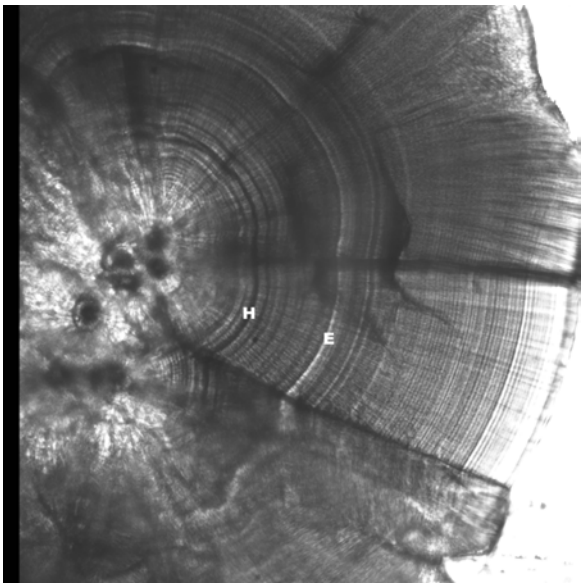

Figure 4.3. Magnified image (16x) of a rainbow trout otolith from Lee's Ferry captured on Sept., 2003 showing emergence (E) and hatch (H) checks. Each pair of dark and light rings represents one day of growth.

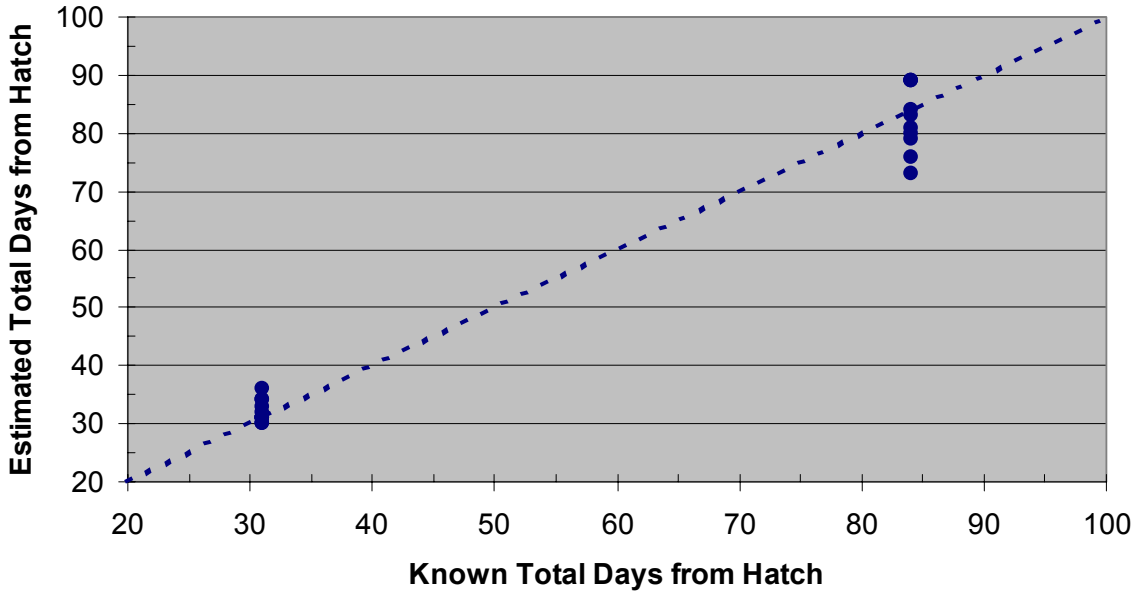

Figure 4.4. Comparison of estimated and known young-of-year age from hatch of wild rainbow trout that were spawned in a hatchery, hatched on Jun. 23, 2003, and sampled on Jul., 24, 2003 (at 31 days from hatch), and Sep. 15, 2003 (at 84 days from hatch).

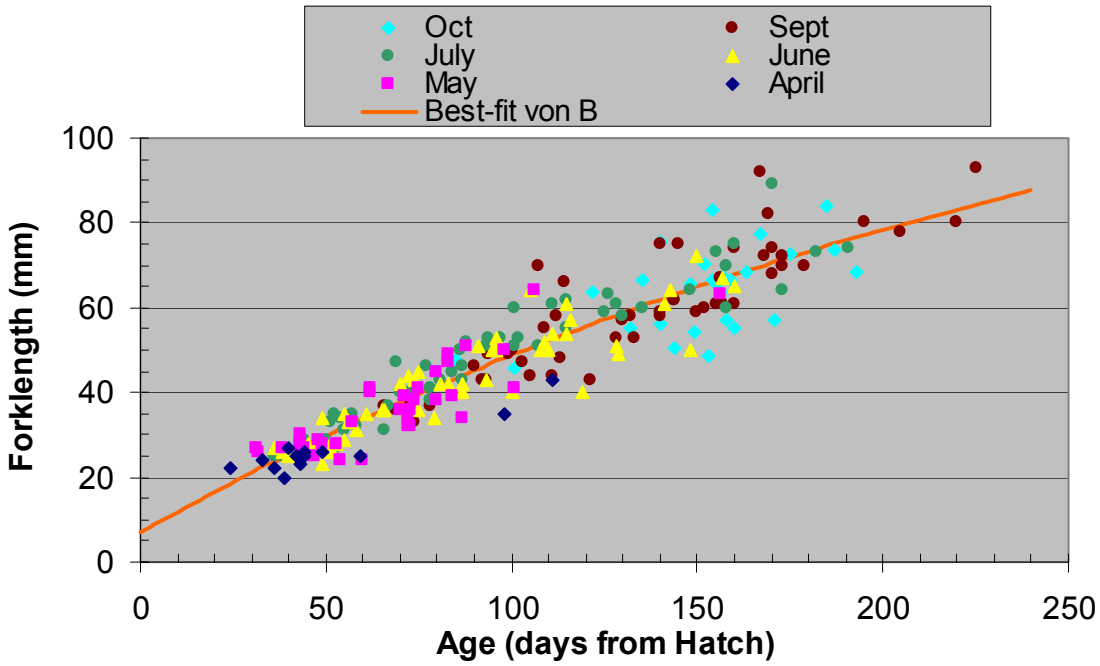

Figure 4.5. Relationship between forklength and the estimated age from hatch for YoY collected over 7 months in the Lee's Ferry reach, 2003. The best-fit von Bertalanffy model to all the data is also shown.

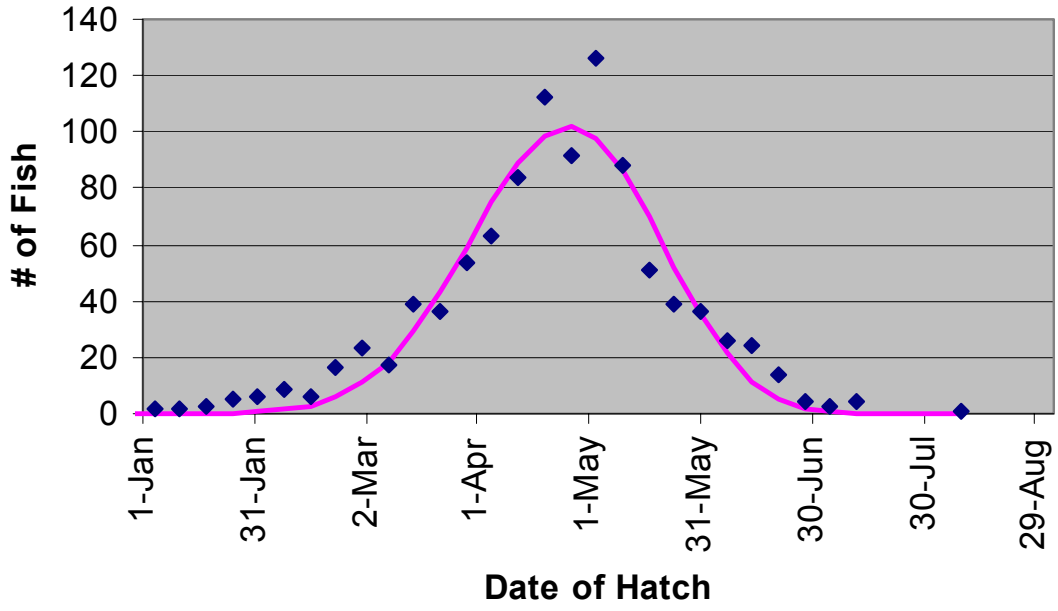

Figure 4.6. Back-calculation of the week of hatch for 991 YoY fish captured in the Lee's Ferry reach from Apr. – Oct. 2003. Diamonds represent the data and the solid line represents the best-fit beta distribution to the data that was used as one of the methods to drive fry recruitment rates in the stock synthesis model.

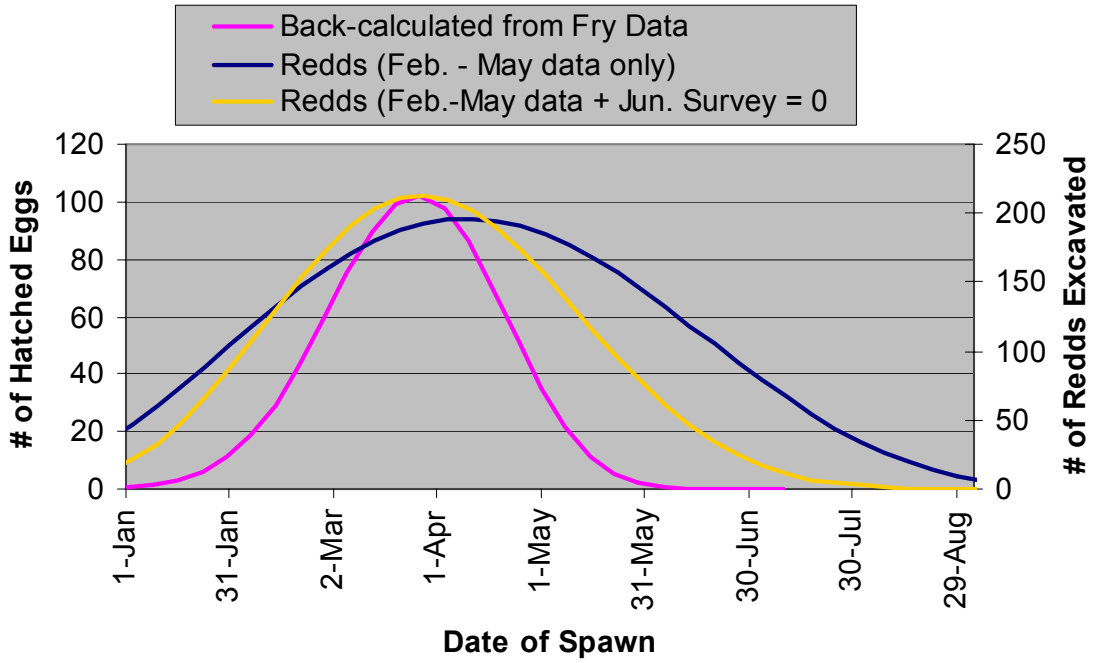

Figure 4.7. Comparison of spawn-timing curves based on redd counts (assuming a redd survey life of 5 wks) and the back-calculated curve based on the estimated timing of hatch from the fry data (Fig. 4.6) and an assumed egg incubation of 30 days. The redd-derived spawn-timing curves are based on either the Feb.-May redd survey data only (blue line), or the same data and the assumption that spawning was completed by the end of May (orange line).

a)

b)

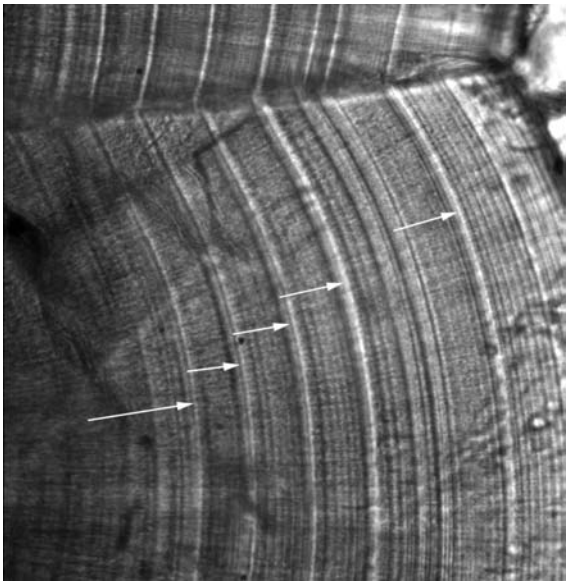

Figure 4.8. Images of a YoY rainbow trout otolith from the Lee's Ferry reach sampled in Apr. showing a weekly striping pattern (identified by white arrows) at magnifications of a) 16x and b) 400x.

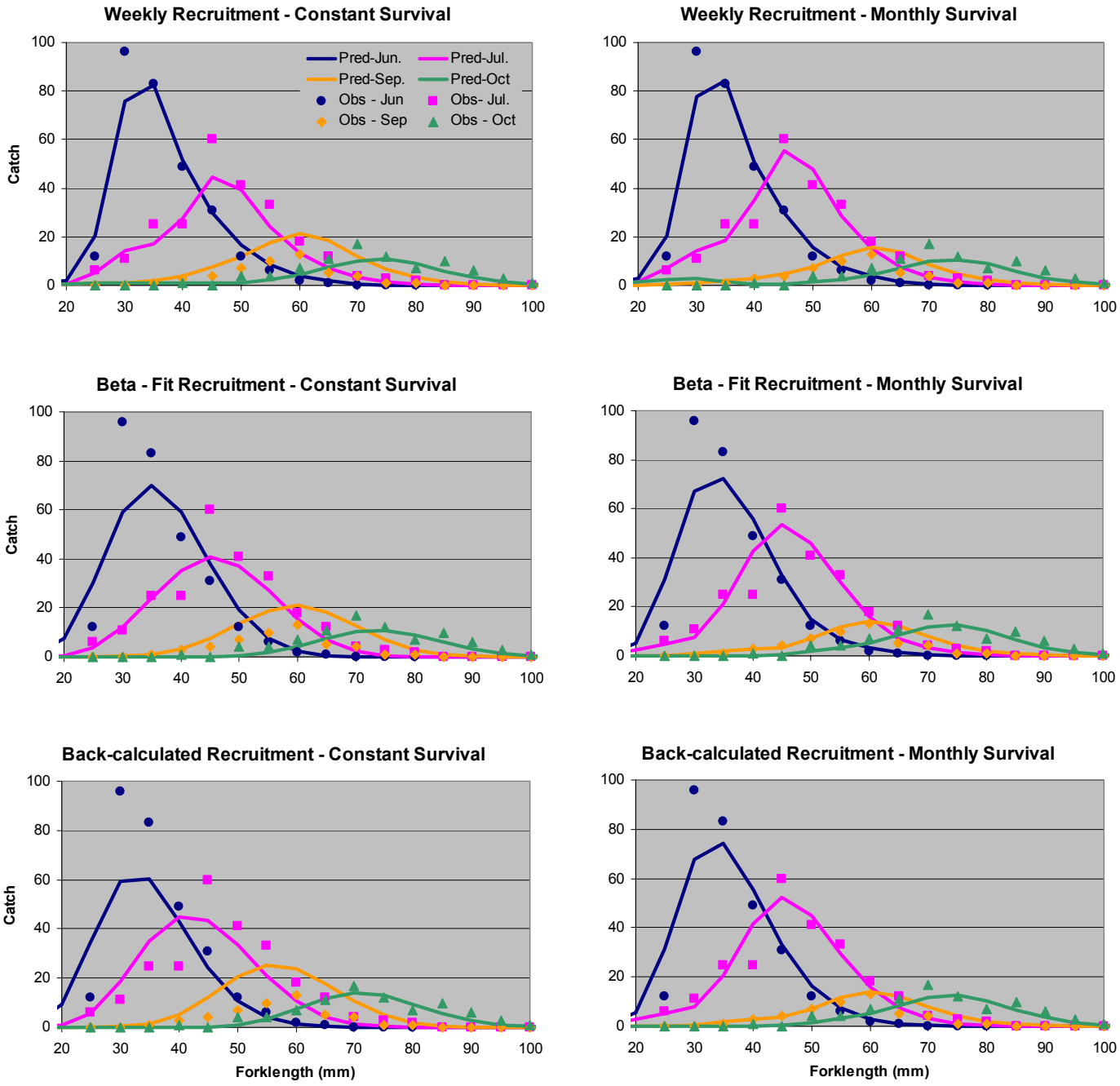

Figure 4.9. Best-fit stock synthesis model fits (lines) to observed (points) length-frequency data based on alternate models that simulate weekly survival rate (constant over simulation or varying by month) and recruitment (independent weekly values, weekly values estimated from a 3-parameter Beta distribution, and weekly values estimated by fitting the magnitude parameter of the Beta distribution with shape parameters determined by back-calculation of hatch dates from catch data and length-age relationship).

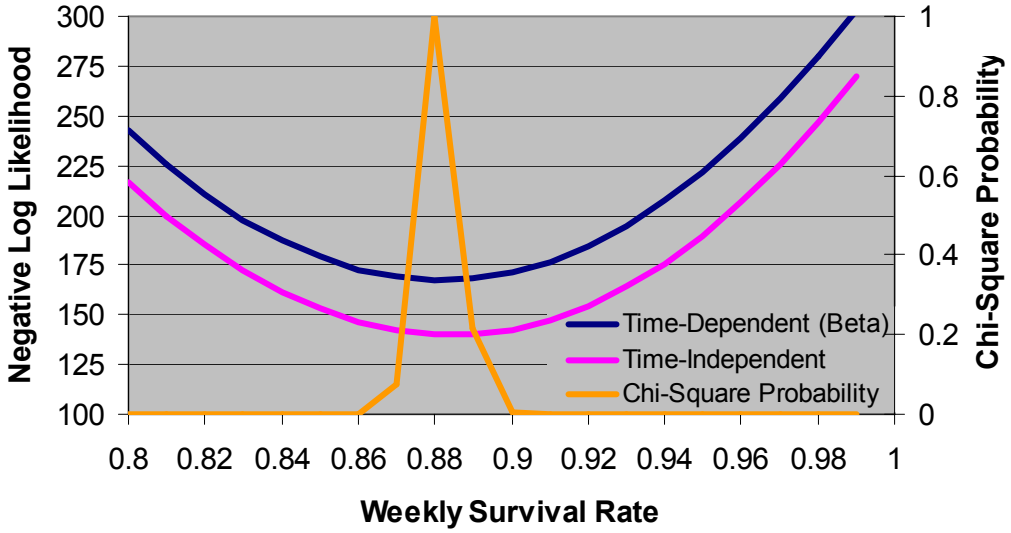

Figure 4.10. Likelihood profiles of weekly survival rate estimates (constant-survival model) for the time-independent and time-dependent best-fit Beta distribution recruitment models. Differences between the minimum negative log likelihood and other values are virtually the same within recruitment models, so the resulting probability profiles are indistinguishable. Confidence limits can be derived by finding the x-axis value below the intersection of the orange line and the one minus the desired confidence interval specified on the right-hand axis (e.g. a 95% limit would be found at Chi-Square probability of 0.05).

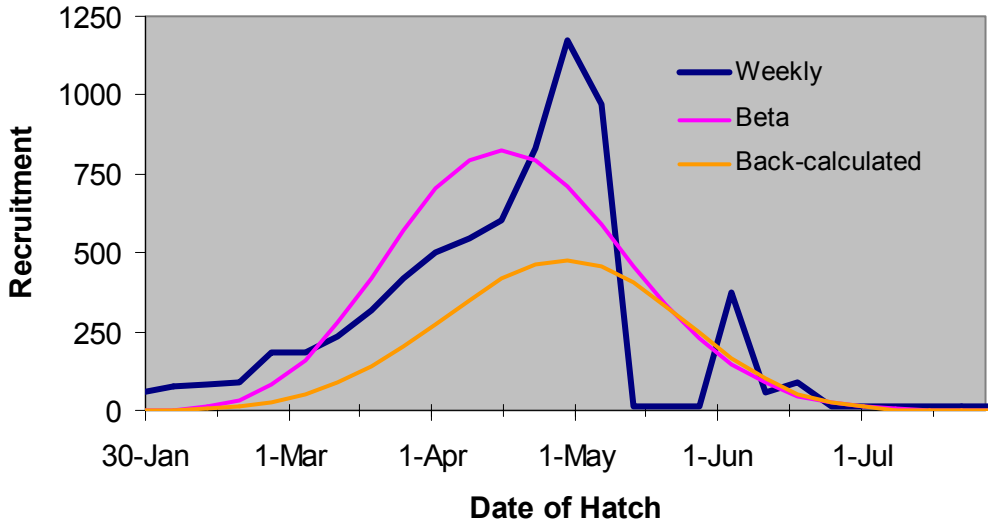

Figure 4.11. Best-fit weekly fry recruitment patterns (number of eggs that hatch) for the constant-survival model based on alternate methods of simulating recruitment (independent weekly values, weekly values estimated from a 3-parameter Beta distribution, and weekly values estimated by fitting the magnitude parameter of the Beta distribution with shape parameters determined by back-calculation of hatch dates from catch data and length-age relationship).